

Results and implications of OLYMPUS

Michael Kohl <kohlm@jlab.org> *

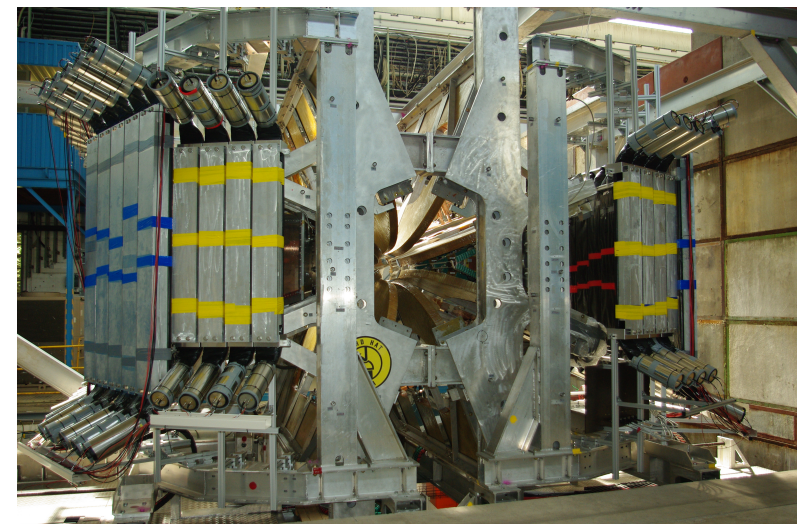
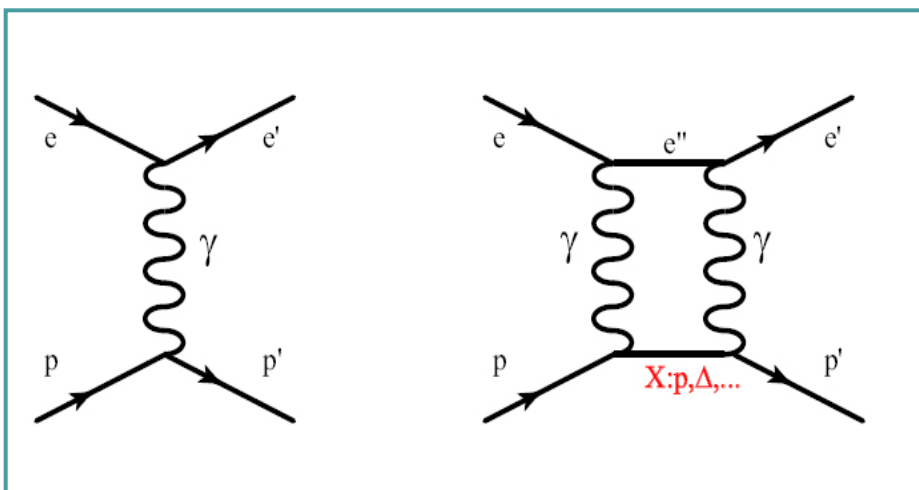
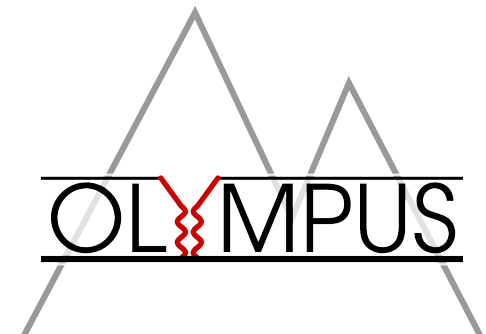
Hampton University, Hampton, VA 23668
Jefferson Laboratory, Newport News, VA 23606



* Presently supported by DOE DE-SC0013941, NSF HRD-1649909, PHY-1505934 and PHY-1436680

Outline

- Proton form factors in the context of one-photon exchange (OPE)
- The limit of OPE or:
 - What is G_E^p ?
 - What is the nature of lepton scattering?
- Two-photon exchange (TPE): New observables
- Current and future experiments to probe TPE
→ OLYMPUS & more
- Latest Review:
A. Afanasev, P.G. Blunden, D. Hasell, and B.A. Raue, *PPNP* 95, 245 (2017)



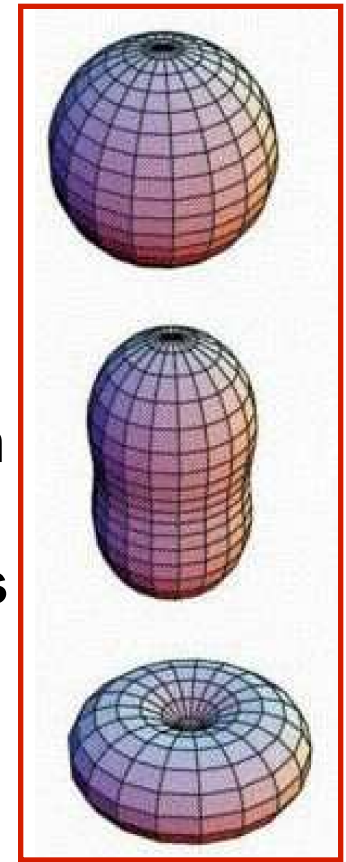
OLYMPUS @ DESY

Nucleon elastic form factors ...

- Fundamental quantities
- Defined in context of single-photon exchange
- Describe internal structure of the nucleons
- Related to spatial distribution of charge and magnetism
- Rigorous tests of nucleon models
- Determined by quark structure of the nucleon
- Role of orbital angular momentum and diquark correlation
- Ultimately calculable by Lattice-QCD
- Input to nuclear structure and parity violation experiments

60+ years of ever increasing activity

- Considerable progress in experiment and theory over last two decades
- New techniques / polarization experiments
- Unexpected results



G. Miller,
PRC68, 022201 (2003)

Recent proton FF, TPE, and PR experiments

Recoil polarization and polarized target (Jlab)

- E04-108 – high-Q² recoil polarization (GEp-III) – published (2010+2017)
- E04-019 – ϵ dependence of recoil pol. (2-Gamma) – published (2011+2017)
- E08-007 – part I: low-Q² recoil polarization – published (2011)
- E08-007 – part II: low-Q² polarized target – analysis in progress
- E07-003 – high-Q² polarized target (SANE) – to be published
- E12-07-109 – high Q² recoil pol. (GEp-V/SBS) – in preparation

Unpolarized cross sections (Jlab)

- E05-017 – high-Q² Rosenbluth (Super-Rosen) – first results, to be published
- E12-07-108 – high-Q² unpolarized (GMp) – first results, to be published

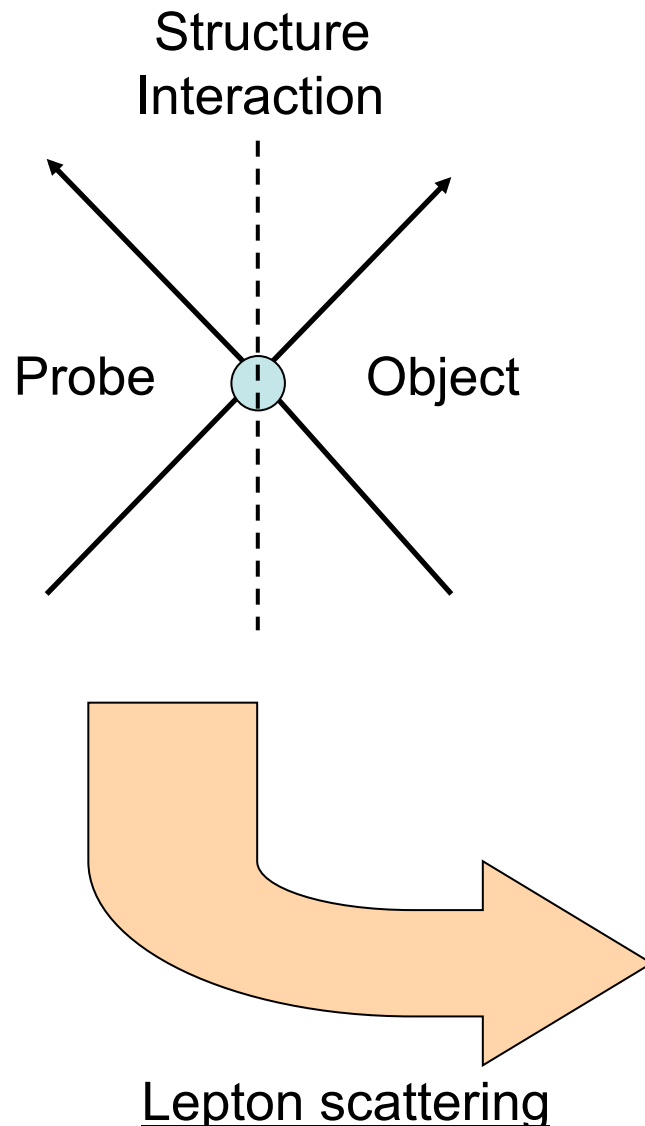
Positron-electron comparisons

- Novosibirsk/VEPP-3 – published (2015)
- CLAS/JLab – published (2015+2017)
- OLYMPUS/DESY – published (2017)

Proton radius measurements

- MAMI / A1 (e-scattering) – published (2010+2014)
- MAMI / A1 (ISR) – published (2017), t.b. cont'd
- MAMI / A2 (TPC); MESA / MAGIX – in preparation
- Jlab / PRad @ CEBAF (e-scattering) – analysis in progress
- Orsay / ProRad @ PRAE; Sendai (Tohoku U.) – in preparation
- PSI / MUSE @ piM1 (e \pm , $\mu\pm$ scattering) – in preparation
- CERN / COMPASS @ SPS ($\mu\pm$ scattering) – in preparation

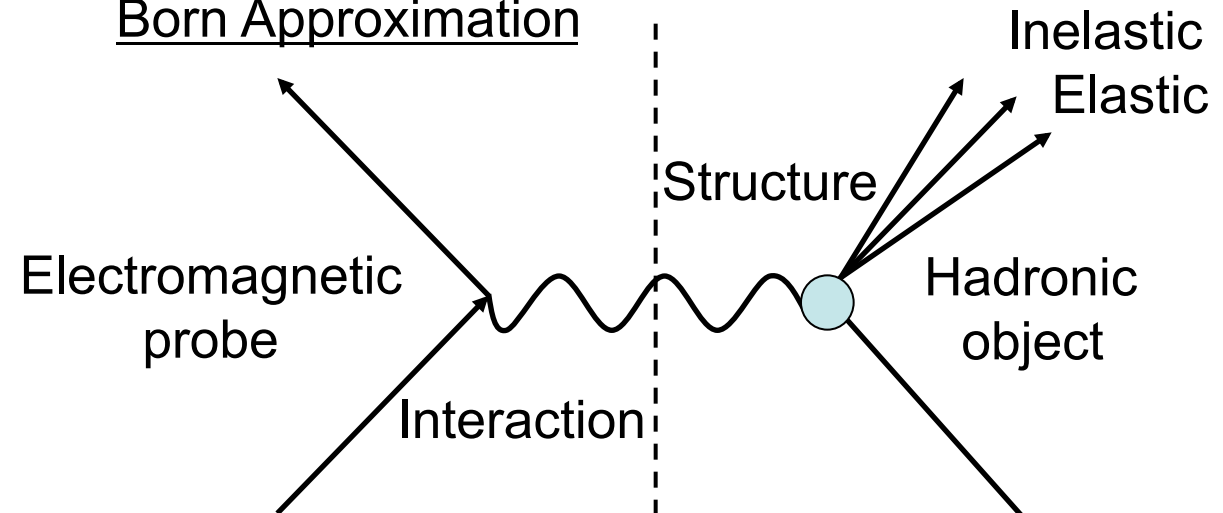
Hadronic structure and EM interaction



Factorization!

$$|\text{Form factor}|^2 = \frac{\sigma(\text{structured object})}{\sigma(\text{pointlike object})}$$

Born Approximation



One-Photon Exchange Approximation

The beginnings

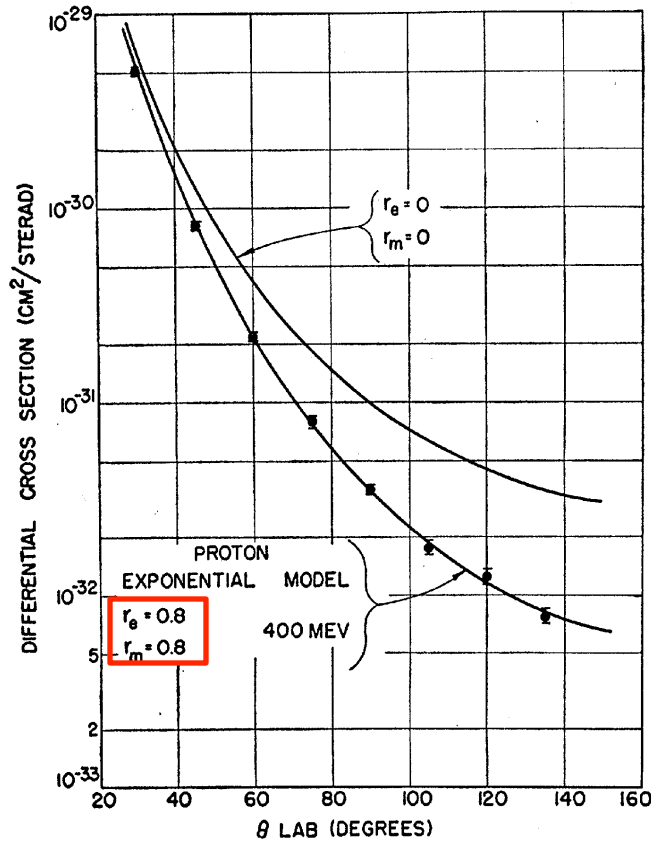


FIG. 26. Typical angular distribution for elastic scattering of 400-Mev electrons against protons. The solid line is a theoretical curve for a proton of finite extent. The model providing the theoretical curve is an exponential with rms radii = 0.80×10^{-13} cm.

R. Hofstadter, Rev. Mod. Phys. 56 (1956) 214

ed-elastic
Finite size + nuclear structure

Robert Hofstadter
Nobel prize 1961

ep-elastic
finite size of the proton
 $R_p \sim 0.8 \text{ fm}$

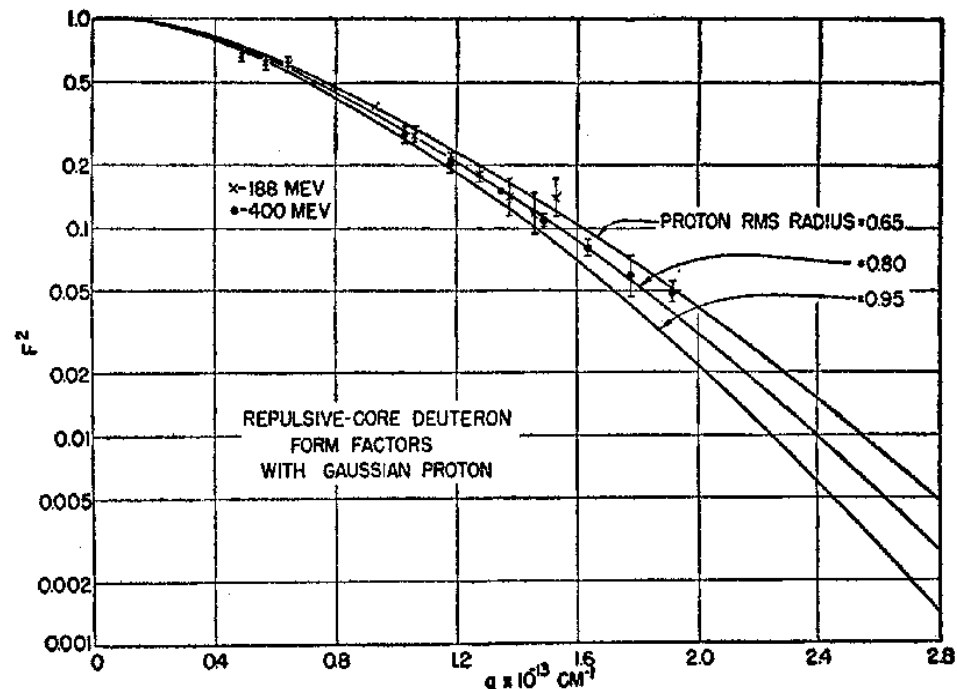
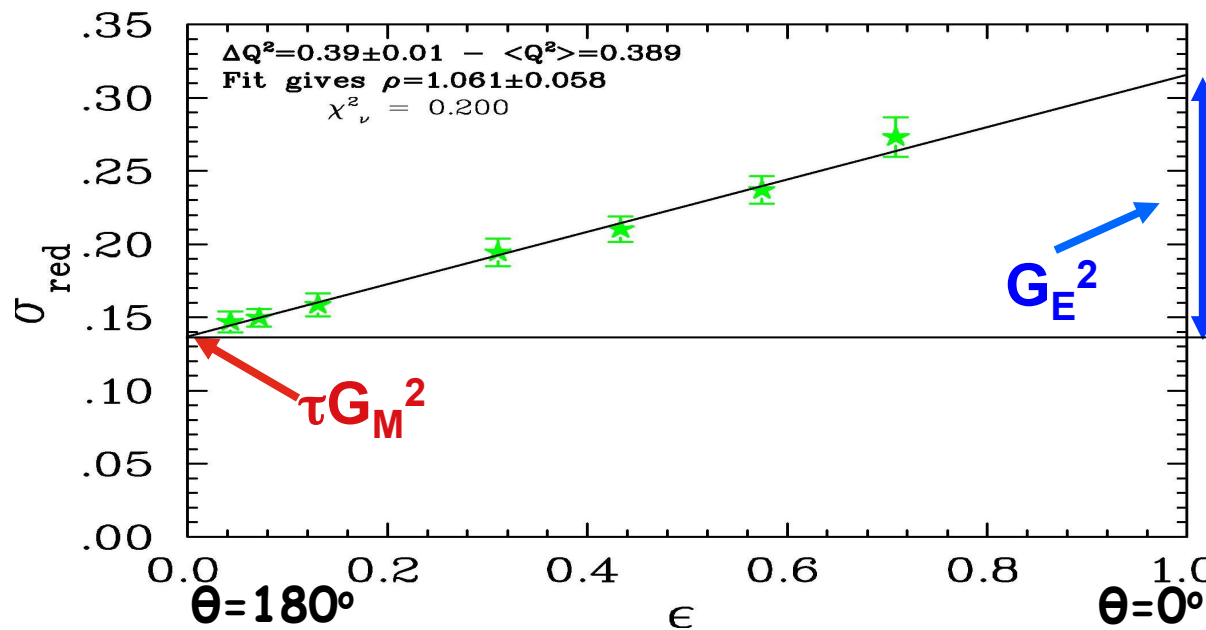


FIG. 31. Introduction of a finite proton core allows the experimental data to be fitted with conventional form factors (McIntyre).

Form factors from Rosenbluth method



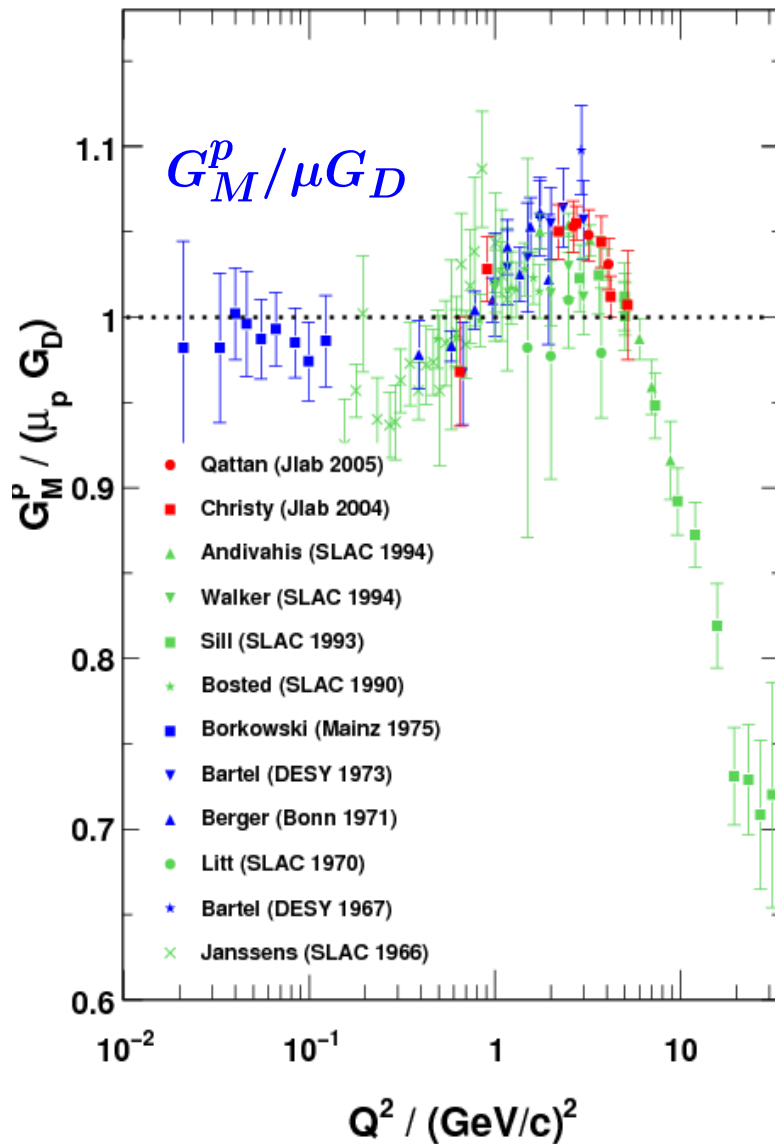
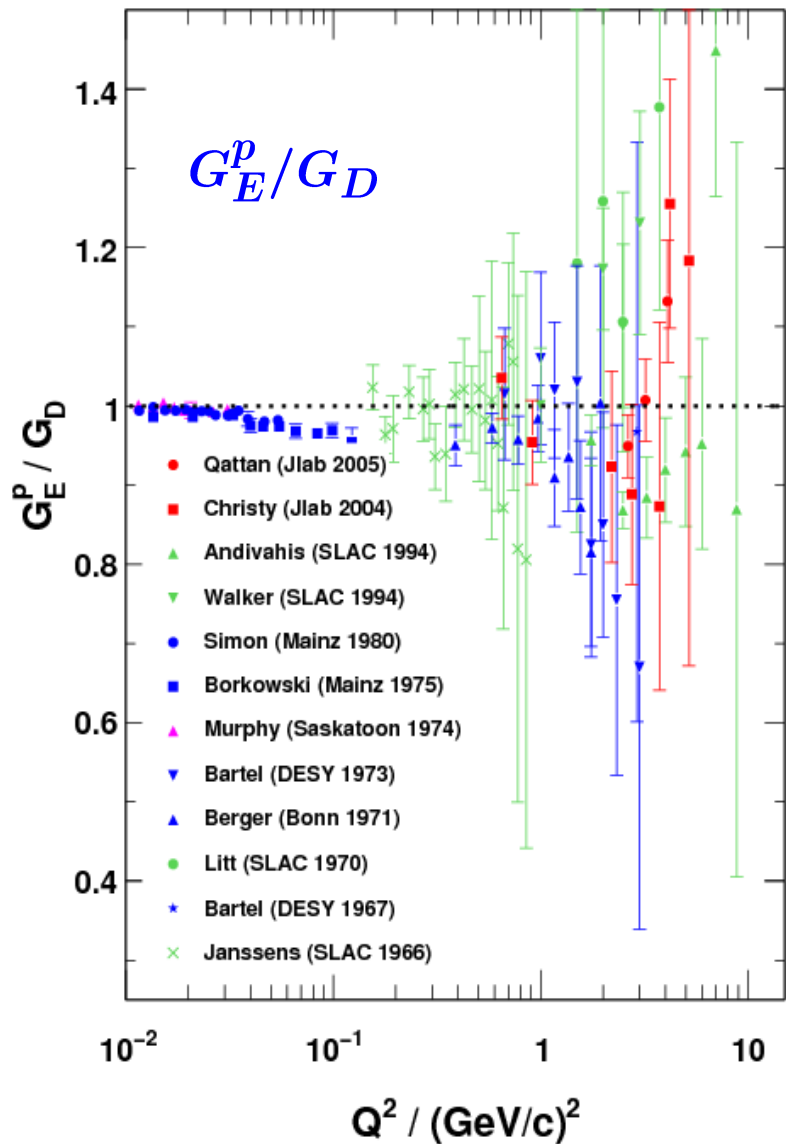
$$\sigma_{\text{red}} = \epsilon G_E^2 + \tau G_M^2$$

→ Determine
 $|G_E|$, $|G_M|$,
 $|G_E/G_M|$

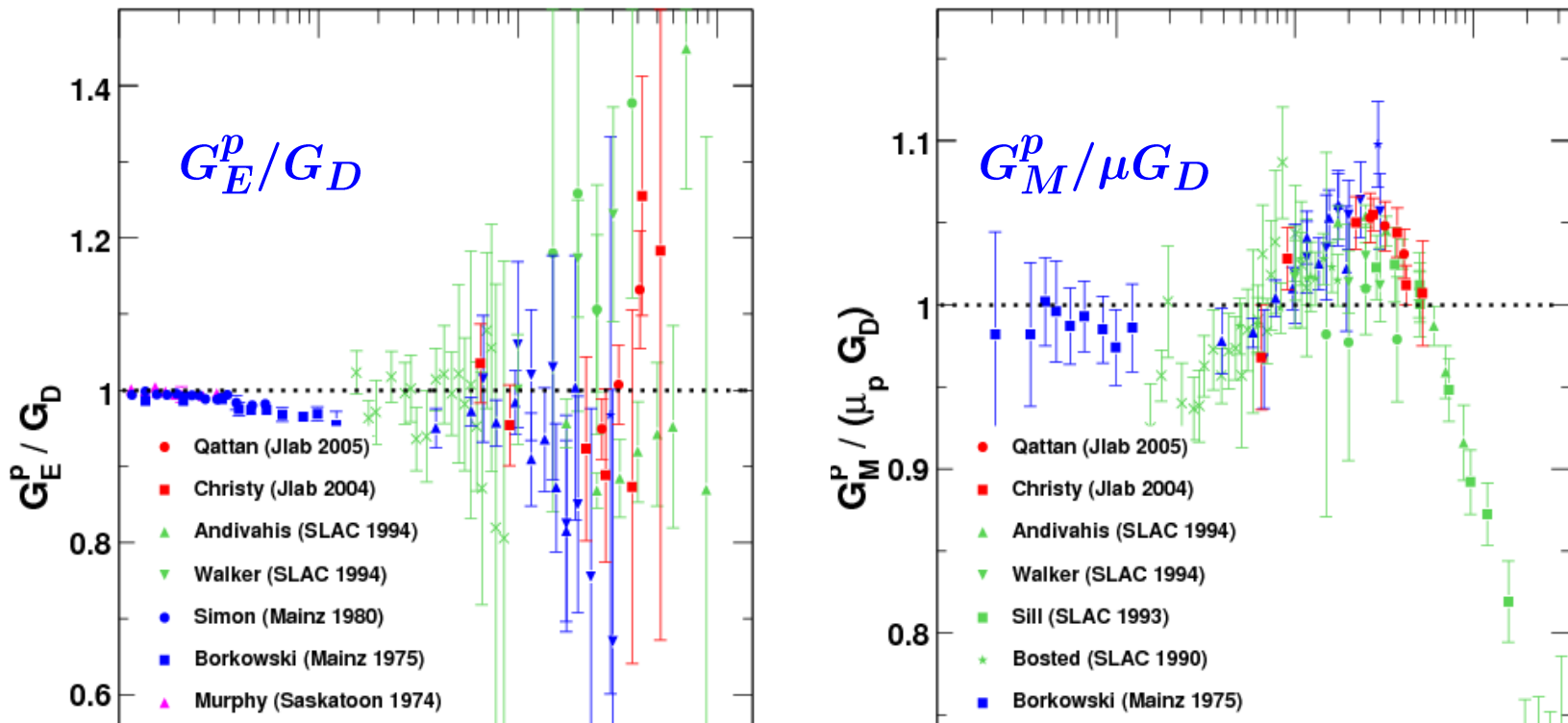
- In One-photon exchange, form factors are related to radiatively corrected elastic electron-proton scattering cross section

$$\begin{aligned}
 \frac{d\sigma/d\Omega}{(d\sigma/d\Omega)_{Mott}} &= S_0 = A(Q^2) + B(Q^2) \tan^2 \frac{\theta}{2} \\
 &= \frac{G_E^2(Q^2) + \tau G_M^2(Q^2)}{1 + \tau} + 2\tau G_M^2(Q^2) \tan^2 \frac{\theta}{2} \\
 &= \frac{\epsilon G_E^2 + \tau G_M^2}{\epsilon (1 + \tau)}, \quad \epsilon = \left[1 + 2(1 + \tau) \tan^2 \frac{\theta}{2} \right]^{-1}
 \end{aligned}$$

G_E^p and G_M^p from unpolarized data



G_E^p and G_M^p from unpolarized data

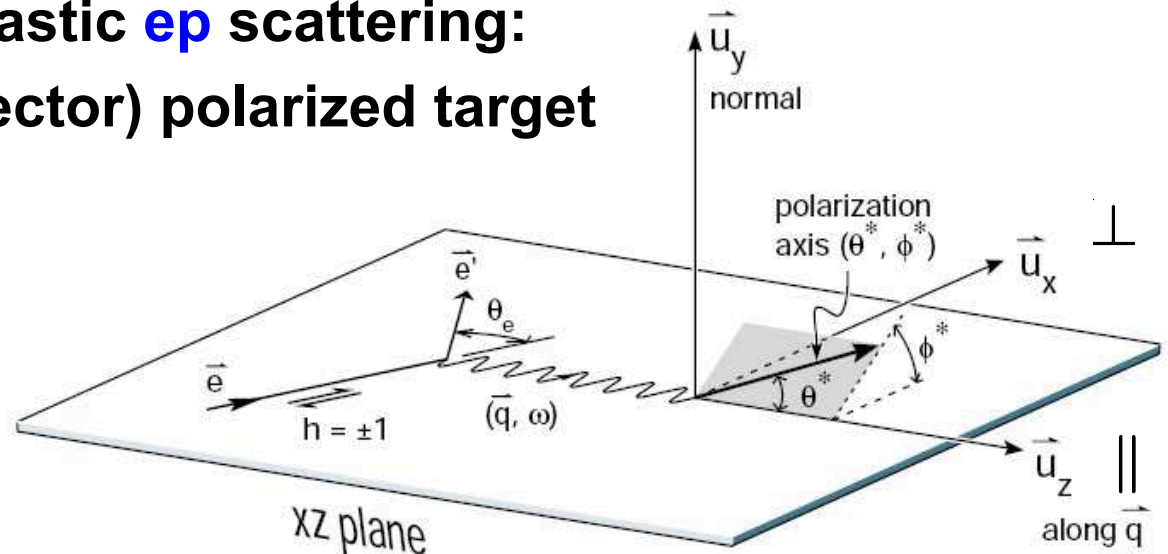


- $G(Q^2)$ $\xleftrightarrow{\text{Fourier}}$ $\rho(r)$ charge and magnetization density (Breit fr.)
- Dipole form factor $G_D = \frac{1}{\left(1 + \frac{Q^2}{0.71}\right)^2}$ \leftrightarrow $\rho_D(r) = \rho_0 e^{-\sqrt{0.71}r}$
- $G_E^p \approx G_M^p / \mu_p \approx G_M^n / \mu_n \approx G_D$ within 10% for $Q^2 < 10$ (GeV/c) 2

Nucleon form factors and polarization

- Double polarization in elastic $e p$ scattering:
Recoil polarization or (vector) polarized target

$$^1H(\vec{e}, e' \vec{p}), \quad ^1H(\vec{e}, e' p)$$



- Polarized cross section

$$\sigma = \sigma_0 \left(1 + P_e \vec{P}_p \cdot \vec{A} \right)$$

- Double polarization observable = spin correlation

$$-\sigma_0 \vec{P}_p \cdot \vec{A} = \sqrt{2\tau\epsilon(1-\epsilon)} G_E G_M \sin \theta^* \cos \phi^* + \tau \sqrt{1-\epsilon^2} G_M^2 \cos \theta^*$$

- Asymmetry ratio (“Super ratio”)

independent of
polarization or analyzing power

$$\frac{P_{\perp}}{P_{\parallel}} = \frac{A_{\perp}}{A_{\parallel}} \propto \frac{G_E}{G_M}$$

Dombey (1969)
Donnelly and Raskin (1986)

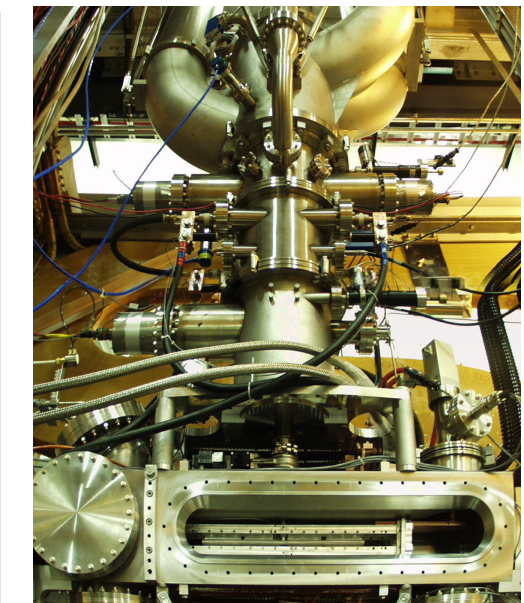
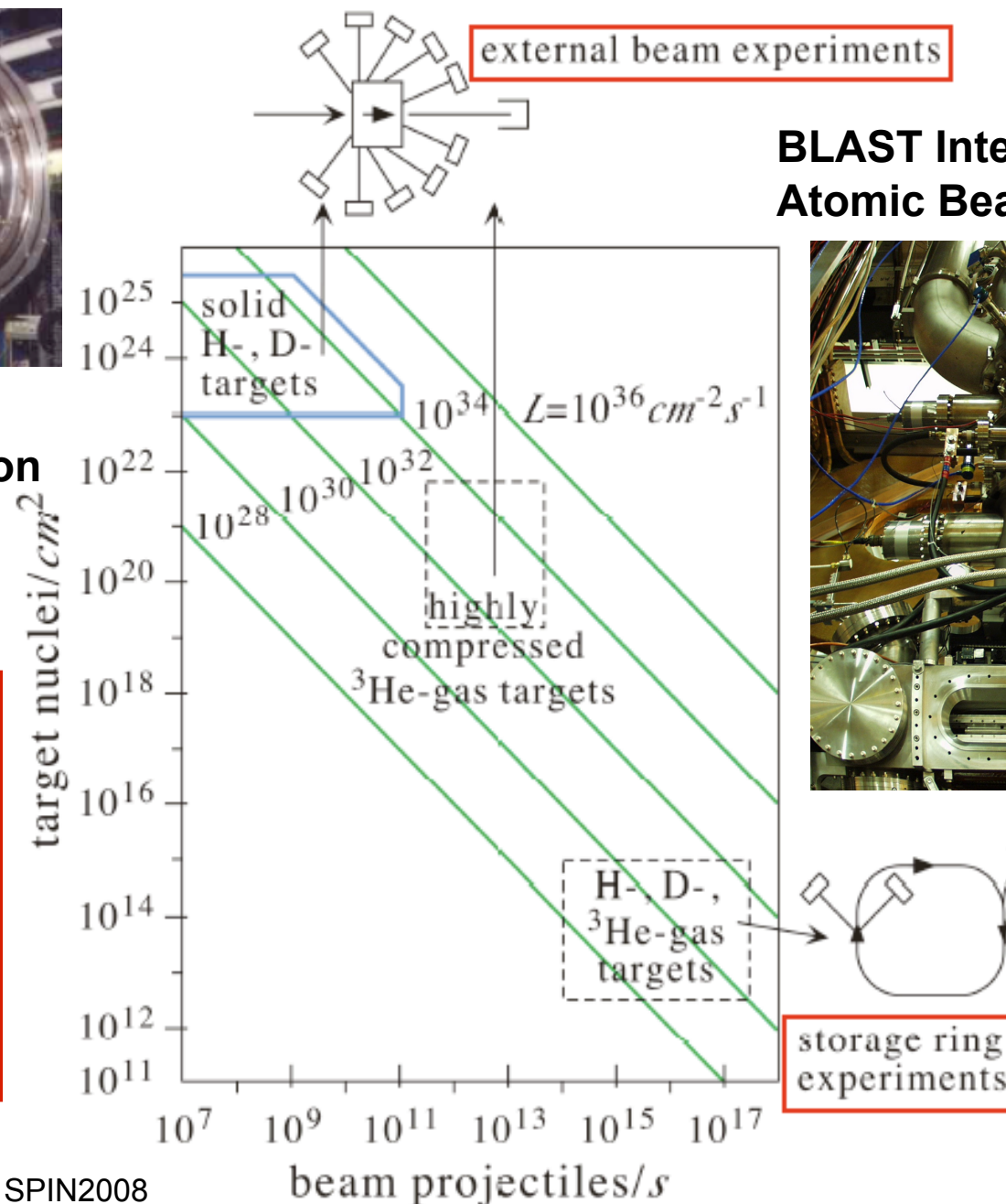
Polarized targets



**UVA / "SLAC"-Target:
Dynamic Nuclear Polarization**

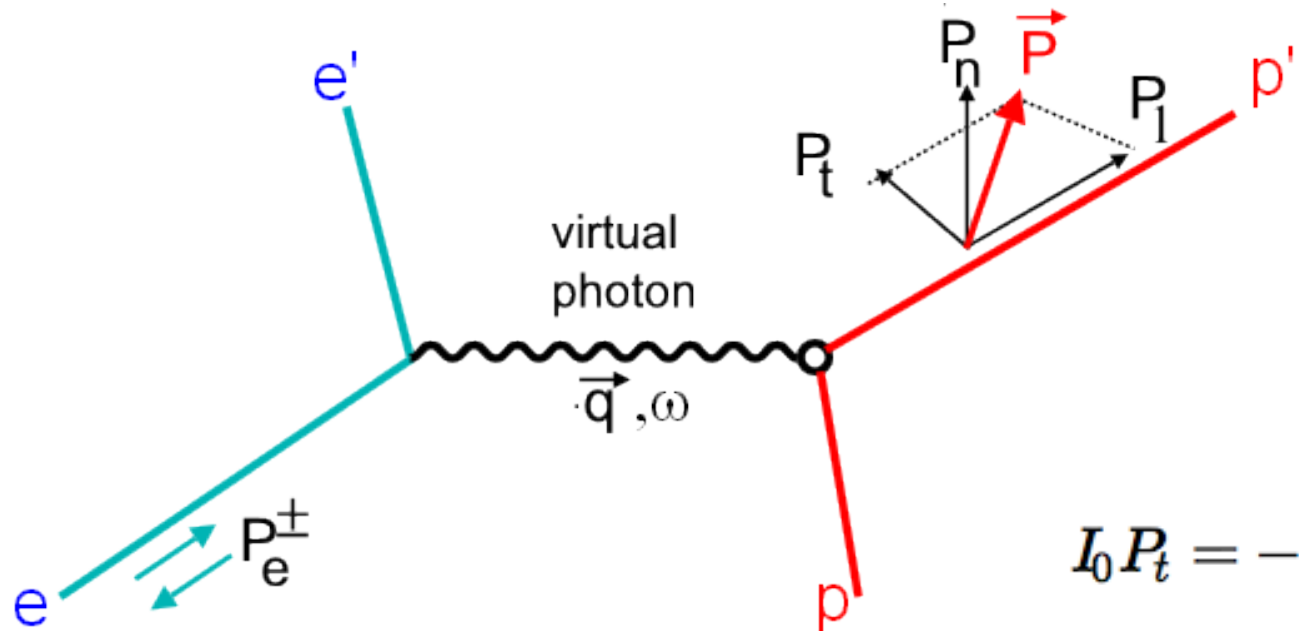
**Limited luminosity for
polarized hydrogen/
deuterium targets**

**Very precise at low to
moderately high Q^2**



**BLAST Internal Target:
Atomic Beam Source**

Recoil polarization technique



$$I_0 P_t = -2 \sqrt{\tau(1+\tau)} G_E G_M \tan \frac{\theta_e}{2}$$

$$I_0 P_\ell = \frac{1}{M} (E_e + E'_e) \sqrt{\tau(1+\tau)} G_M^2 \tan^2 \frac{\theta_e}{2}$$

$$\frac{G_E}{G_M} = -\frac{P_t}{P_\ell} \frac{(E_e + E'_e)}{2M_p} \tan\left(\frac{\theta_e}{2}\right)$$

$$I_0 \propto G_E^2 + \frac{\tau}{\epsilon} G_M^2$$

Applicable to protons and neutrons

Akhiezer and Rekalo (1968+1974)
Arnold, Carlson and Gross (1981)

Recoil polarization technique

- Pioneered at MIT-Bates
- Pursued in Halls A and C, and MAMI A1
- In preparation for Jlab @ 12 GeV

V. Punjabi *et al.*,
Phys. Rev. C 71, 05520 (2005)

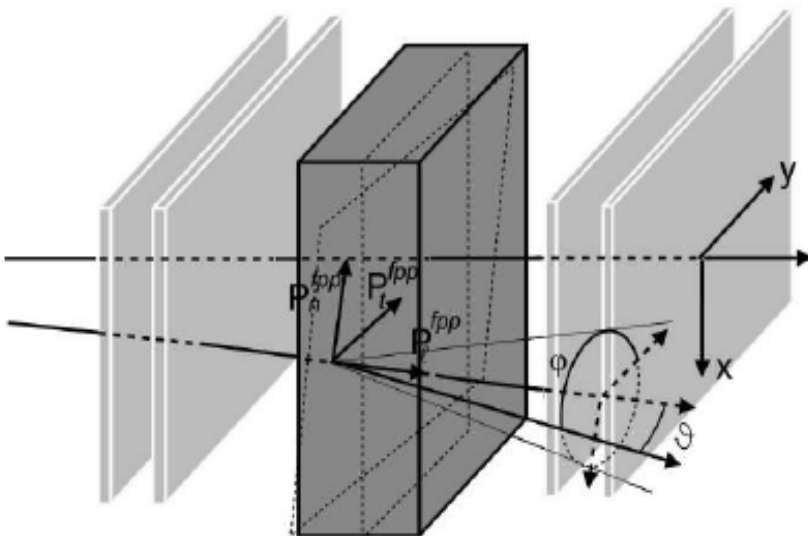


FIG. 9: Schematic of the polarimeter chambers and analyzer, showing a non-central trajectory; ϑ is the polar angle, and φ is the azimuthal angle from the y -direction counterclockwise.

Focal-plane polarimeter

Secondary scattering of polarized proton from unpolarized analyzer
requiring polarization in transverse plane

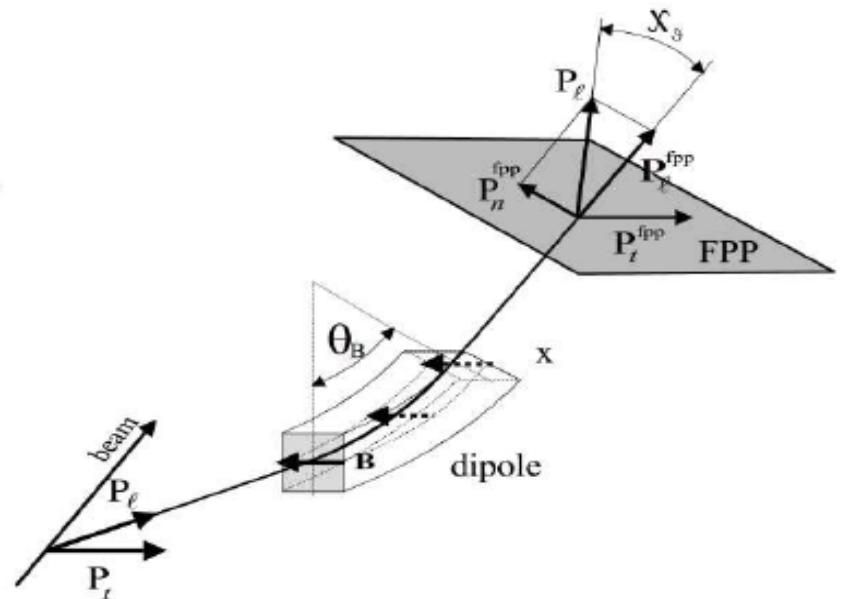
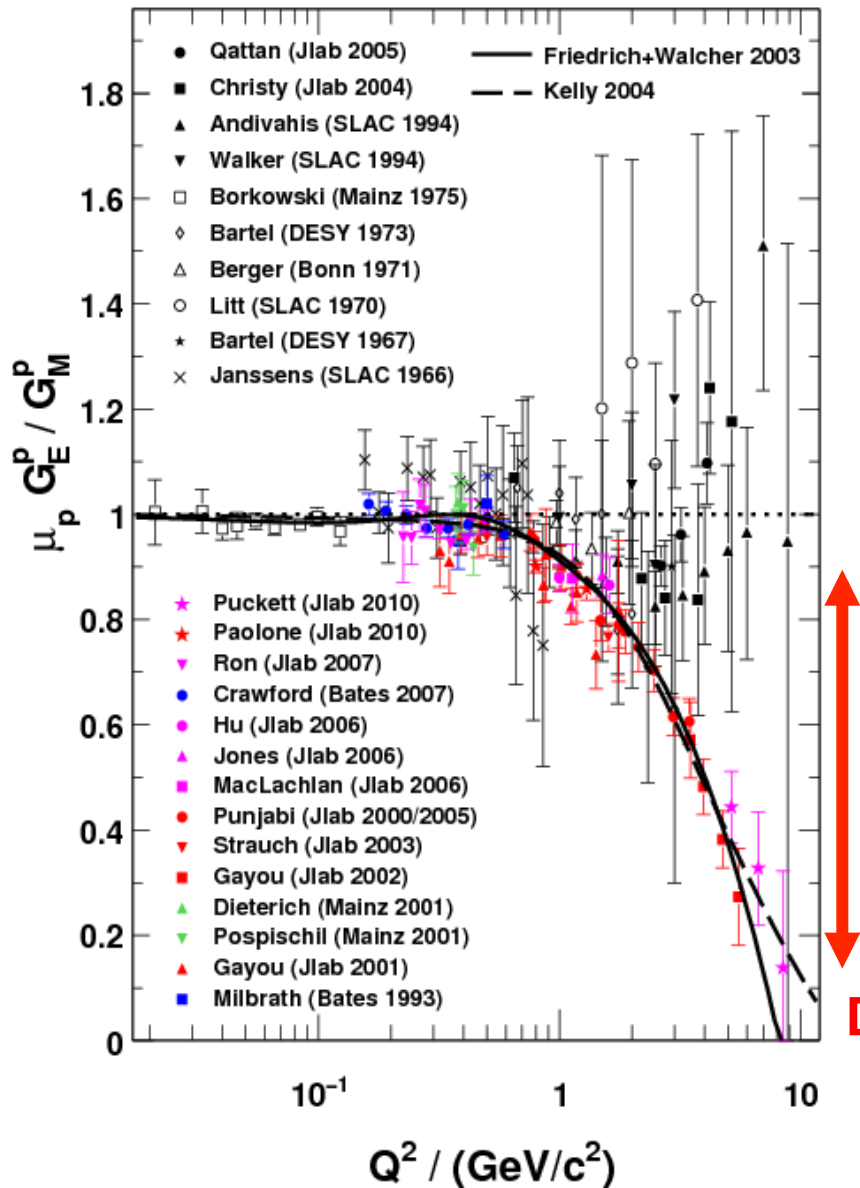


FIG. 15: Schematic drawing showing the precession by angle χ_θ of the P_e component of the polarization in the dipole of the HRS.

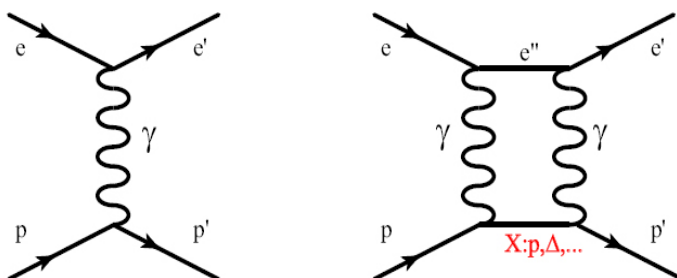
Spin transfer formalism to account for spin precession through spectrometer required to measure longitudinal polariz.

Proton form factor ratio



Jefferson Lab 2000–

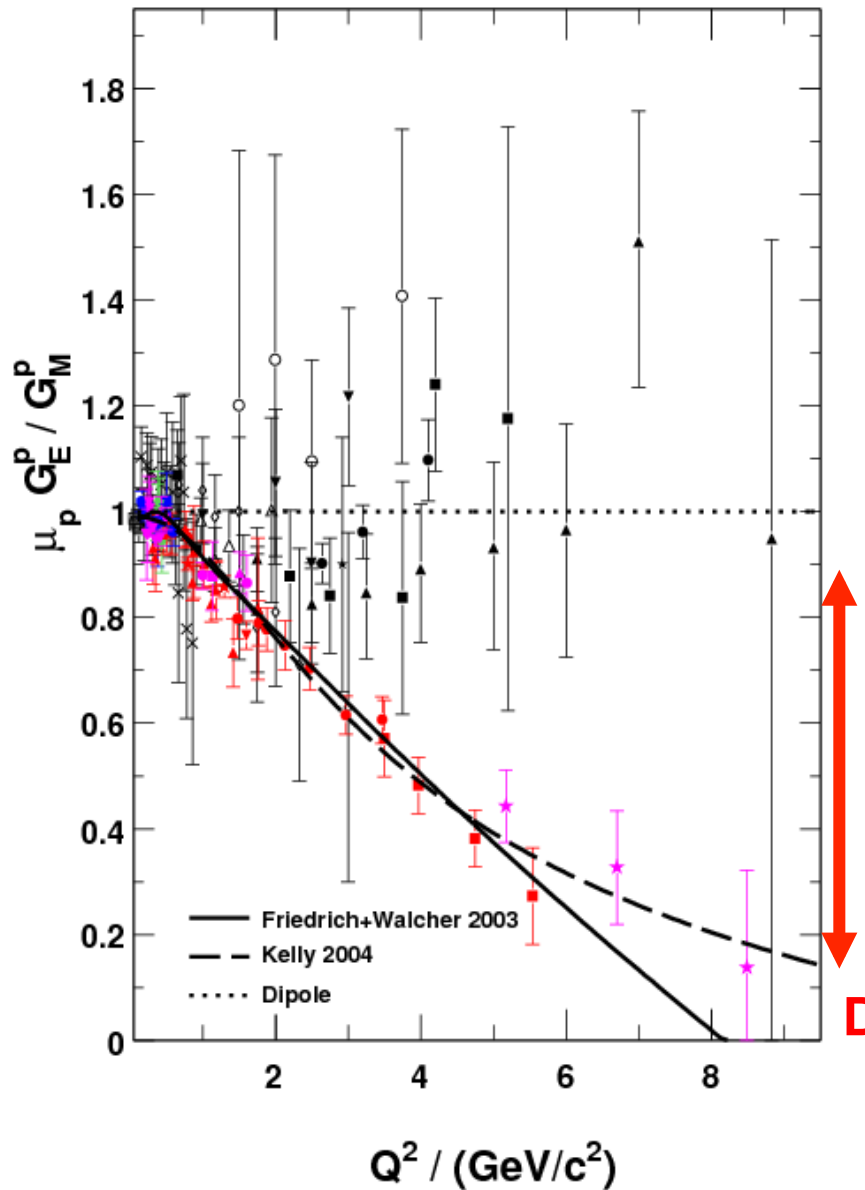
- All Rosenbluth data from SLAC and Jlab in agreement
- Dramatic discrepancy between Rosenbluth and recoil polarization technique
- Multi-photon exchange considered best candidate



Dramatic discrepancy!

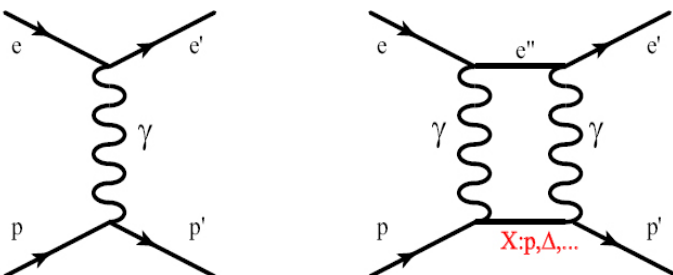
>800 citations

Proton form factor ratio



Jefferson Lab 2000–

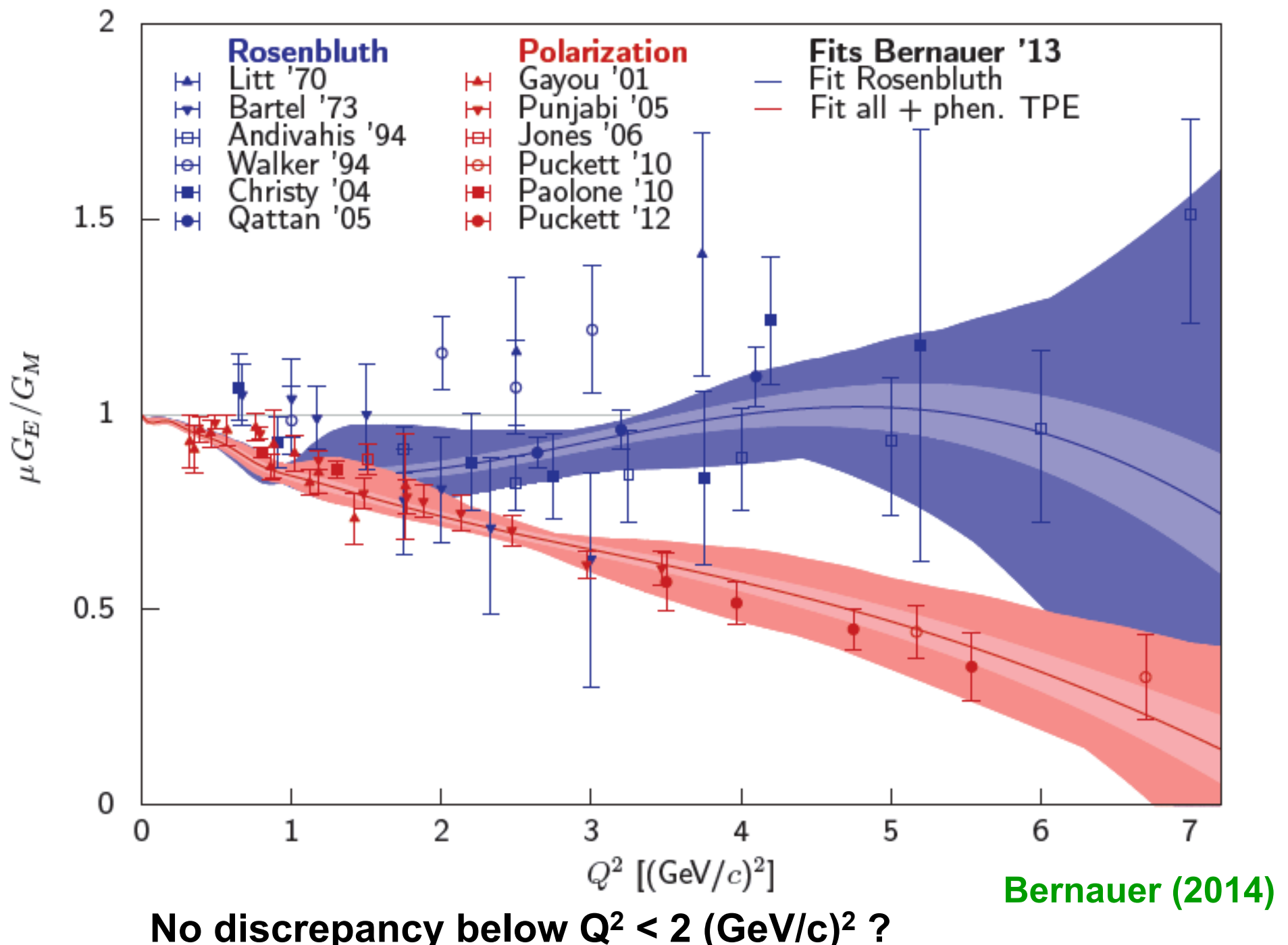
- All Rosenbluth data from SLAC and Jlab in agreement
- Dramatic discrepancy between Rosenbluth and recoil polarization technique
- Multi-photon exchange considered best candidate



Dramatic discrepancy!

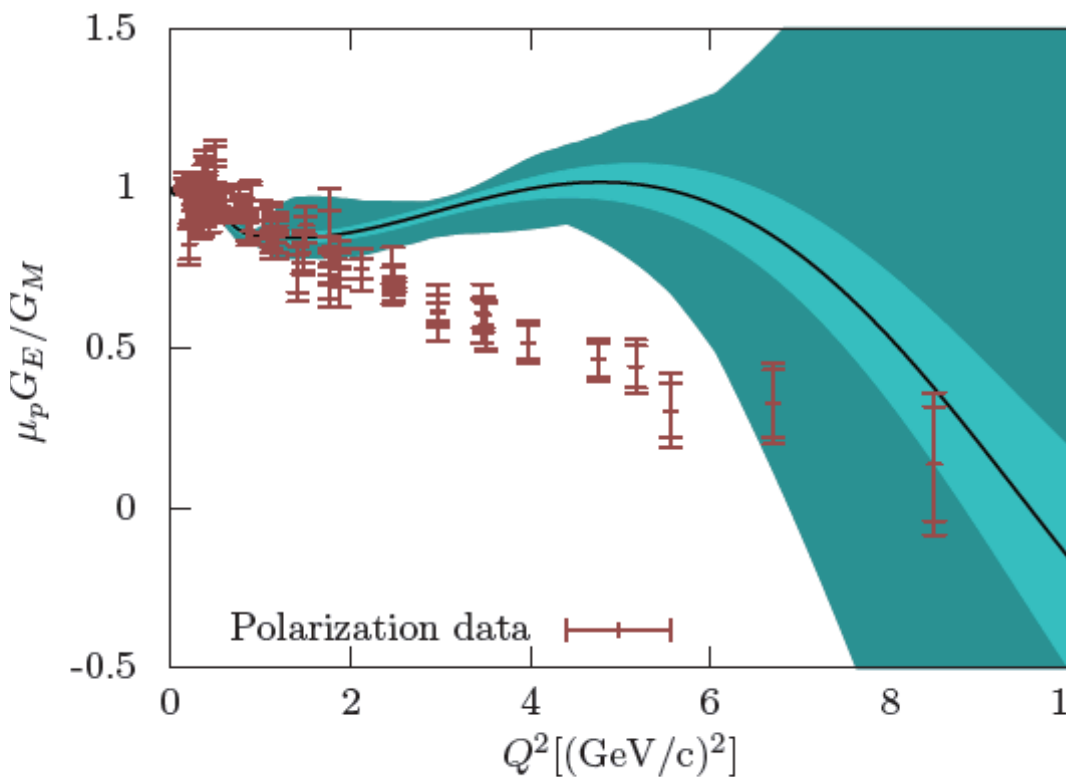
>800 citations

Another look

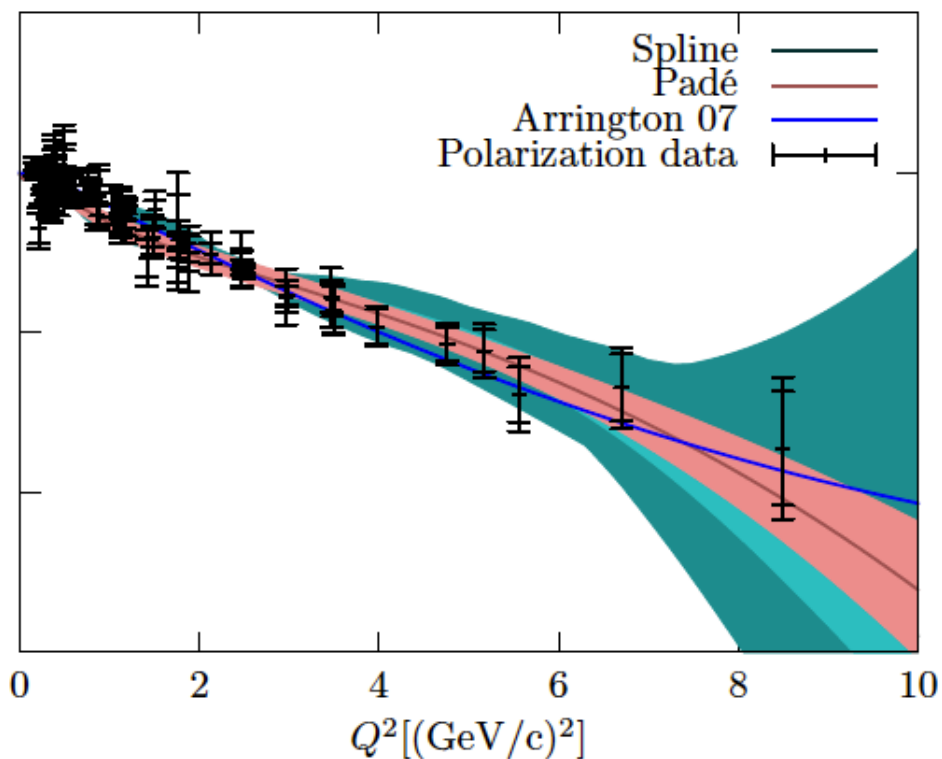


Global analysis

Fit to unpolarized data

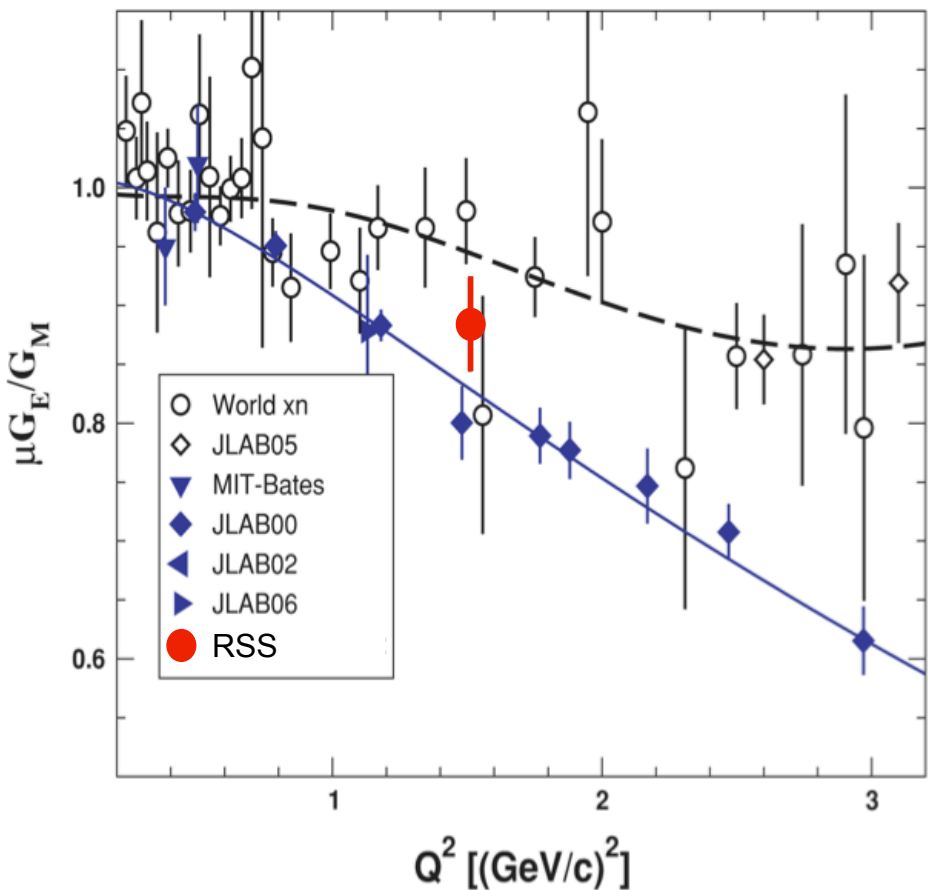


Fit including polarized data
+ TPE parameterization



J.C. Bernauer *et al.*, PRC 90, 015206 (2014) [arXiv:1307.6227v2]

Polarized target data at high Q^2



Polarized Target:

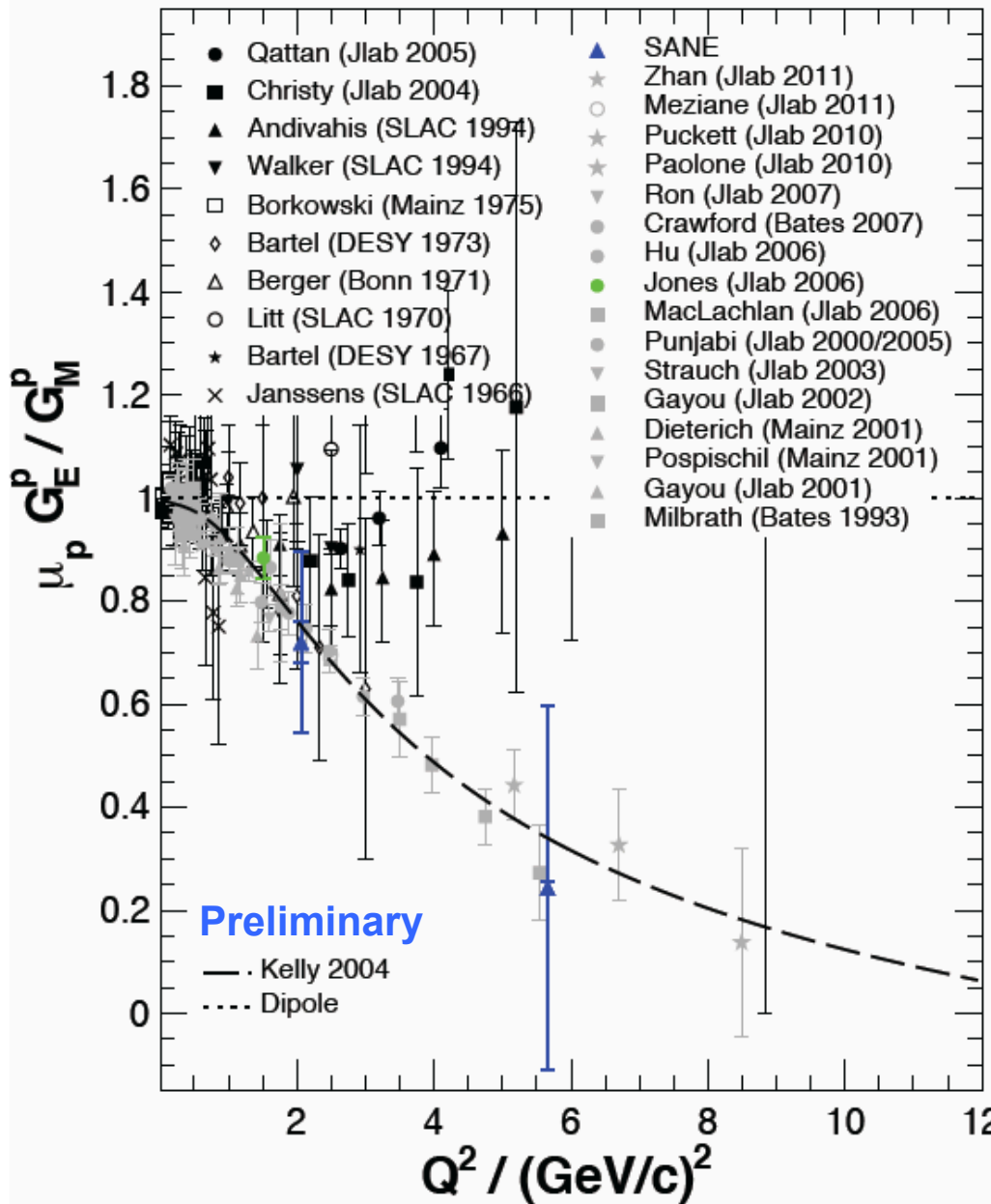
Independent verification of recoil polarization result is crucial

Polarized internal target / low Q^2 : **BLAST**
 $Q^2 < 0.65 \text{ (GeV}/c)^2$ not high enough to see deviation from scaling

RSS /Hall C: $Q^2 \approx 1.5 \text{ (GeV}/c)^2$

M.K. Jones *et al.*, PRC74, 035201 (2006)

Polarized target data at high Q^2



Polarized Target:

Independent verification of recoil polarization result is crucial

Polarized internal target / low Q^2 : **BLAST**
 $Q^2 < 0.65 \text{ (GeV/c)}^2$ not high enough to see deviation from scaling

RSS /Hall C: $Q^2 \approx 1.5 \text{ (GeV/c)}^2$

SANE/Hall C: completed March 2009
BigCal electron detector
Recoil protons in HMS parasitically
 G_E/G_M at $Q^2 \approx 2.1$ and 5.7 (GeV/c)^2

Decline of G_E/G_M has been confirmed!

Future precision measurements at high Q^2 are feasible

New unpolarized data at high Q^2

- **GMp (E12-07-108):**

Magnetic form factor of the proton at high Q^2 (cross section)

Scattered electron detection (single-arm)

Data taking completed in 2016

Preliminary results available

Final results by fall 2018

- **Super-Rosen (E05-017):**

High- Q^2 Rosenbluth separation up to $Q^2 < 5.7 \text{ (GeV/c)}^2$

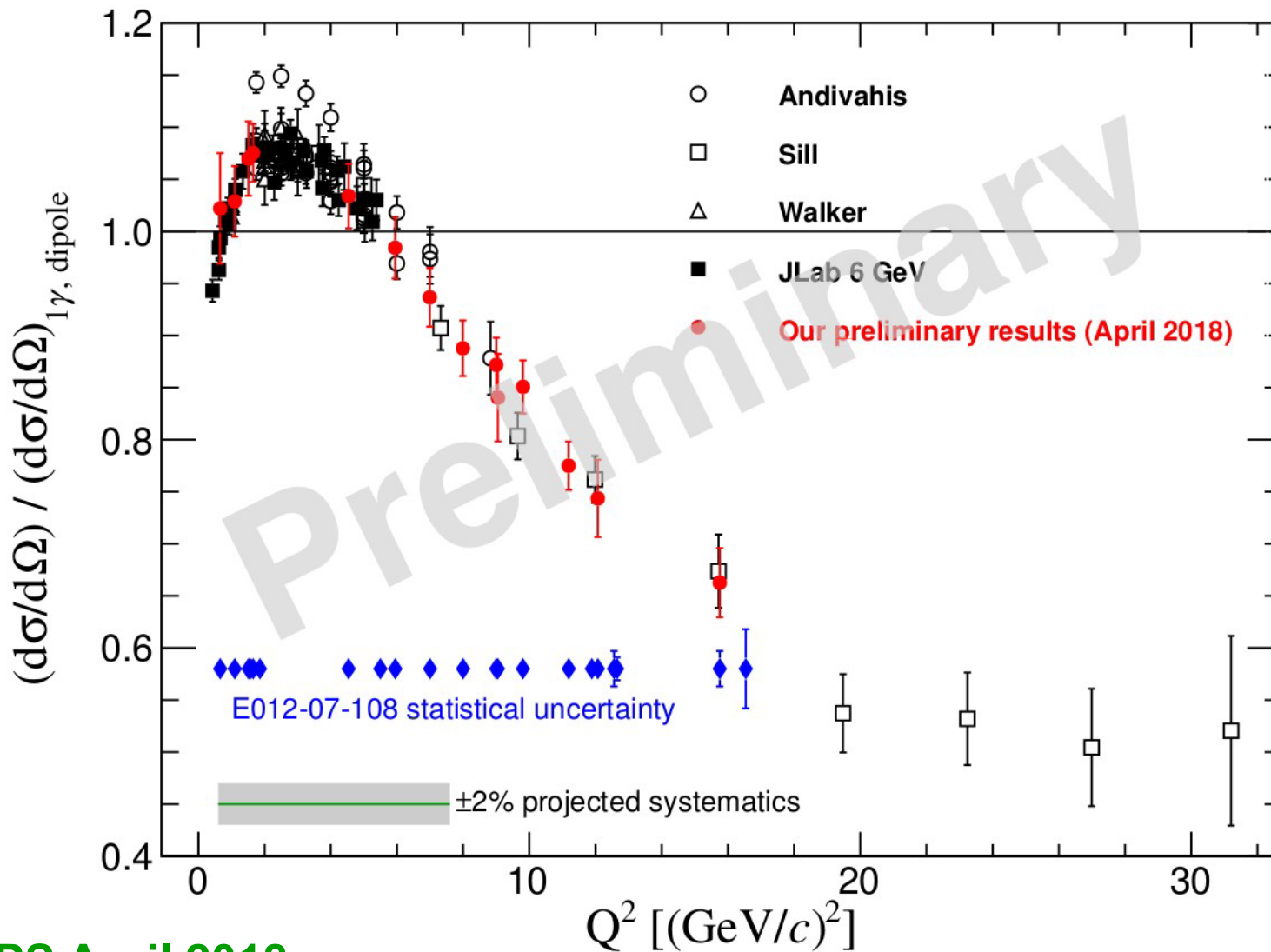
Recoil proton detection (single-arm)

Preliminary results available

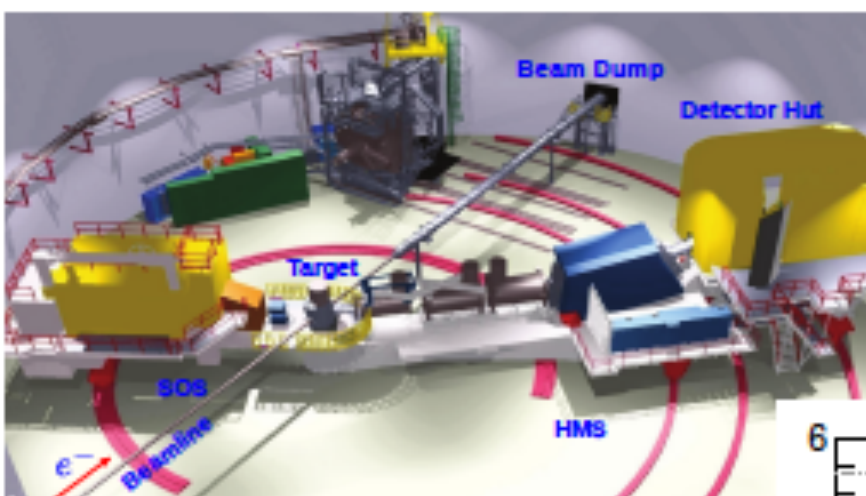
GMP (E12-07-108) at high Q^2

- Preliminary cross-section results are presented below with 5% total uncertainty
- Final results will be available by fall 2018 with <2% systematic uncertainty

JLab E012-07-108, e - p elastic cross section



E05-017 HALL C, JLAB



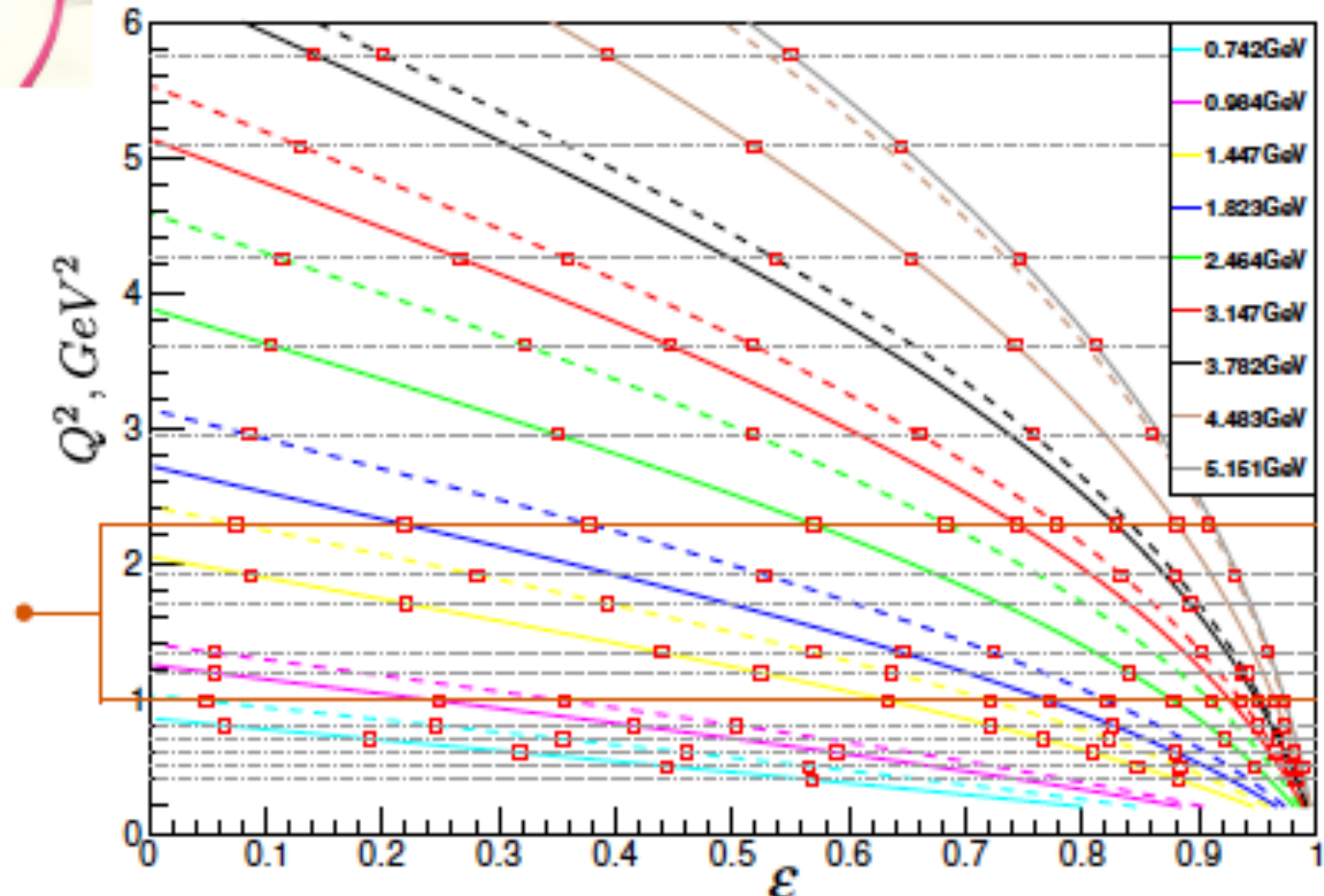
Experimental Hall C Layout

102 Kinematics points

10 points at $Q^2 = 2.284$

13 points at $Q^2 = 0.983$

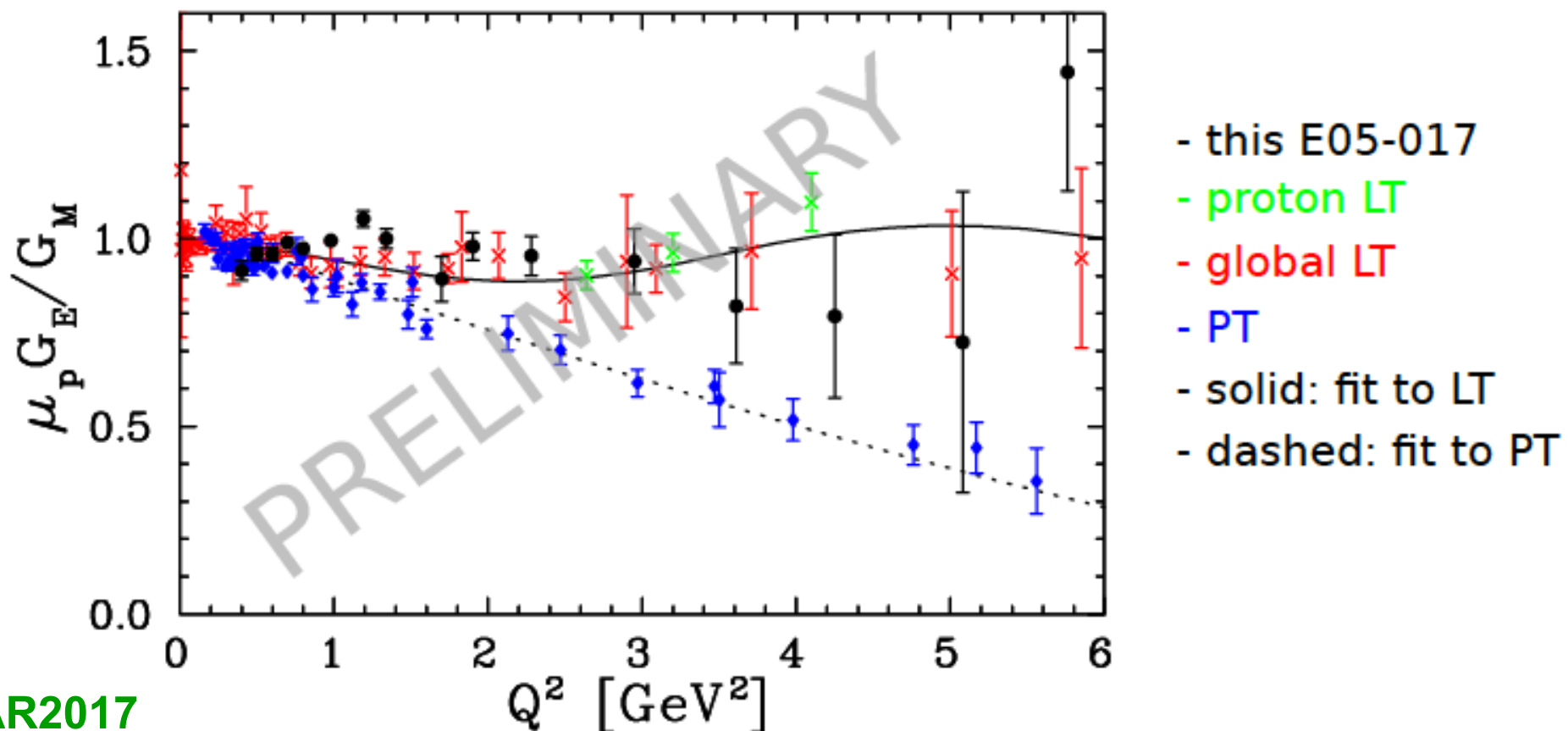
- 4 cm LH₂ and dummy targets
- recoil proton detected in HMS
- 17 settings of beam energy



NSTAR2017

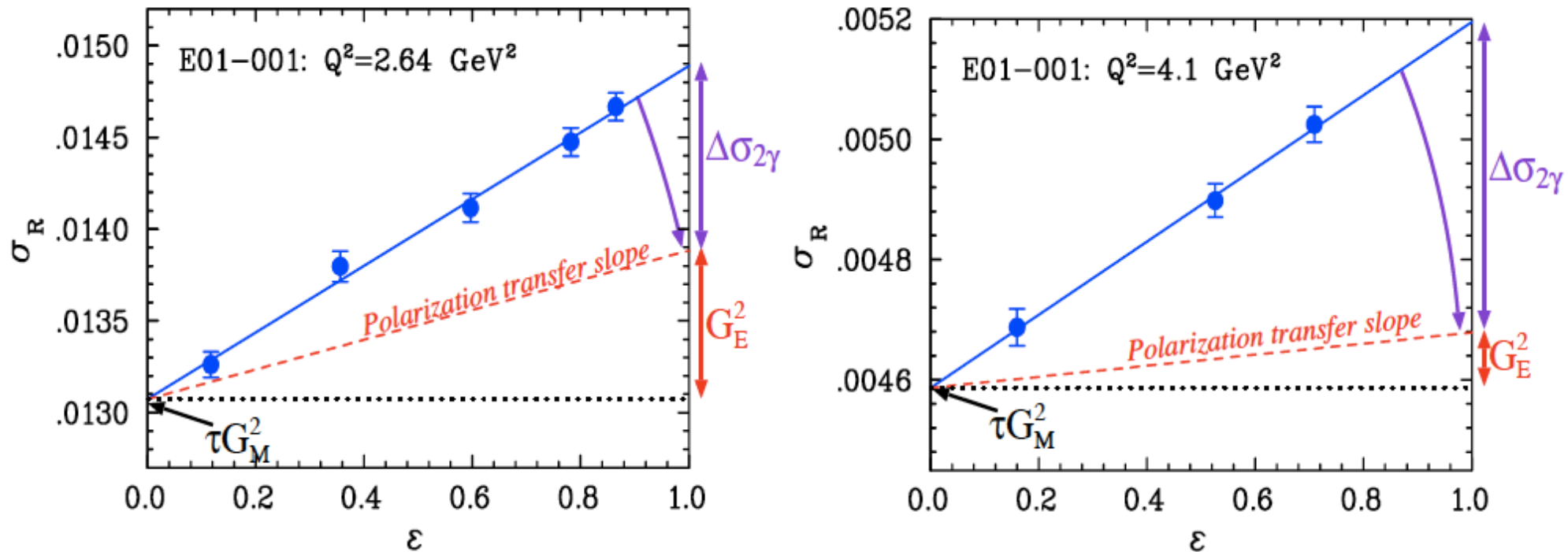
PRELIMINARY RESULTS

- $\mu_p G_E/G_M$ extraction:
 - from analysis that focused on low Q^2 settings
- expected uncertainty reduction:
 - slope by factor of 2 everywhere
 - point-to-point by factor 1.3 at $Q^2 < 2$ and by 1.5 above



Effect of two-photon exchange

J. Arrington, P. Blunden, W. Melnitchouk, Prog. Part. Nucl. Phys. 66, 782 (2011)



By construction, theorists sought mechanism that affects the “slope” in the Rosenbluth plot (ε -dependence)

At high Q^2 , the contribution of G_E to the cross section is of similar order as the TPE effect (few %)

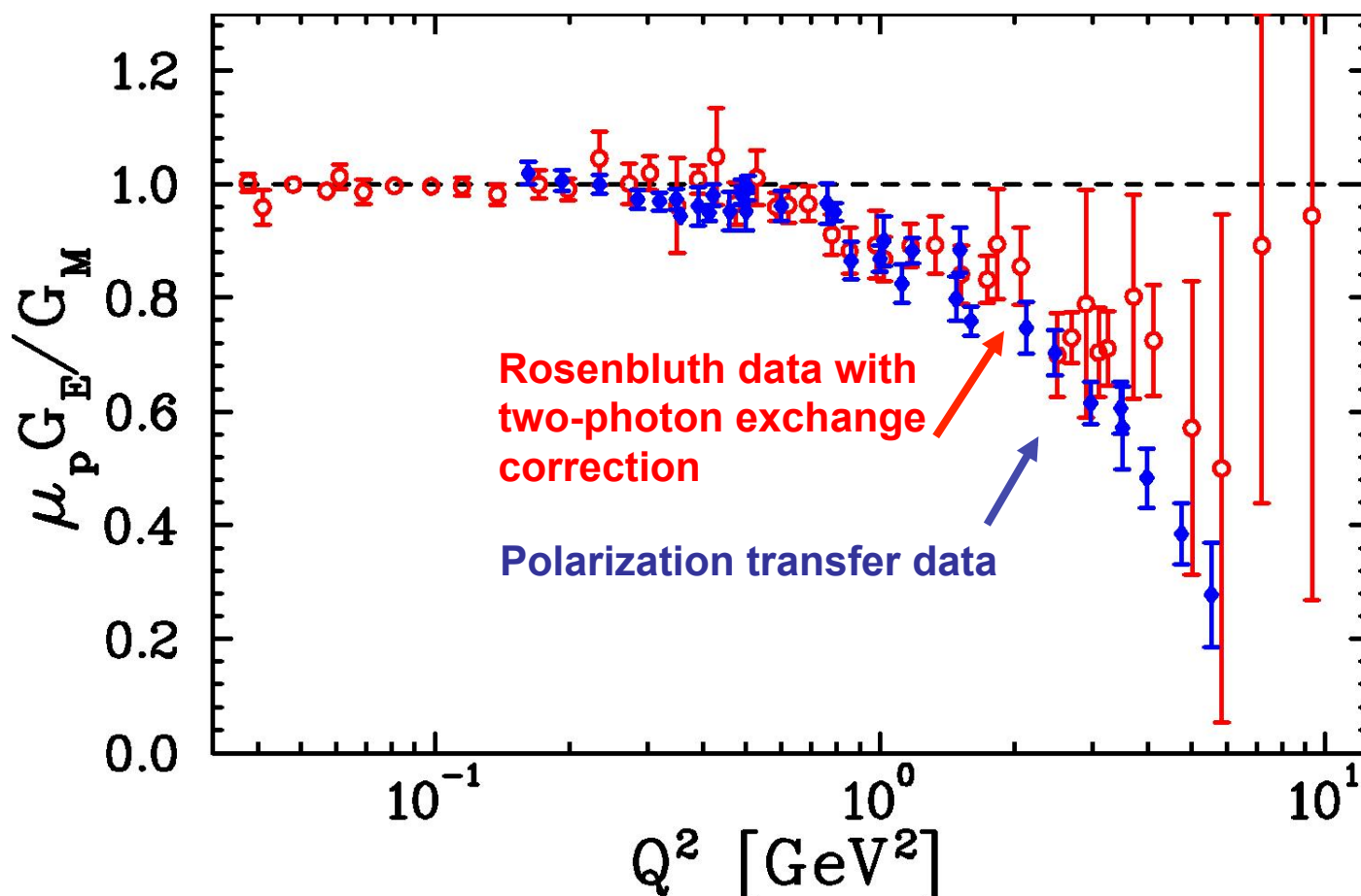
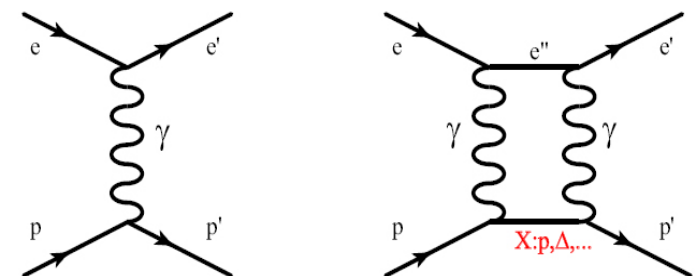
Two-photon exchange: exp. evidence

Two-photon exchange theoretically suggested

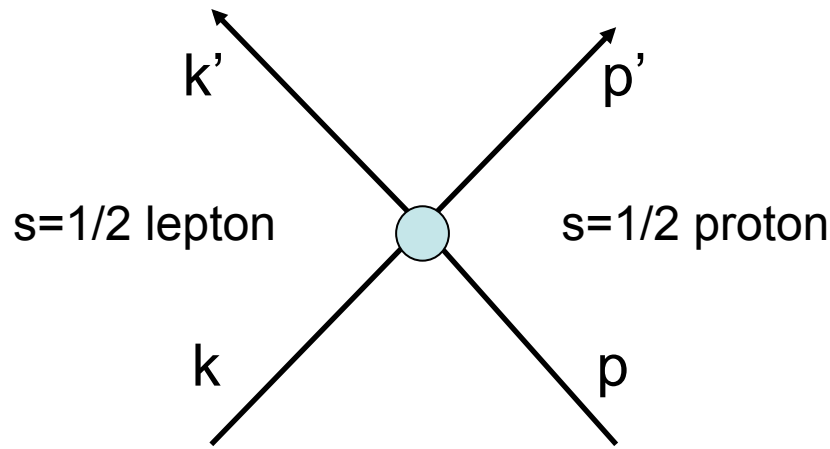
TPE can explain form factor discrepancy

J. Arrington, W. Melnitchouk, J.A. Tjon,

Phys. Rev. C 76, 035205 (2007)



Elastic ep scattering beyond OPE



$$P \equiv \frac{p + p'}{2}, \quad K \equiv \frac{k + k'}{2}$$

Kinematical invariants :

$$\begin{aligned} Q^2 &= -(p - p')^2 \\ \nu &= K \cdot P = (s - u)/4 \end{aligned}$$

Next-to Born approximation:

$$\begin{aligned} T_{h' \lambda'_N, h \lambda_N}^{non-flip} &= \frac{e^2}{Q^2} \bar{u}(k', h') \gamma_\mu u(k, h) \\ (\text{m}_e = 0) &\times \bar{u}(p', \lambda'_N) \left(\tilde{G}_M \gamma^\mu - \tilde{F}_2 \frac{P^\mu}{M} + \tilde{F}_3 \frac{\gamma \cdot K P^\mu}{M^2} \right) u(p, \lambda_N) \end{aligned}$$

The T-matrix still factorizes, however a new response term \tilde{F}_3 is generated by TPE
Born-amplitudes are modified in presence of TPE; modifications $\sim \alpha^3$

$$\begin{aligned} \tilde{G}_M(\nu, Q^2) &= G_M(Q^2) + \delta \tilde{G}_M & \tilde{G}_E \equiv \tilde{G}_M - (1 + \tau) \tilde{F}_2 \\ \tilde{F}_2(\nu, Q^2) &= F_2(Q^2) + \delta \tilde{F}_2 & \tilde{G}_E(\nu, Q^2) = G_E(Q^2) + \delta \tilde{G}_E \\ \tilde{F}_3(\nu, Q^2) &= 0 + \delta \tilde{F}_3 \end{aligned}$$

New amplitudes are complex!

Inherited from M. Vanderhaeghen

Observables involving real part of TPE

$$\begin{aligned}
 P_t &= -\sqrt{\frac{2\varepsilon(1-\varepsilon)}{\tau}} \frac{G_M^2}{d\sigma_{red}} \left\{ R + R \frac{\Re(\delta\tilde{G}_M)}{G_M} + \frac{\Re(\delta\tilde{G}_E)}{G_M} + Y_{2\gamma} \right\} \\
 P_l &= \sqrt{(1+\varepsilon)(1-\varepsilon)} \frac{G_M^2}{d\sigma_{red}} \left\{ 1 + 2 \frac{\Re(\delta\tilde{G}_M)}{G_M} + \frac{2}{1+\varepsilon} \varepsilon Y_{2\gamma} \right\} \\
 \frac{P_t}{P_l} &= -\sqrt{\frac{2\varepsilon}{(1+\varepsilon)\tau}} \left\{ R - R \frac{\Re(\delta\tilde{G}_M)}{G_M} - \frac{\Re(\delta\tilde{G}_E)}{G_M} + 2 \left(1 - R \frac{2\varepsilon}{1+\varepsilon} \right) Y_{2\gamma} \right\}
 \end{aligned}$$

E04-019
(Two-gamma)

$$d\sigma_{red} / G_M^2 = 1 + \frac{\varepsilon R^2}{\tau} + 2 \frac{\Re(\delta\tilde{G}_M)}{G_M} + 2R \frac{\varepsilon \Re(\delta\tilde{G}_E)}{\tau G_M} + 2 \left(1 + \frac{R}{\tau} \right) \varepsilon Y_{2\gamma}$$

$$\Re(\tilde{G}_E) = G_E(Q^2) + \Re(\delta\tilde{G}_E(Q^2, \varepsilon))$$

$$\Re(\tilde{G}_M) = G_M(Q^2) + \Re(\delta\tilde{G}_M(Q^2, \varepsilon))$$

$$R = G_E / G_M \quad Y_{2\gamma} = 0 + \sqrt{\frac{\tau(1+\tau)(1+\varepsilon)}{1-\varepsilon}} \frac{\Re(\tilde{F}_3(Q^2, \varepsilon))}{G_M}$$

Born Approximation

Beyond Born Approximation

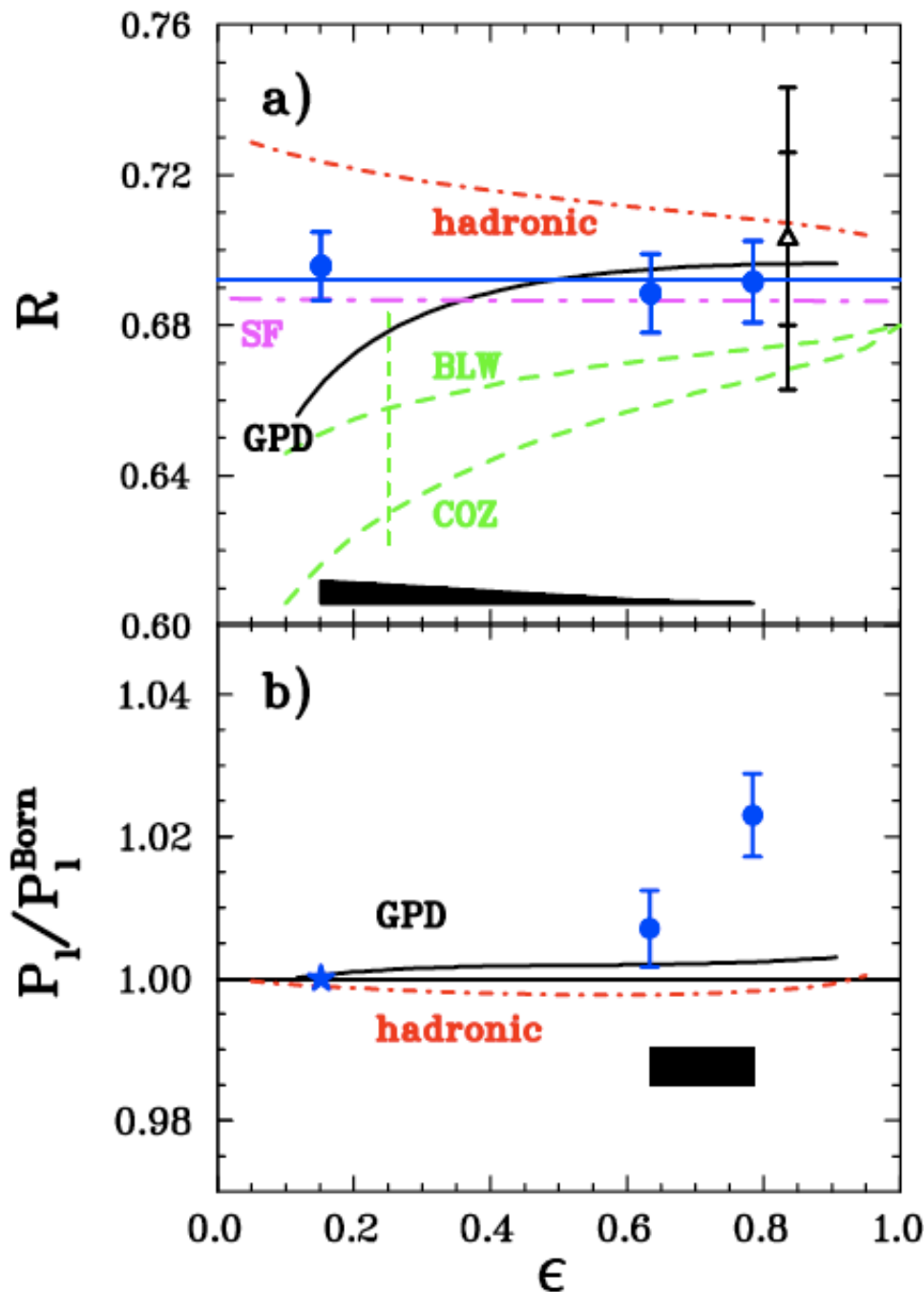
e⁺/e⁻ x-section ratio
CLAS, VEPP3, OLYMPUS
Rosenbluth non-linearity
E05-017

P.A.M. Guichon and M. Vanderhaeghen, Phys.Rev.Lett. 91, 142303 (2003)

M.P. Rekalo and E. Tomasi-Gustafsson, E.P.J. A 22, 331 (2004)

Slide idea:
L. Pentchev

Jefferson Lab E04-019 (Two-gamma)



Jlab – Hall C

$Q^2 = 2.5 \text{ (GeV/c)}^2$

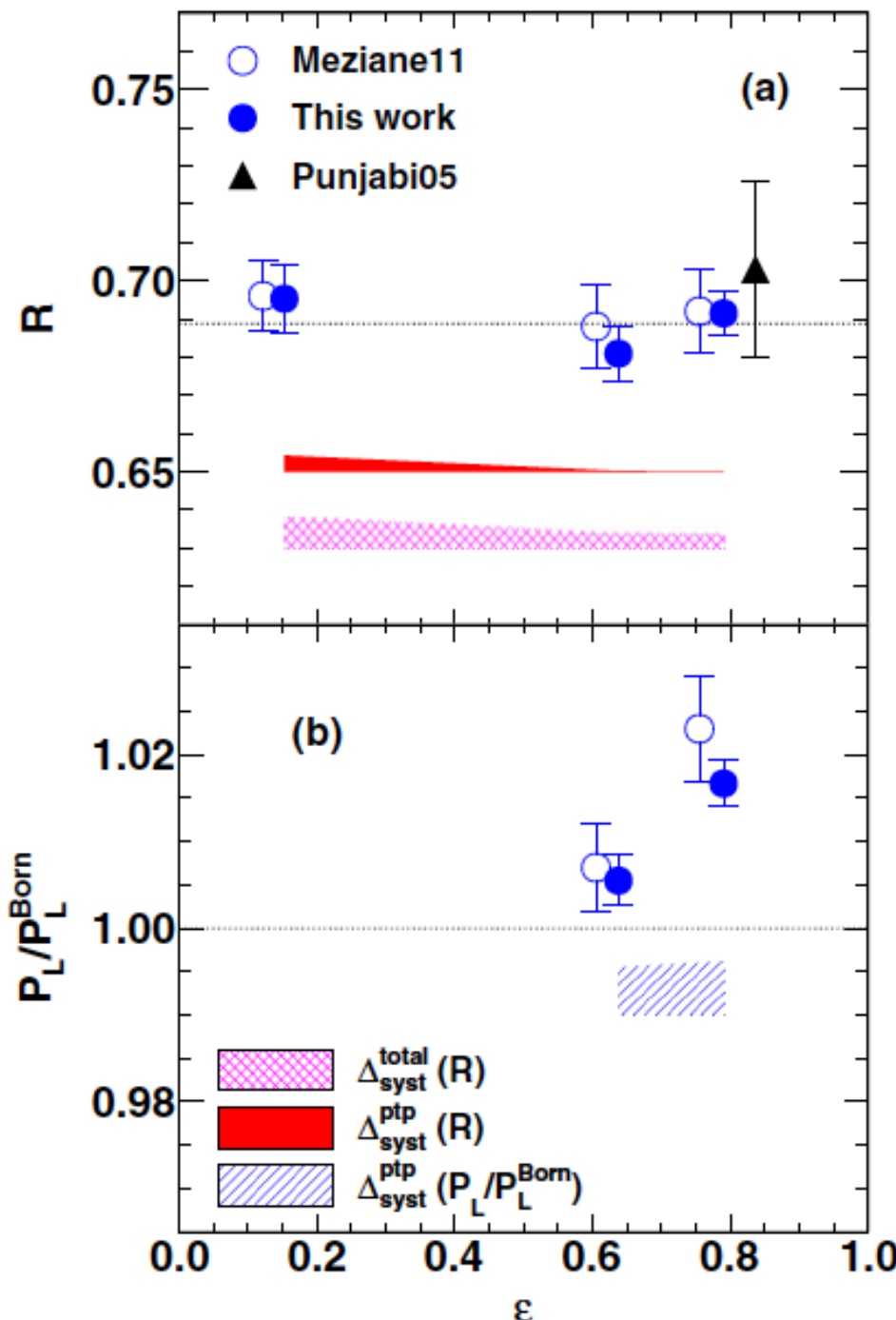
G_E/G_M from P_t/P_l constant vs. ϵ

- no effect in P_t/P_l
- some effect in P_l

Expect larger effect in e^+e^- !

M. Meziane et al., hep-ph/1012.0339v2
Phys. Rev. Lett. 106, 132501 (2011)

Jefferson Lab E04-019 (Two-gamma)



Jlab – Hall C
 $Q^2 = 2.5 \text{ (GeV/c)}^2$

G_E/G_M from P_t/P_l constant vs. ϵ

- no effect in P_t/P_l
- some effect in P_l

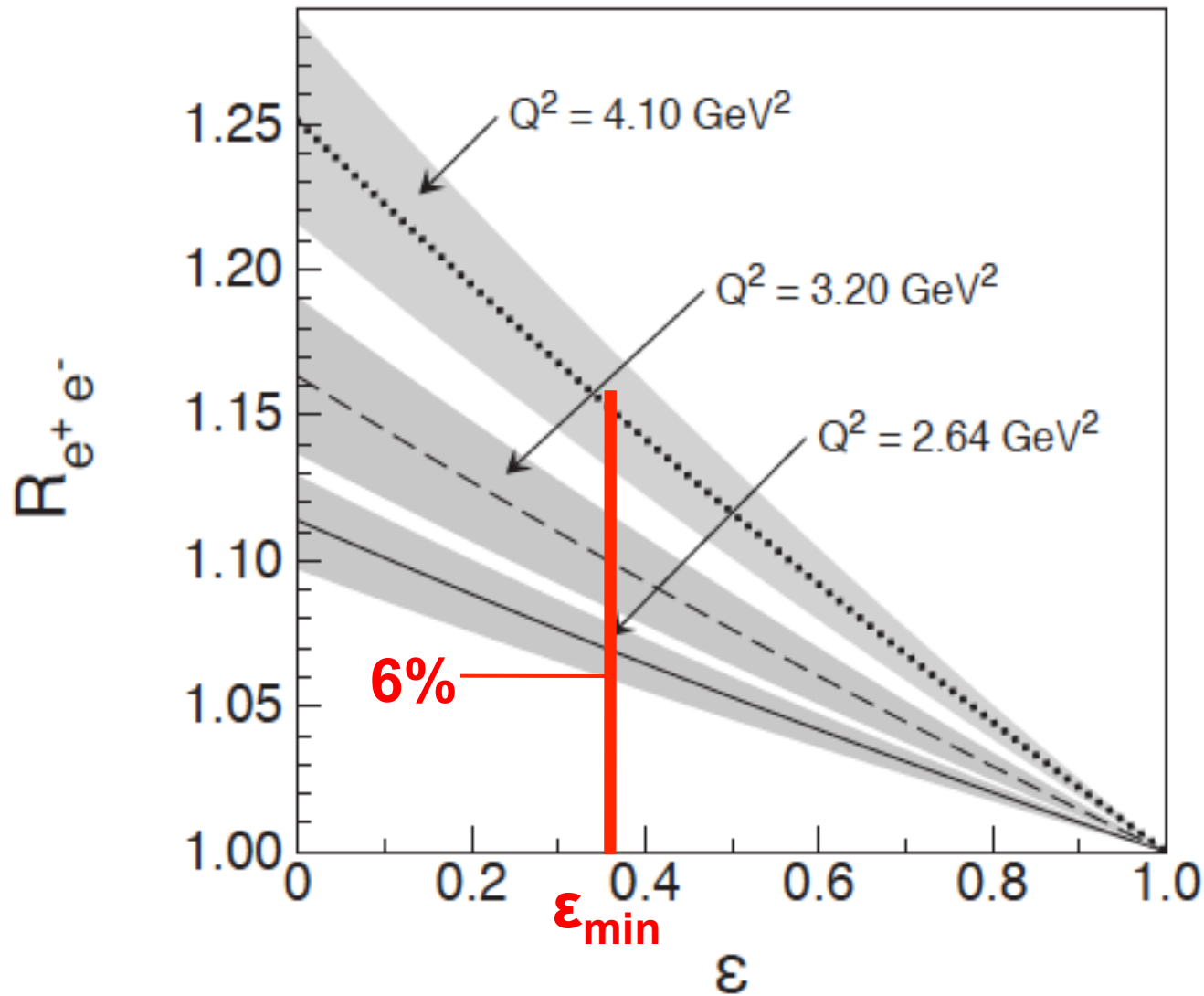
Expect larger effect in e^+e^- !

M. Meziane et al., hep-ph/1012.0339v2
 Phys. Rev. Lett. 106, 132501 (2011)

A. Puckett et al., nucl-ex/1707.08587v2
 Phys. Rev. C 96, 055203 (2017)

Empirical extraction of TPE amplitudes

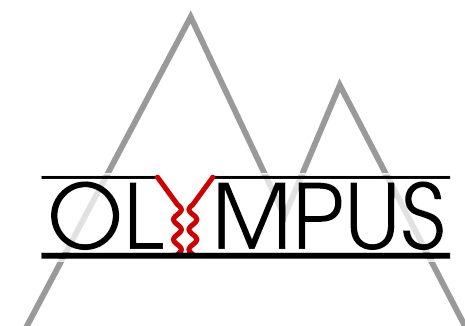
J. Guttmann, N. Kivel, M. Meziane, and M. Vanderhaeghen, EPJA 47, 77 (2011)



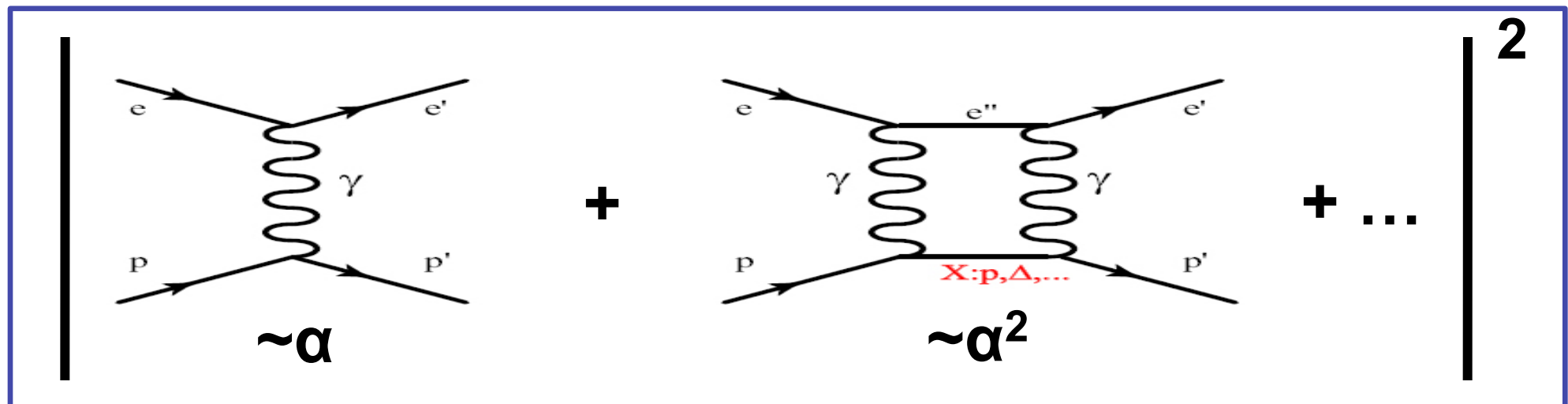
grows with Q^2 !

Expect ~6% effect for
OLYMPUS@2.0GeV

$\epsilon_{\min} > 0.35, Q^2 < 2.2 \text{ (GeV/c)}^2$



Lepton-proton elastic scattering



- Interference term depends on lepton charge sign (**C-odd**)

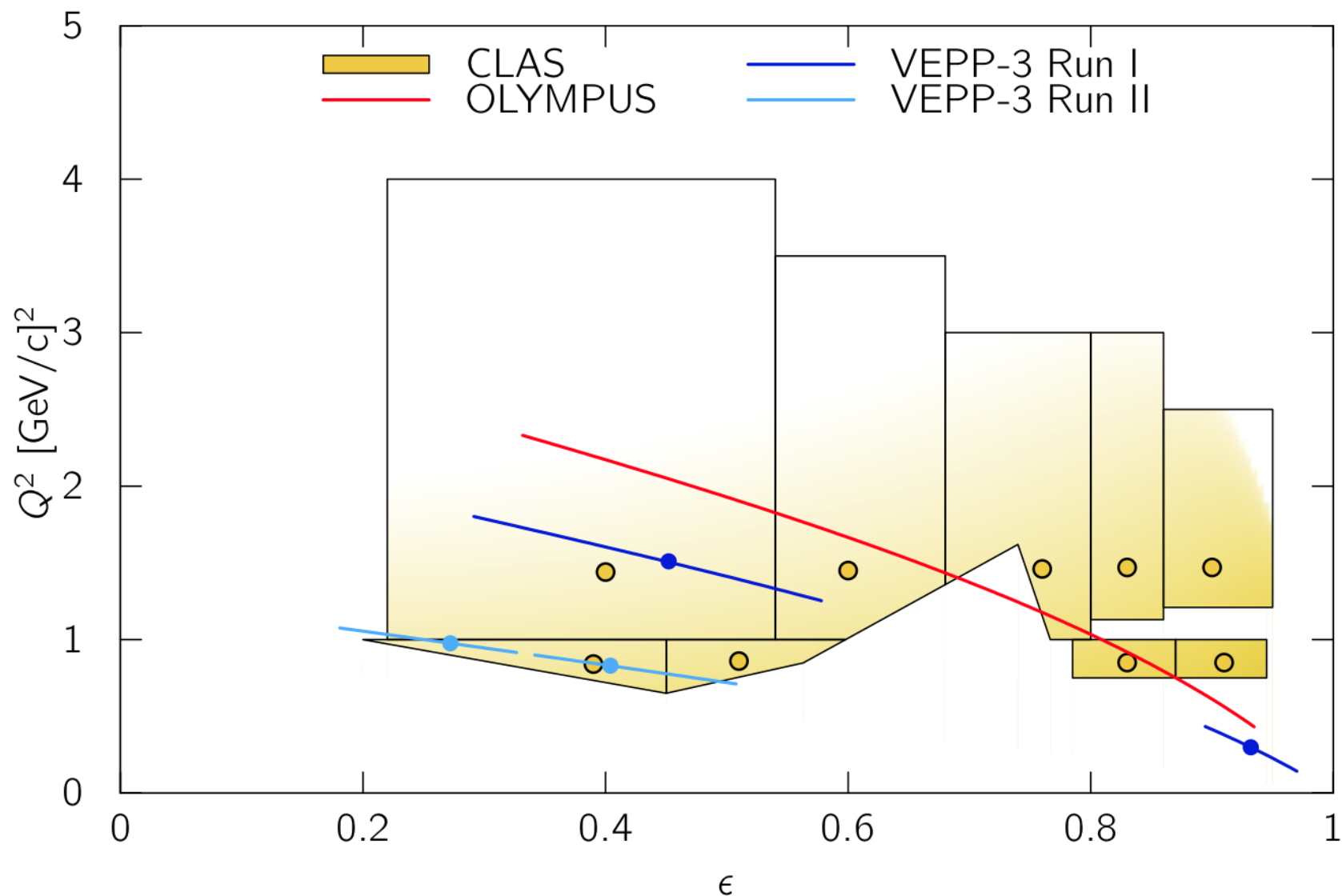
$$\sigma_{e^\pm p} = |\mathcal{M}_{1\gamma}|^2 \pm 2\Re\{\mathcal{M}_{1\gamma}^\dagger \mathcal{M}_{2\gamma}\} + \dots$$

- e^+/e^- ratio deviates from unity by two-photon contribution

$$\frac{\sigma_{e^+ p}}{\sigma_{e^- p}} \approx 1 + 4 \frac{\Re\{\mathcal{M}_{1\gamma}^\dagger \mathcal{M}_{2\gamma}\}}{|\mathcal{M}_{1\gamma}|^2}$$

Comparison of e⁺/e⁻ experiments

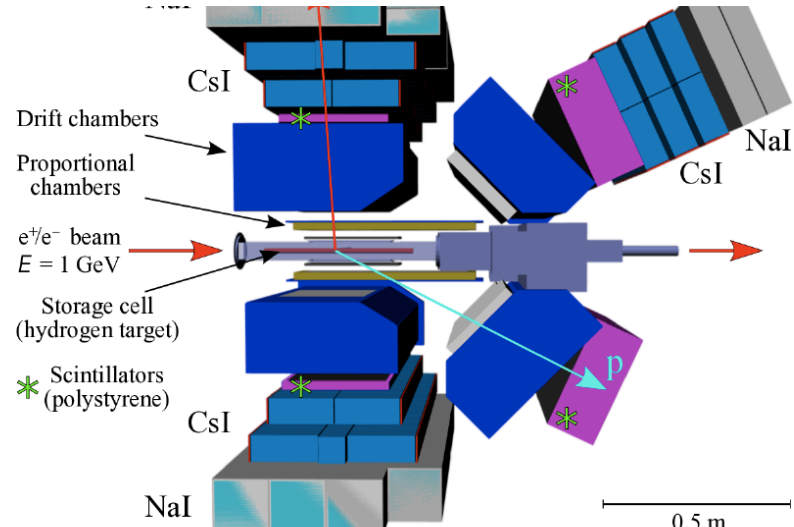
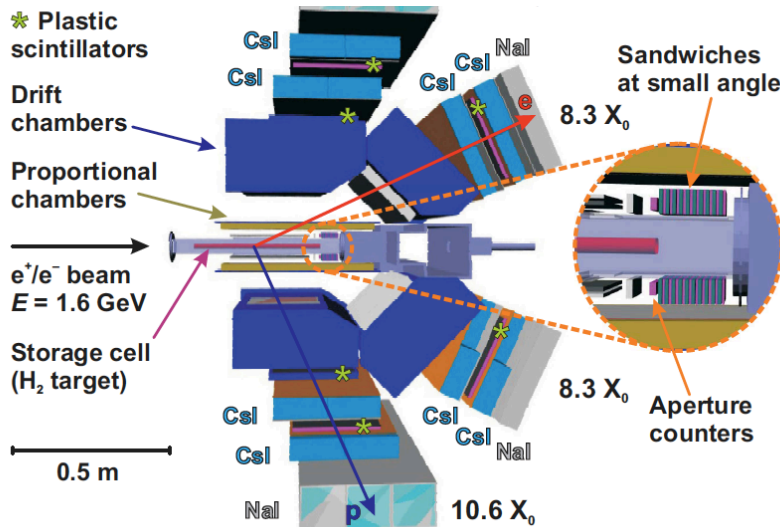
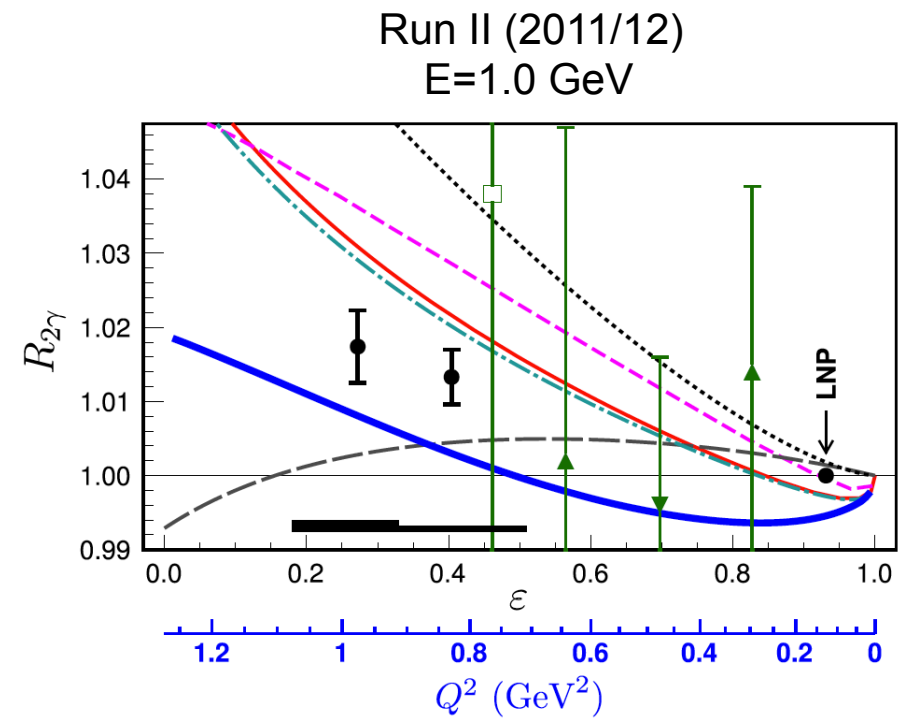
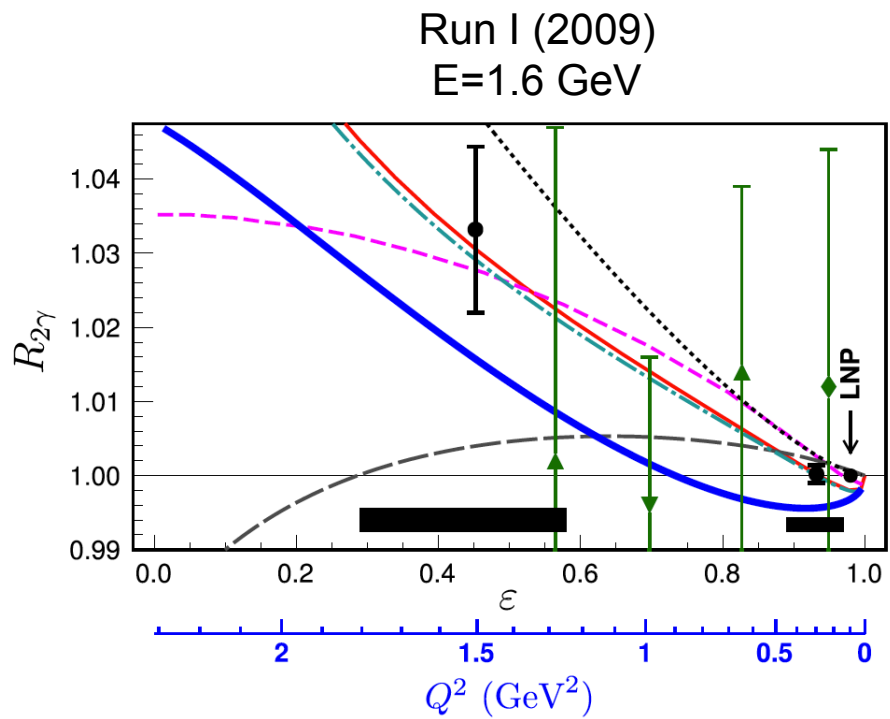
- VEPP-3 @ Novosibirsk: $E_{\text{beam}} = 1.6, 1.0 \text{ (and } 0.6\text{)} \text{ GeV}$
- CLAS @ JLAB : $E_{\text{beam}} = 0.5 - 4.0 \text{ GeV continuous}$
- OLYMPUS @ DESY: $E_{\text{beam}} = 2.0 \text{ GeV}$



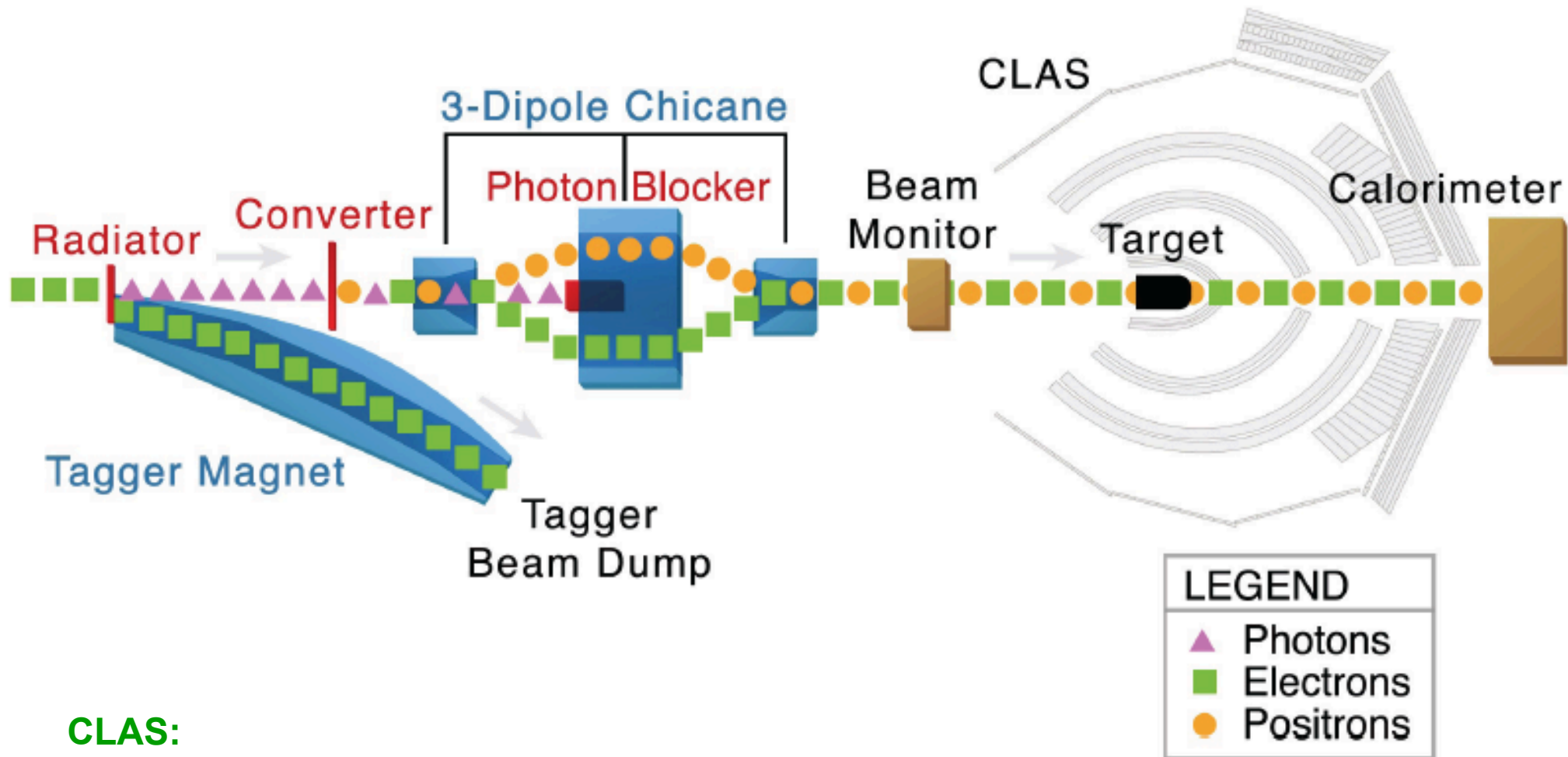
Comparison of e⁺/e⁻ experiments

	VEPP-3 Novosibirsk	OLYMPUS DESY	EG5 CLAS JLab
beam energy	3 fixed	1 fixed	wide spectrum
equality of e [±] beam energy	measured	measured	reconstructed
e ⁺ /e ⁻ swapping frequency	half-hour	24 hours	simultaneously
e ⁺ /e ⁻ lumi monitor	elastic low-Q ²	elastic low-Q ² , Möller/Bhabha	from simulation
energy of scattered e [±]	EM-calorimeter	mag. analysis	mag. analysis
proton PID	ΔE/E, TOF	mag. analysis, TOF	mag. analysis, TOF
e ⁺ /e ⁻ detector acceptance	identical	big difference	big difference
luminosity	1.0×10^{32}	2.0×10^{33}	2.5×10^{32}
beam type	storage ring	storage ring	secondary beam
target type	internal H target	internal H target	liquid H target
data taken	2009, 2011-12	2012	2011
published	2015	2017	2015

TPE experiments: Novosibirsk/VEPP-3



TPE experiments: CLAS (E04-116)



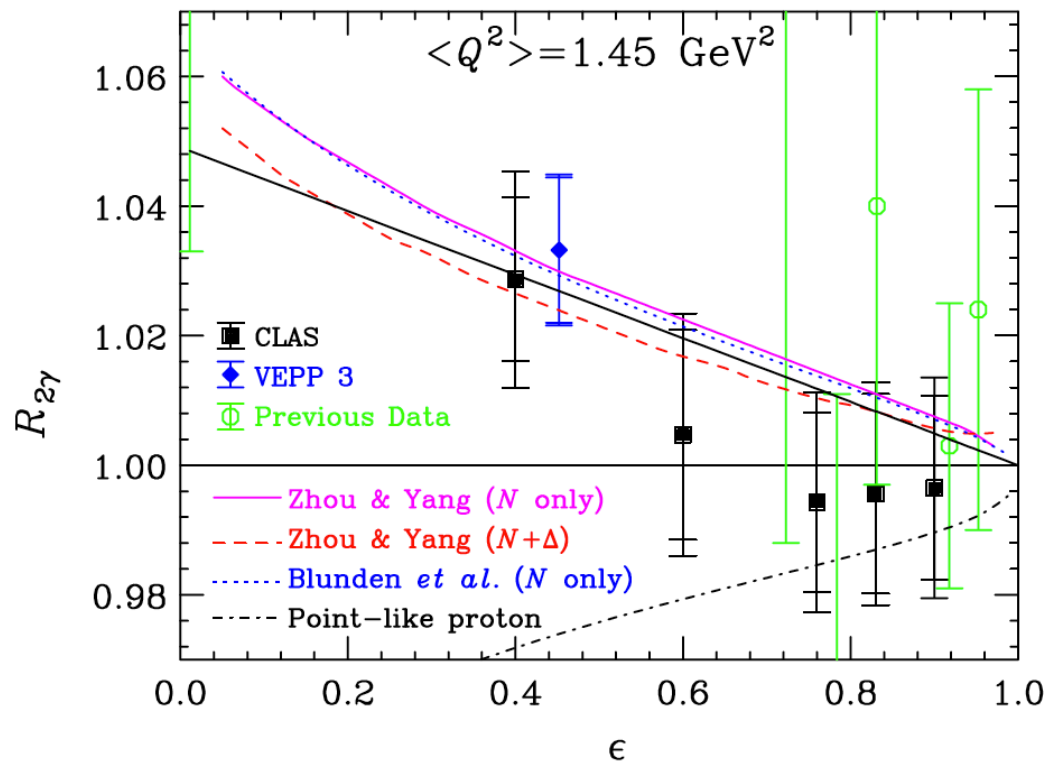
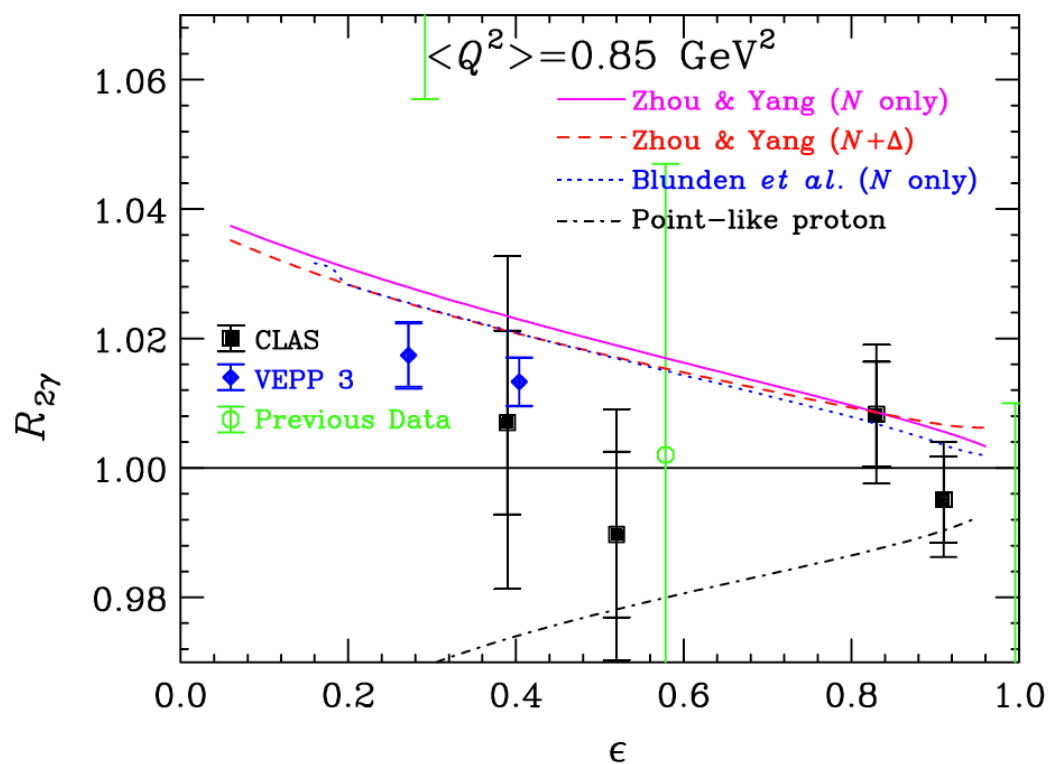
CLAS:

D. Rimal *et al.*, PRC 95, 065201 (2017)

D. Adikaram *et al.*, PRL 114, 062003 (2015)

TPE experiments: CLAS (E04-116)

ϵ dependence



CLAS:

D. Rimal *et al.*, PRC 95, 065201 (2017)

D. Adikaram *et al.*, PRL 114, 062003 (2015)

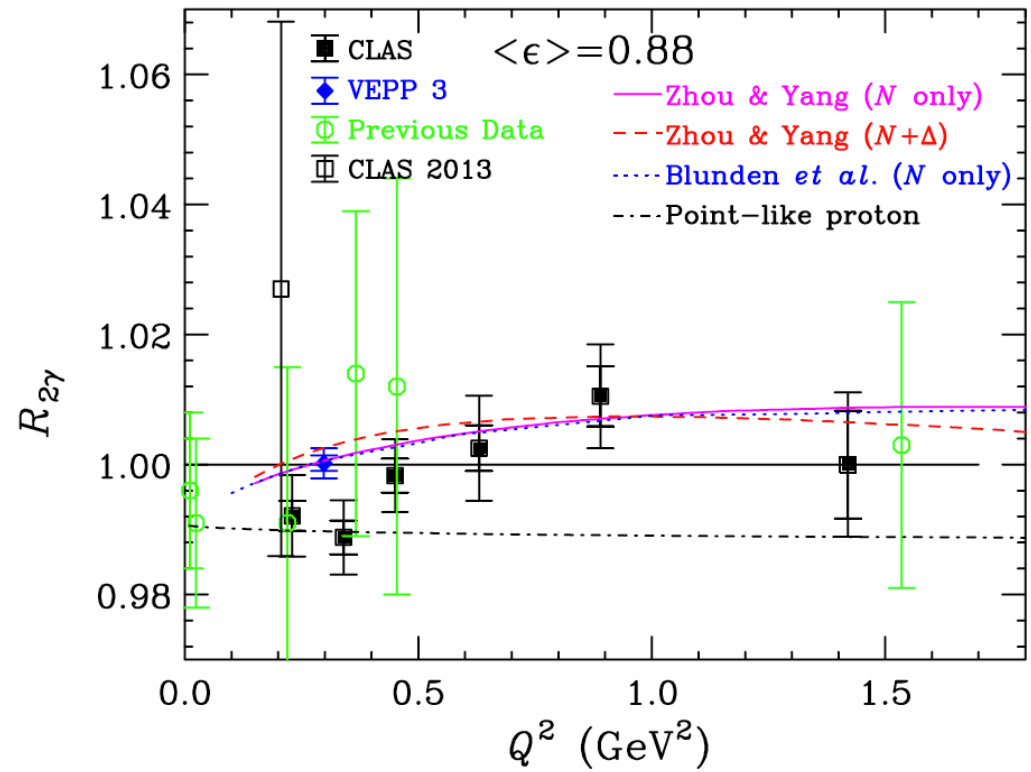
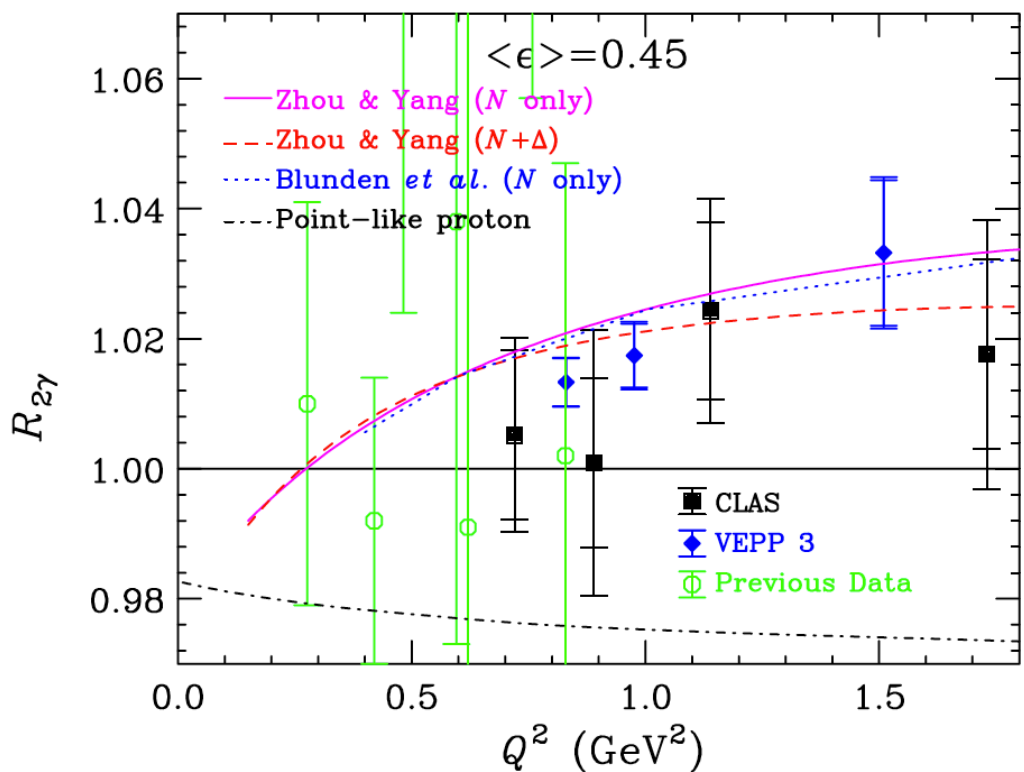
VEPP-3:

I.A. Racheck *et al.*, PRL 114, 062005 (2015)

CLAS result consistent with “standard” TPE prescription
... however, limited precision

TPE experiments: CLAS (E04-116)

Q^2 dependence



CLAS:

D. Rimal *et al.*, PRC 95, 065201 (2017)

D. Adikaram *et al.*, PRL 114, 062003 (2015)

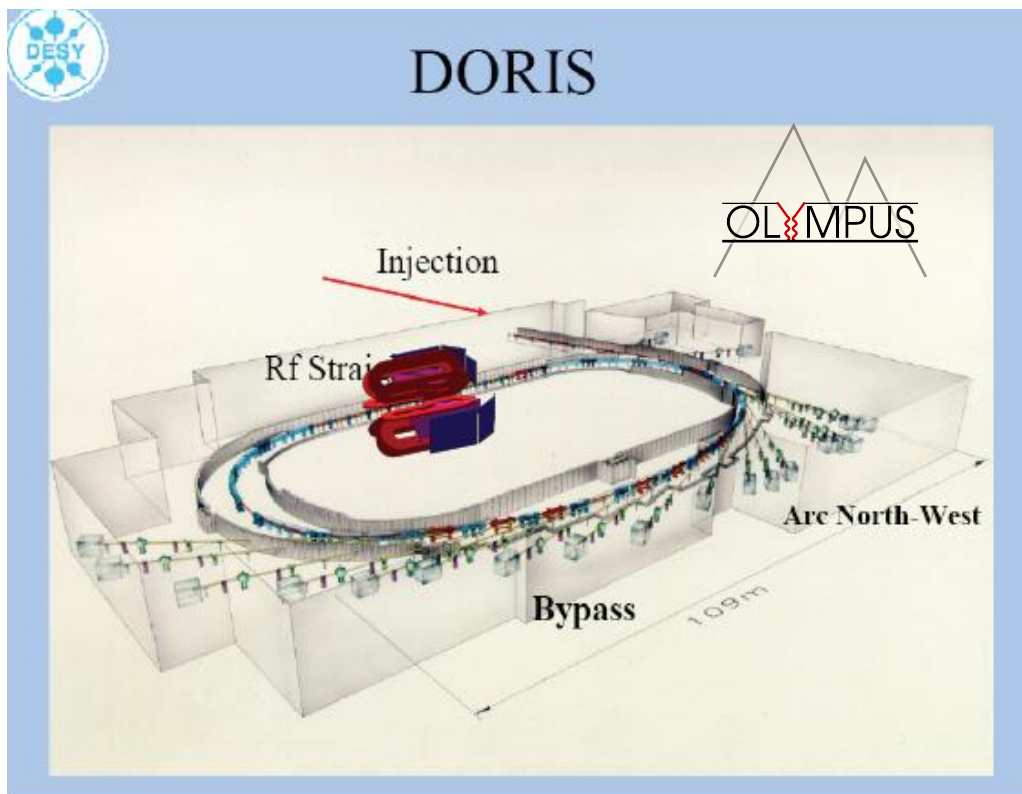
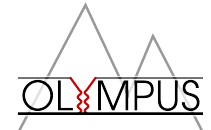
VEPP-3:

I.A. Racheck *et al.*, PRL 114, 062005 (2015)

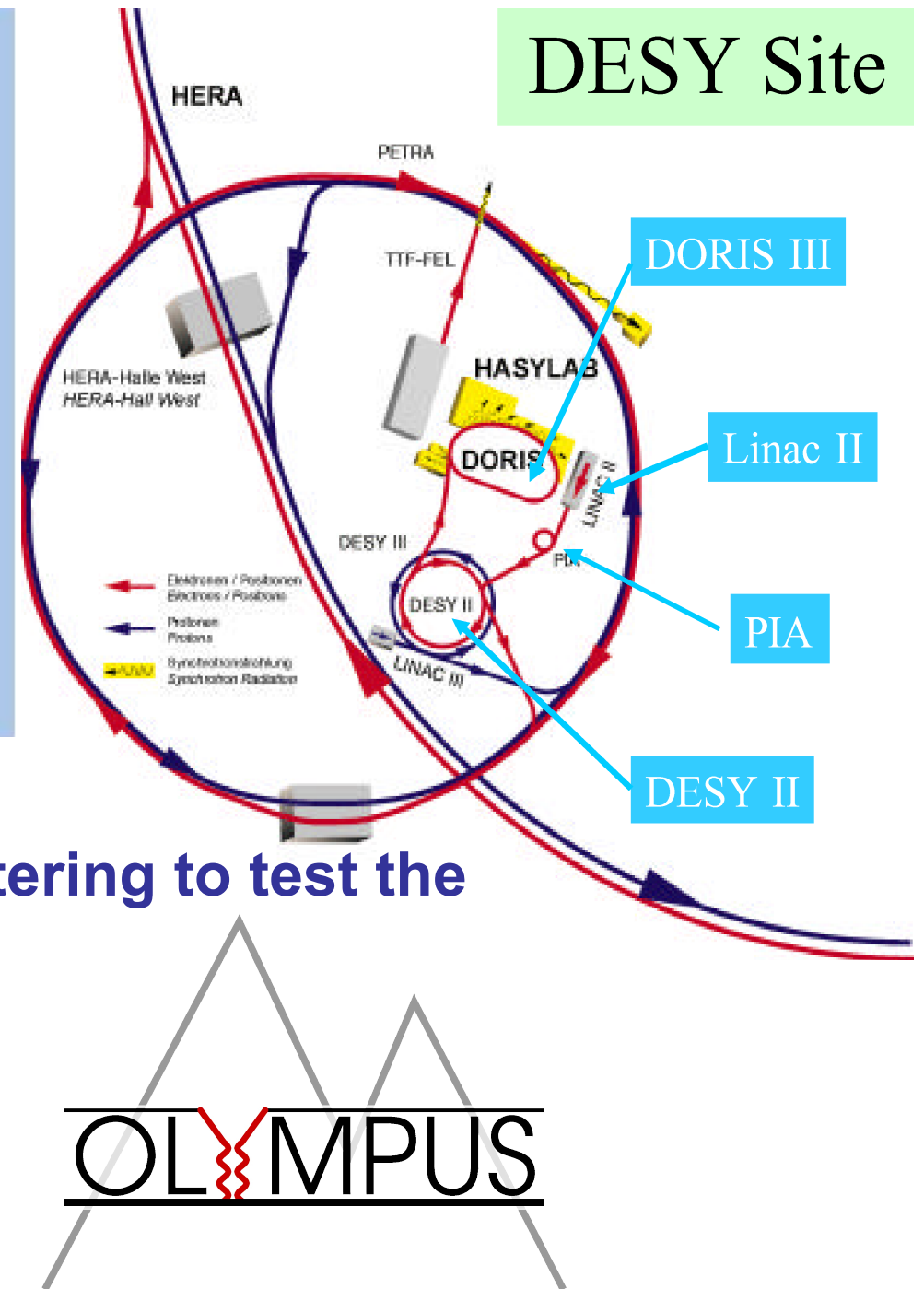
**CLAS result consistent with “standard” TPE prescription
... however, limited precision**

OLYMPUS @ DORIS/DESY

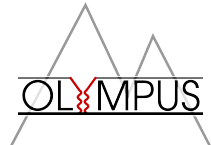
38



DORIS



pOsitron-proton and eLectron-proton elastic scattering to test the hYpothesis of Multi- Photon exchange Using DoriS



OLYMPUS collaboration

~50 physicists from 13 institutions in 6 countries

Elected spokesmen / deputy:	R. Milner / R. Beck	(2009–2011)
	M.K. / A. Winnebeck	(2011–2013)
	D. Hasell / U. Schneekloth	(2013–)

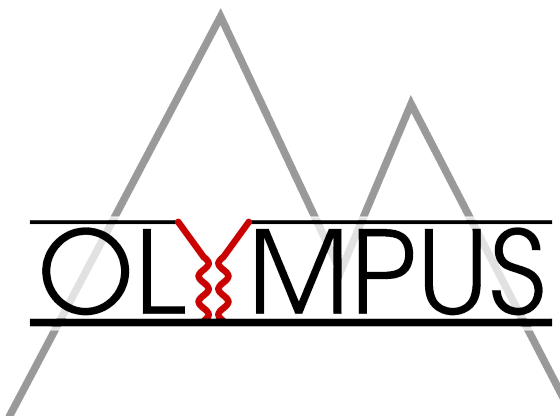
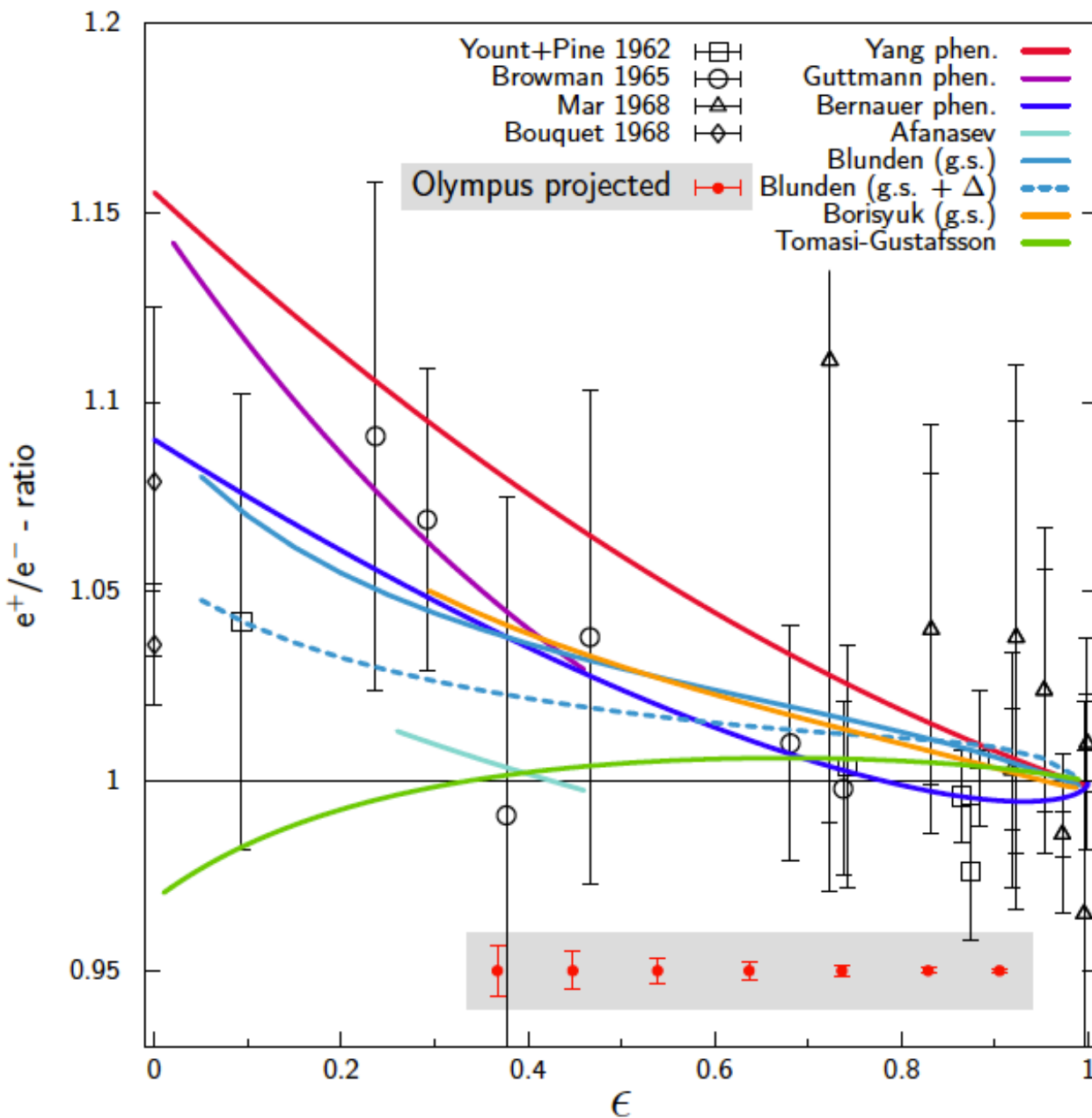
PhDs: O. Ates, A. Schmidt, R. Russell, B. Henderson, L. Ice, C. O'Connor, D. Khanefi

- **Arizona State University:** TOF support, particle identification, magnetic shielding
- **DESY:** Modifications to DORIS accelerator and beamline, toroid support, infrastructure, installation
- **Hampton University:** GEM luminosity monitor
- **INFN Bari:** GEM electronics
- **INFN Ferrara:** Target
- **INFN Rome:** GEM electronics
- **MIT:** BLAST spectrometer, wire chambers, tracking upgrade, target and vacuum system, transportation to DESY, simulations, slow control, analysis framework
- **Petersburg Nuclear Physics Institute:** MWPC luminosity monitor
- **University of Bonn:** Trigger, data acquisition, and online monitor
- **University of Mainz:** Trigger, DAQ, Symmetric Moller monitor
- **University of Glasgow:** TOF scintillators
- **University of New Hampshire:** TOF scintillators
- **A. Alikhanyan National Laboratory (AANL), Yerevan:** TOF scintillators

The OLYMPUS experiment

- Electrons/positrons (100mA) in 2.0–4.5 GeV storage ring
DORIS at DESY, Hamburg, Germany
- Unpolarized internal hydrogen target (buffer system)
 3×10^{15} at/cm² @ 100 mA → $L = 2 \times 10^{33} / (\text{cm}^2\text{s})$
- Large acceptance detector for e-p in coincidence
BLAST detector from MIT-Bates available
- Redundant monitoring of luminosity
Pressure, temperature, flow, current measurements
Small-angle elastic scattering at high epsilon / low Q²
Symmetric Moller/Bhabha scattering
- Measure ratio of positron-proton to electron-proton unpolarized elastic scattering to 1% stat.+sys.

Projected results for OLYMPUS



Data from 1960's

Many theoretical predictions
with little constraint

OLYMPUS:

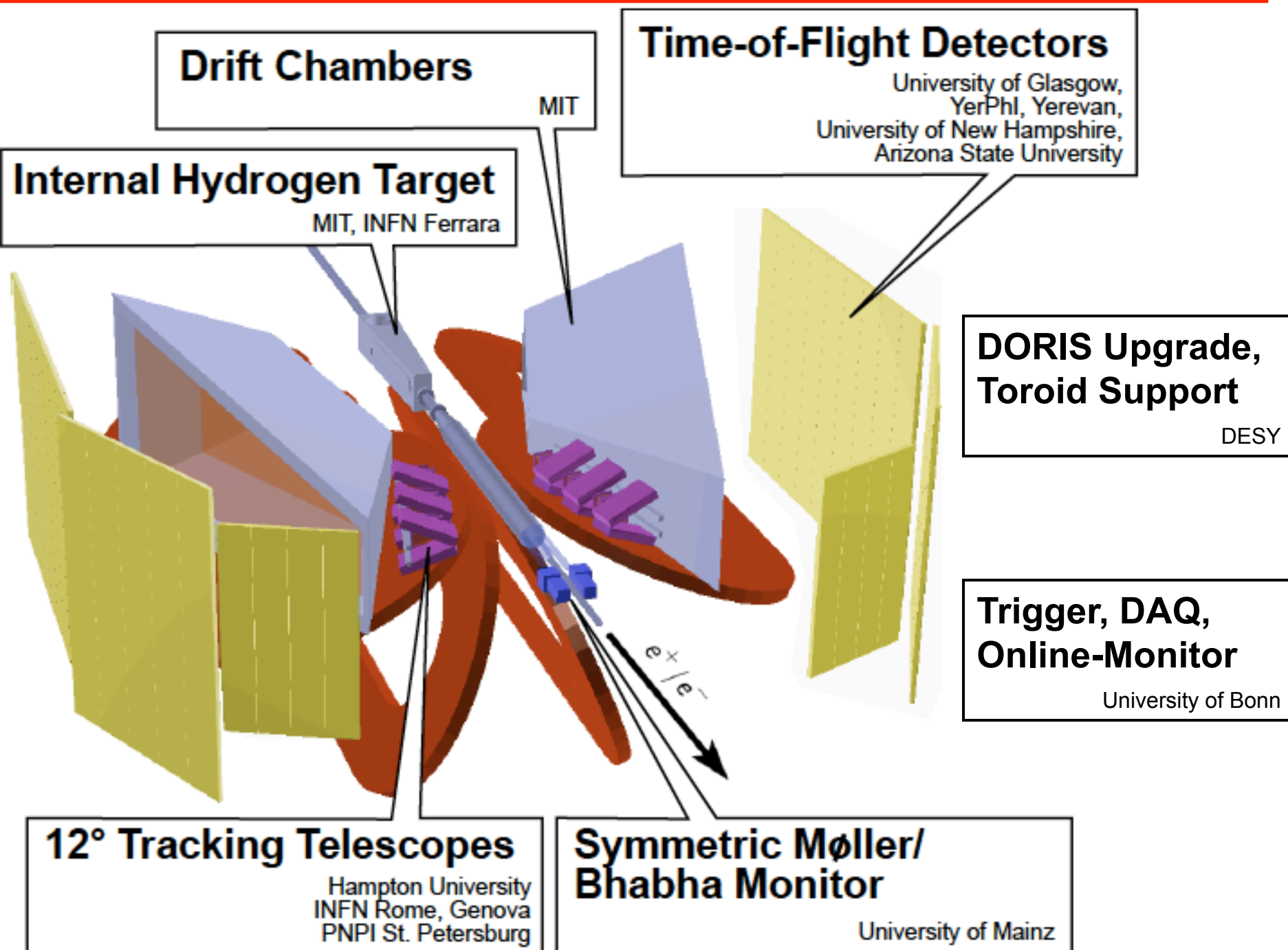
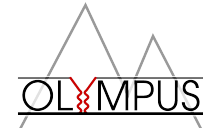
$E = 2.0 \text{ GeV}$

$0.4 < Q^2 / (\text{GeV}/c)^2 < 2.2$

Acquire 3.6 fb^{-1} for $< 1\%$
projected uncertainties

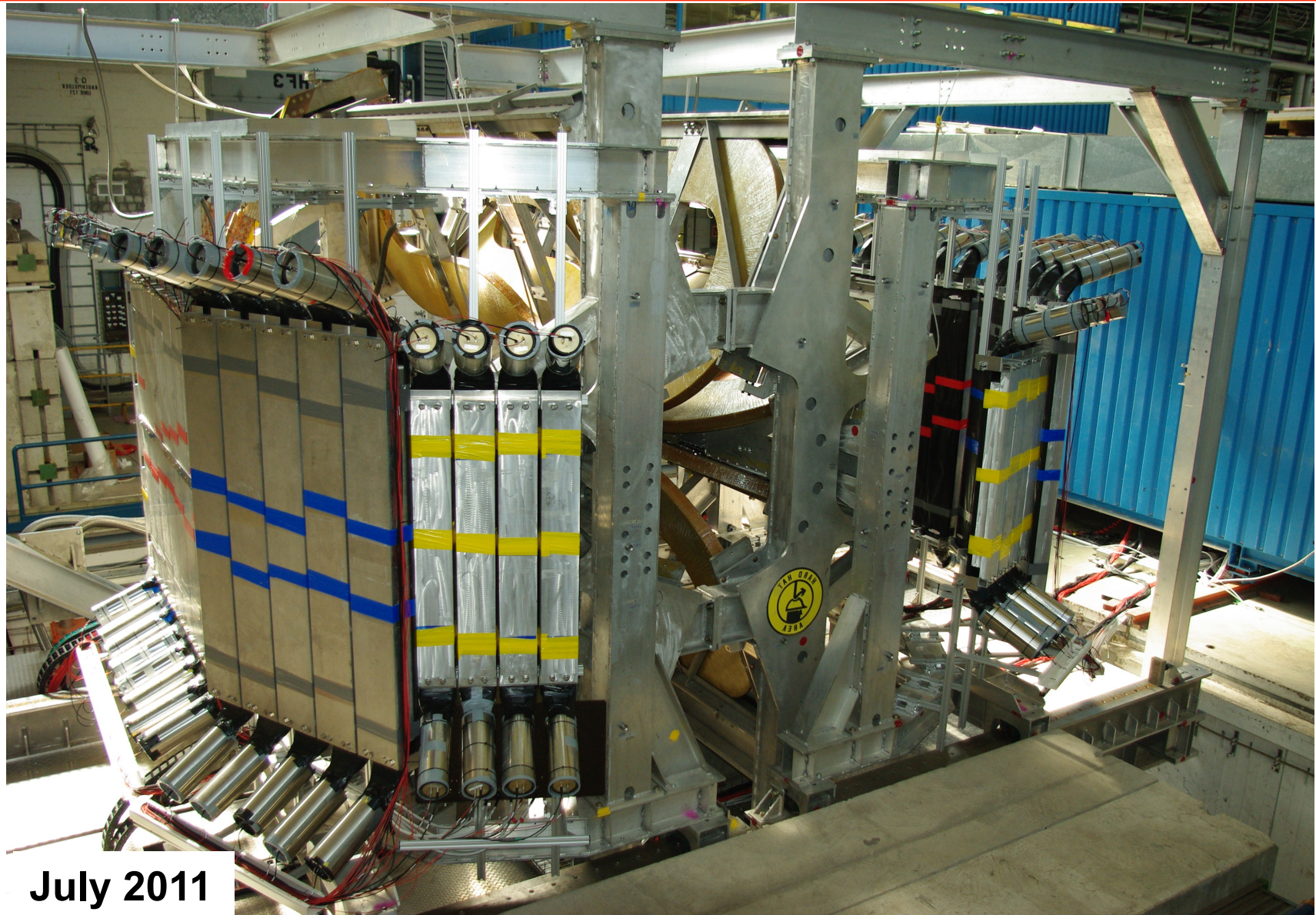
Data taking completed in 2012

The designed OLYMPUS detector



based on a figure by R. Russell

The realized OLYMPUS detector

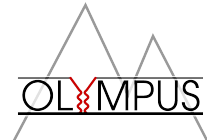


Apparatus: “*The OLYMPUS Experiment*”, R. Milner et al., NIMA 741, 1 (2014)

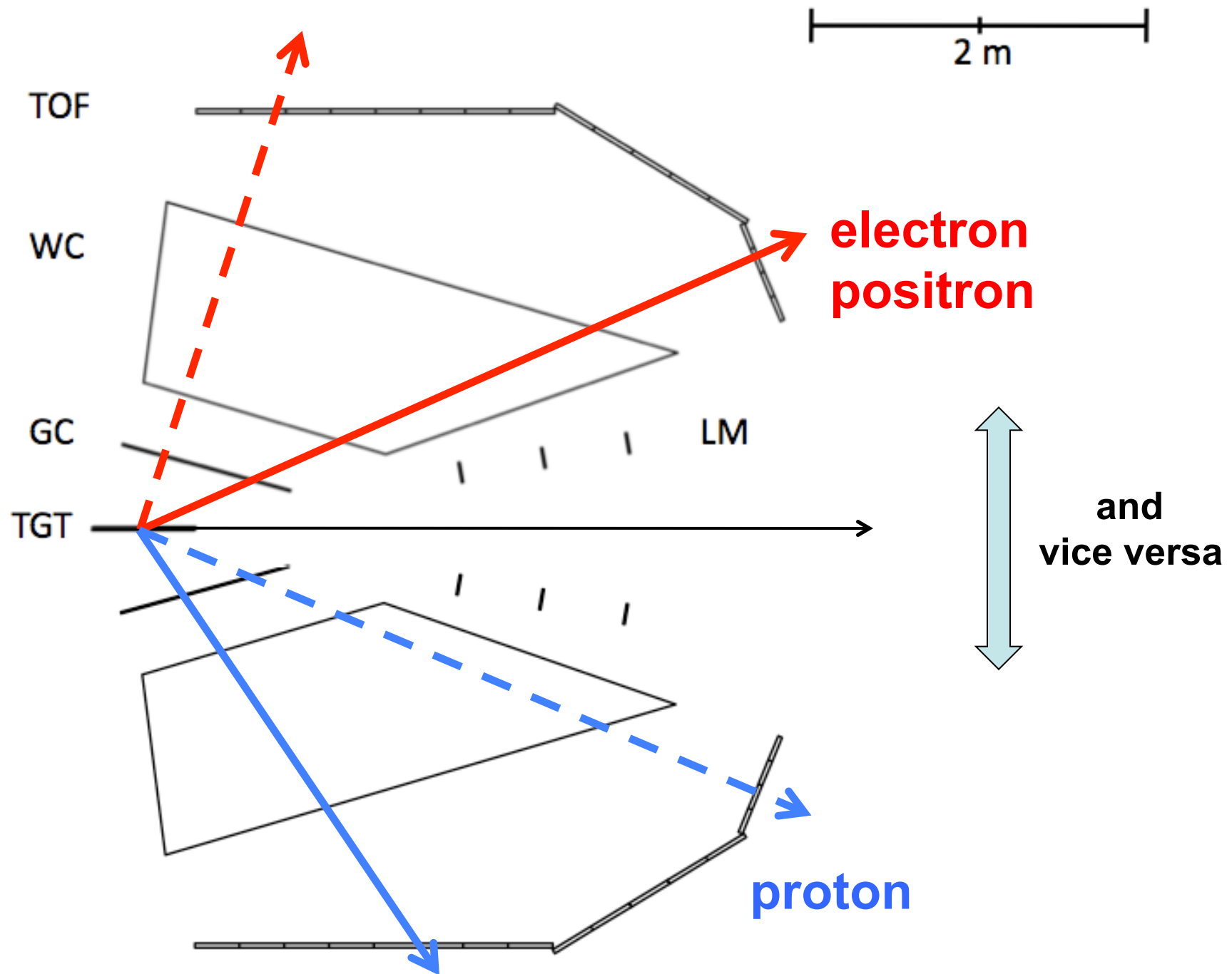
Target: “*The OLYMPUS internal hydrogen target*”, J.C. Bernauer, NIMA 755, 20 (2014)

Magnet: “*Measurement and tricubic interpolation of the magnetic field for the OLYMPUS experiment*”, J.C. Bernauer et al., NIMA 823, 9 (2016)

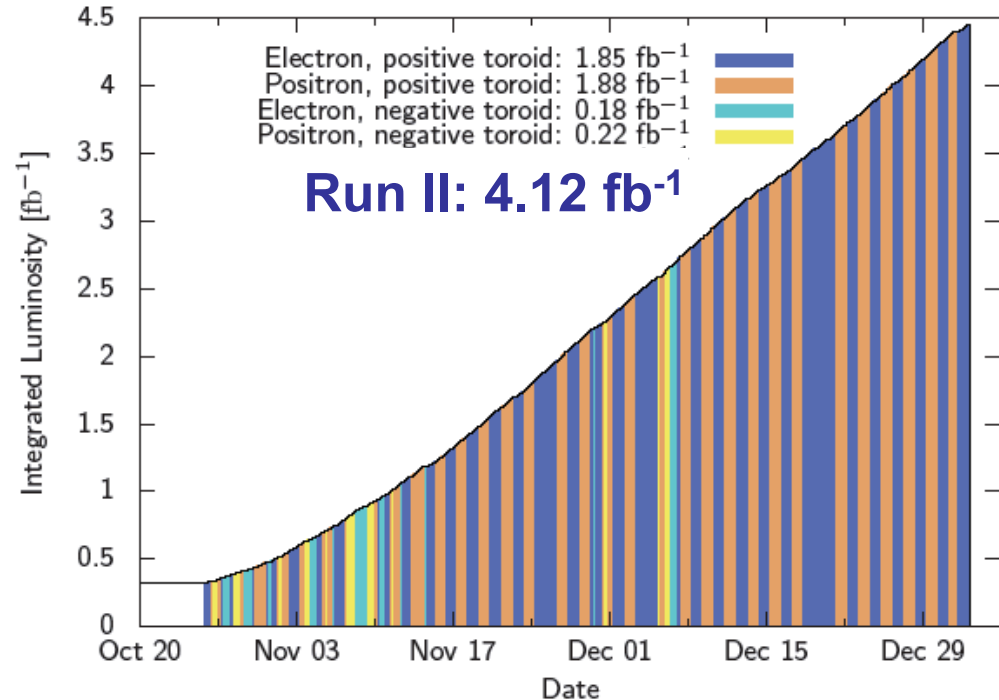
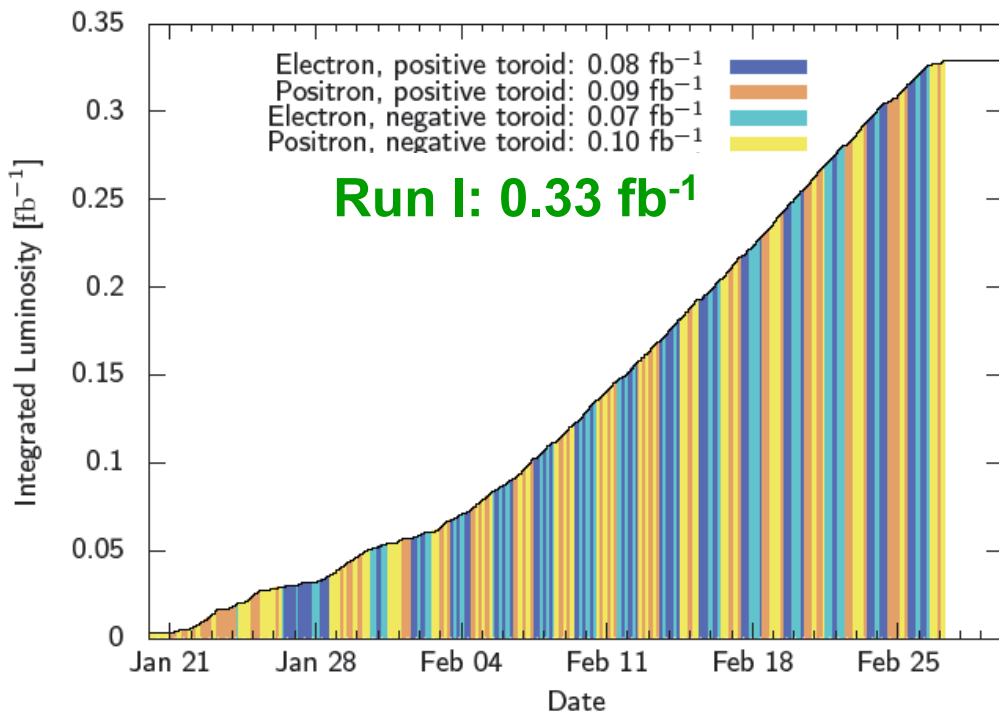
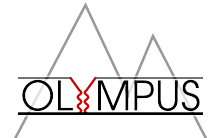
OLYMPUS kinematics at 2.0 GeV



44



Timeline of OLYMPUS



- 2007 Letter of Intent
- 2008 Proposal
- 2009 Technical review
- 2010 Approval and funding
- Summer 2010 BLAST transfer
- Spring 2011 Target test run
- Summer 2011 Detector installed
- Fall 2011 Commissioning

First run Jan 30 – Feb 27, 2012
... acquired $< 0.3 \text{ fb}^{-1}$

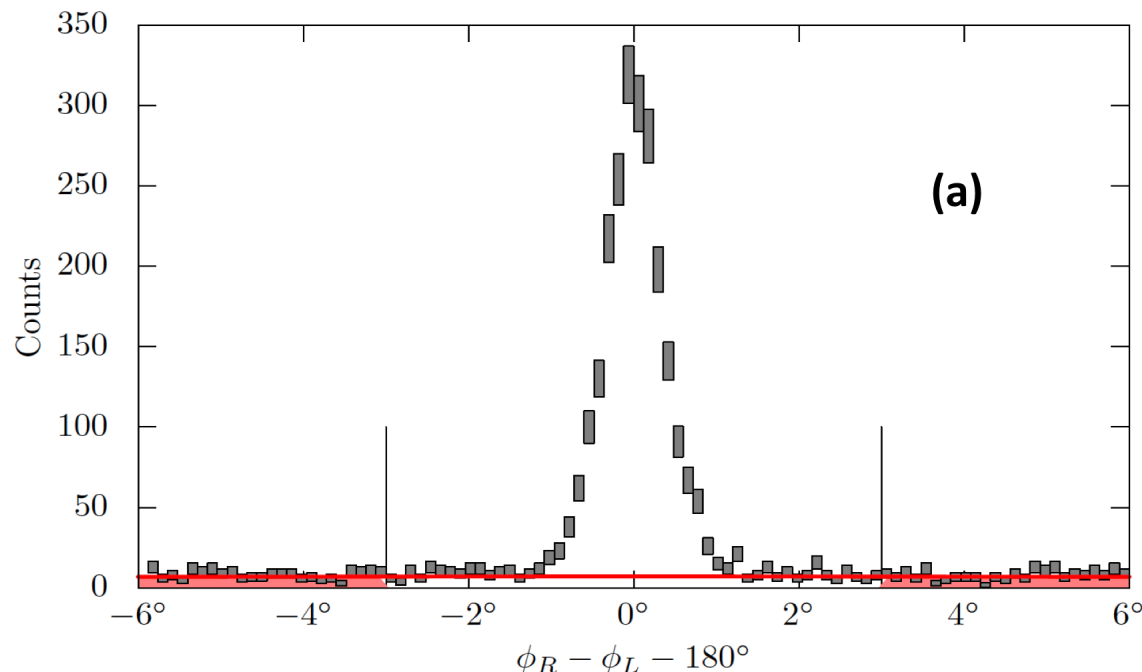
- Summer 2012 Repairs and upgrades

Second run Oct 24, 2012 – Jan 2, 2013
... acquired $> 4.0 \text{ fb}^{-1}$

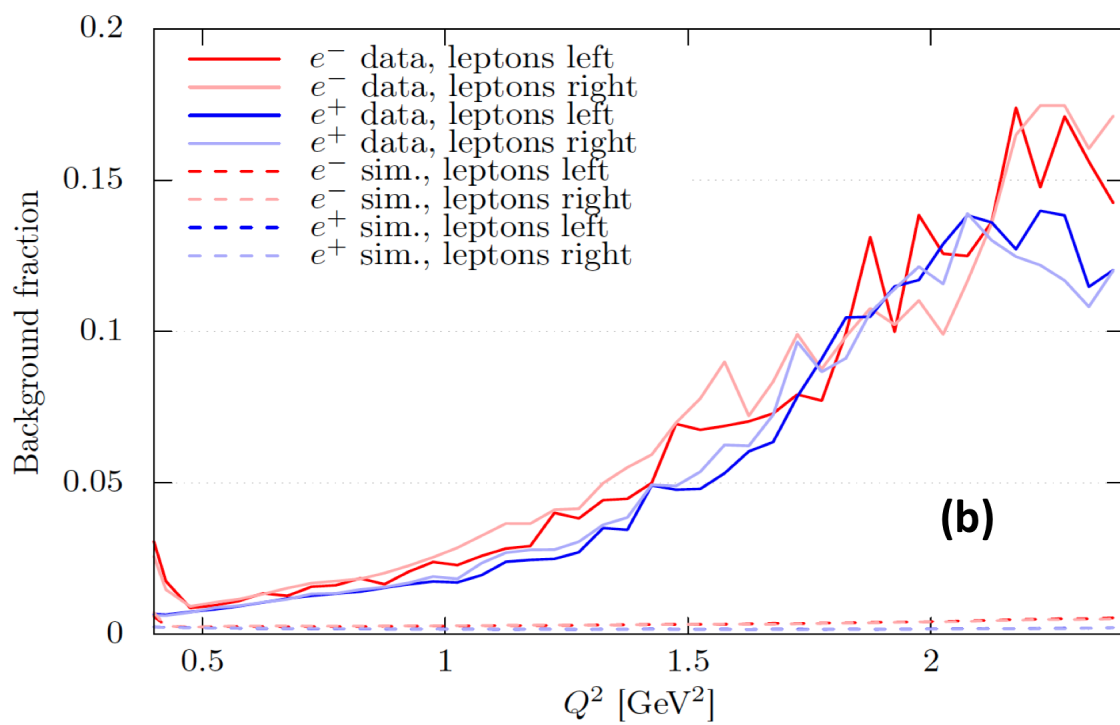
- Smooth performance of machine, target, detector
- Spring 2013 Survey & field mapping
- Analysis progressing – framework, calibrations, tracking, simulations

- **Results released in November 2016**

Backgrounds



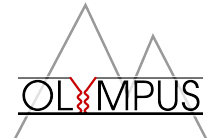
(a)



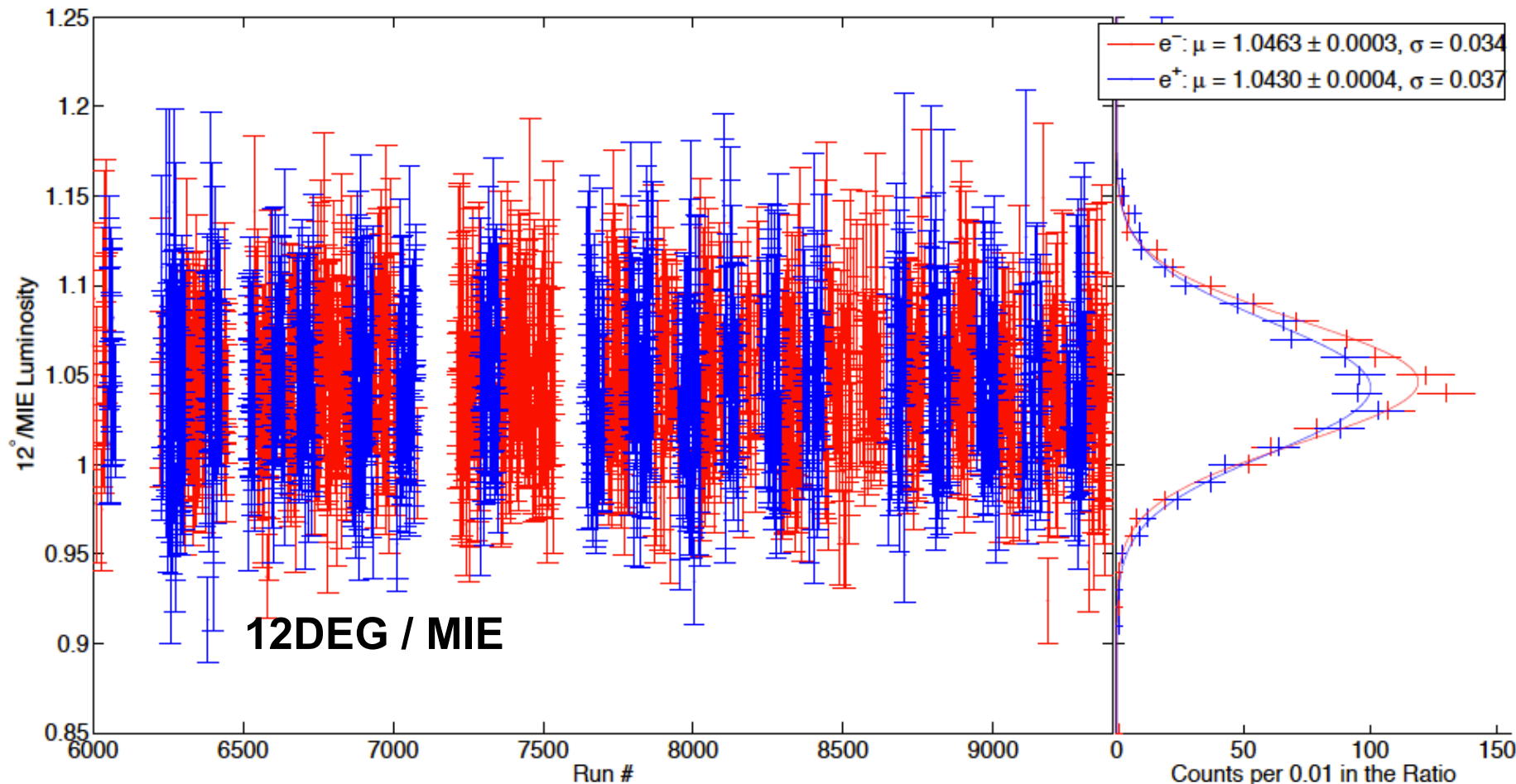
(b)

- Coplanarity peak for background estimation
- Backgrounds range from negligible at forward angles to 15-20% at large angles
- Mostly independent of species

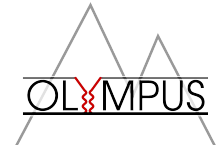
Luminosity monitoring



- Five redundant systems: Slow Control, SYMB, MIE, 12DEG-L,R
- Absolute luminosity from each rate to a few %
- Ratio of e^+/e^- luminosities for $R_{2\gamma}$ to sub %
- Time variation, mean and variance, systematics from comparisons
- Excellent agreement between SC, MIE, and 12DEG-L,R
- Final luminosity ratio from MIE, using 12DEG for high- ϵ data point

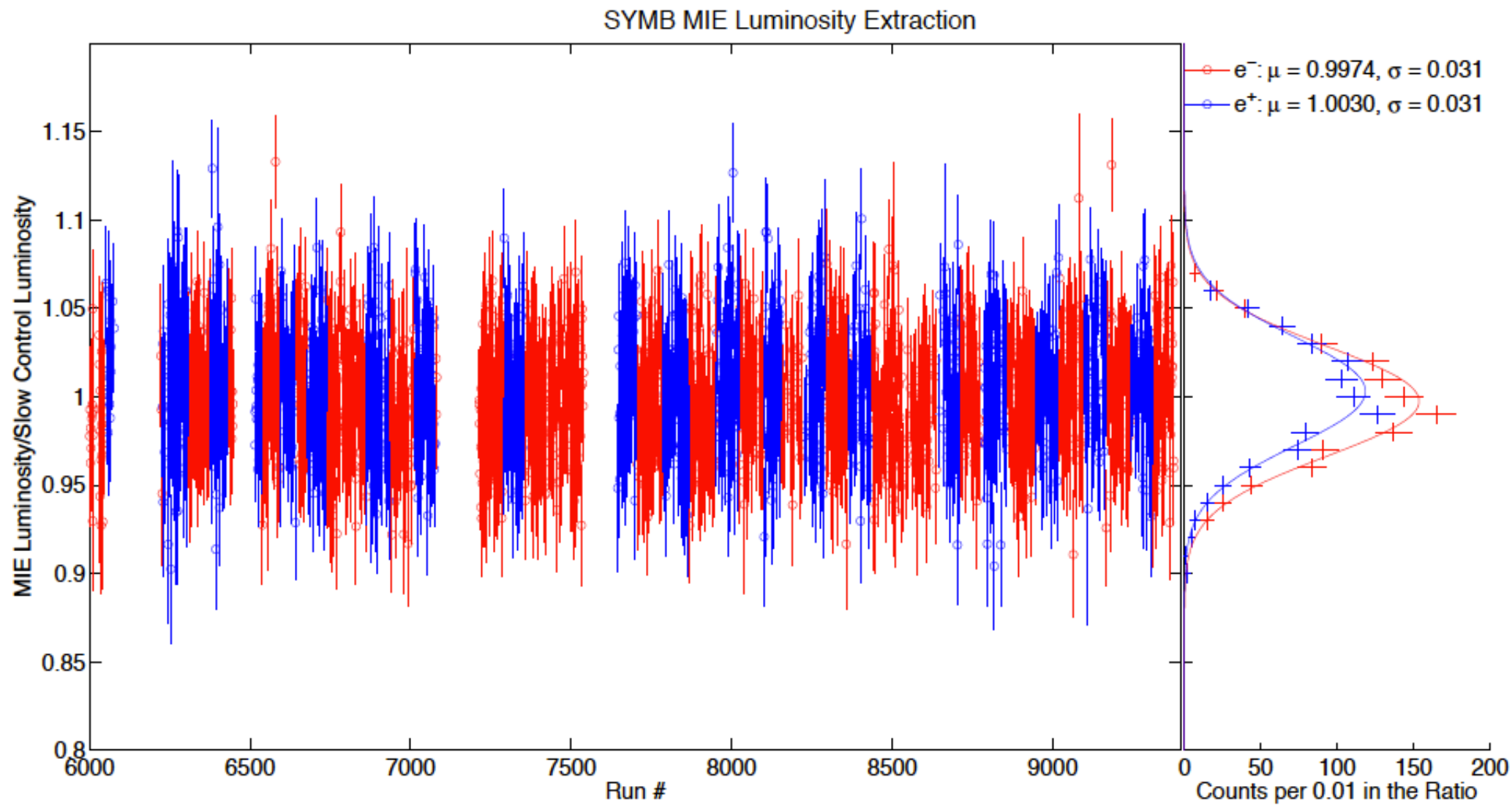


Luminosity monitoring



48

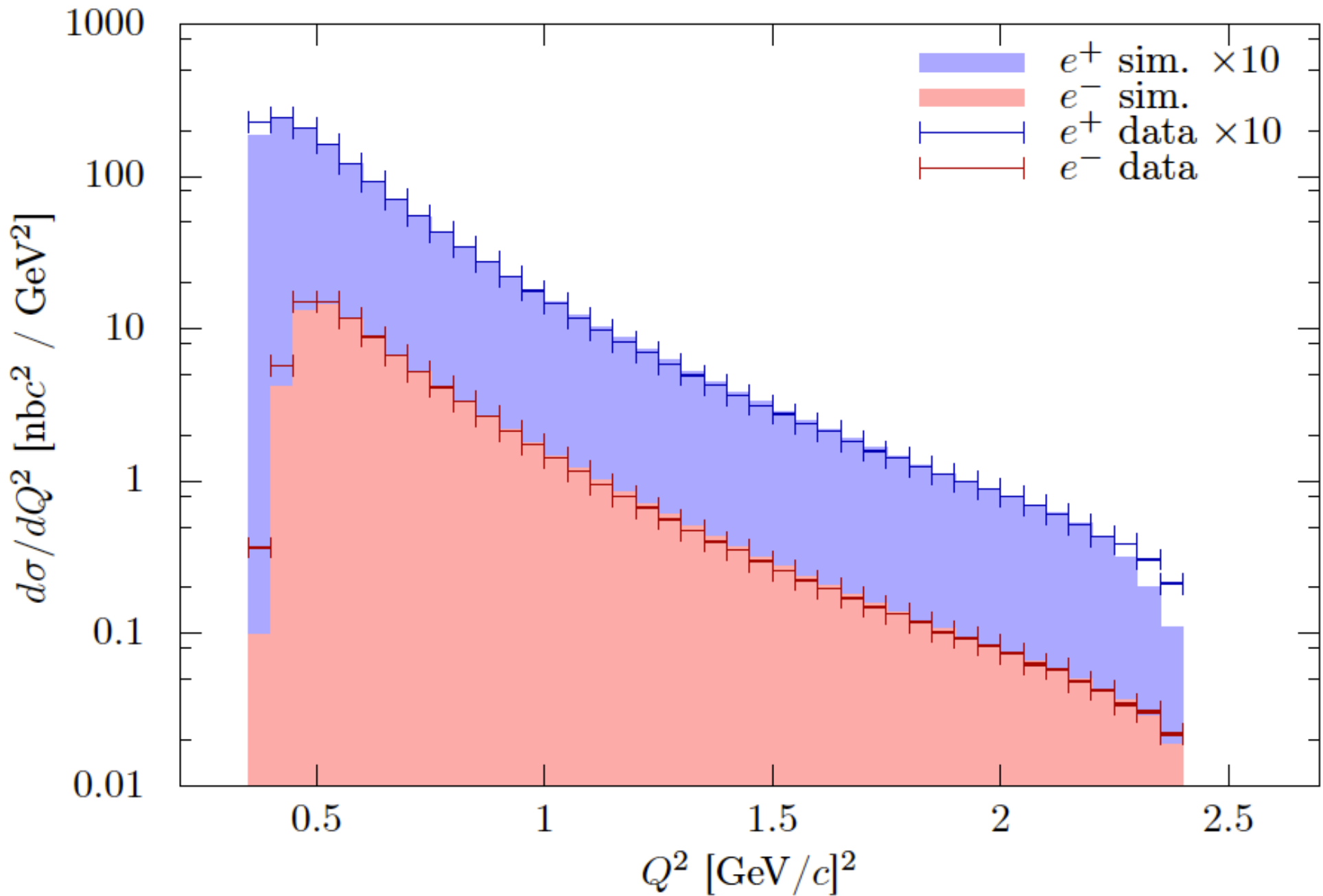
MIE / SC



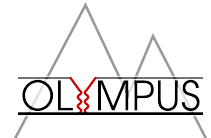
Yields



49

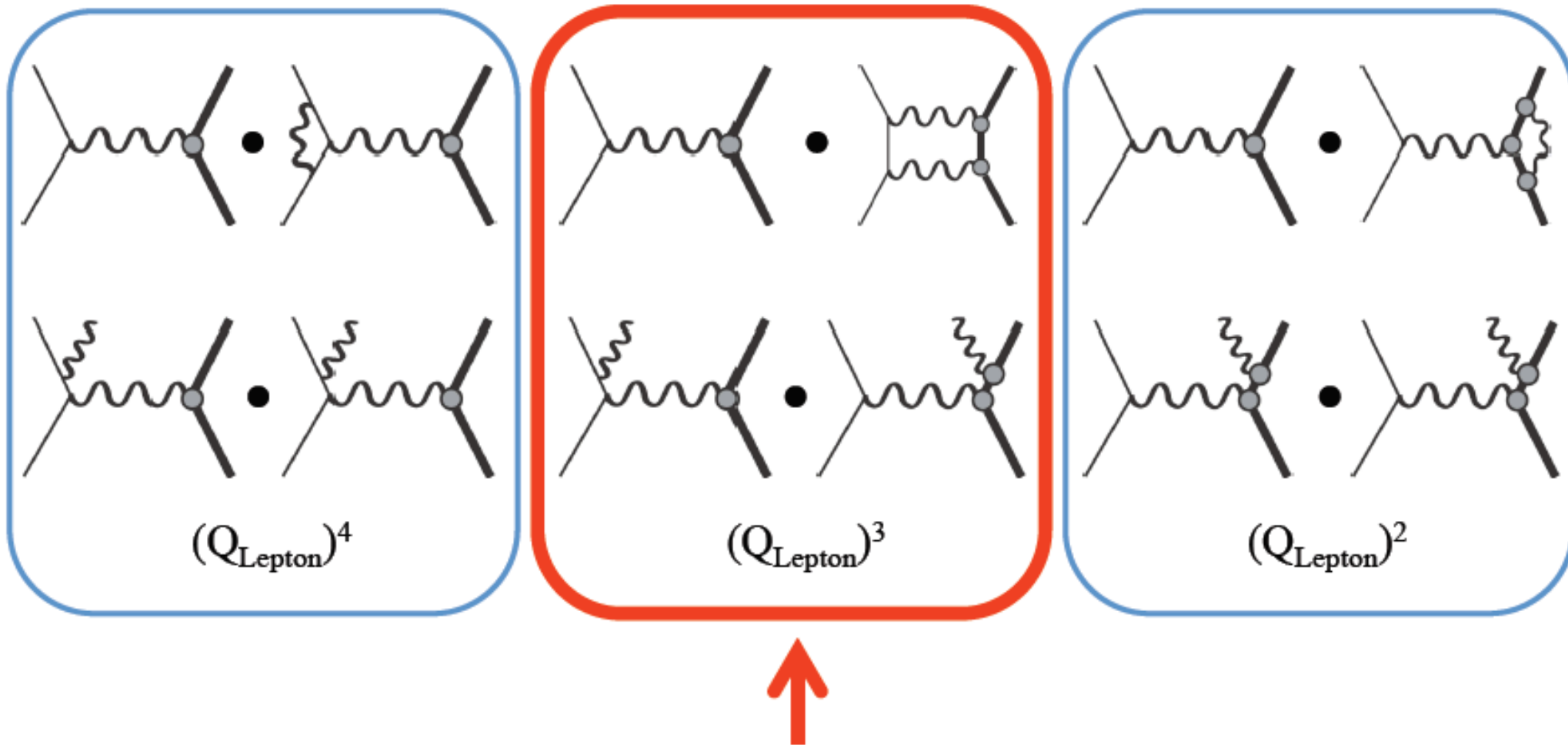


Radiative corrections of order α^3



50

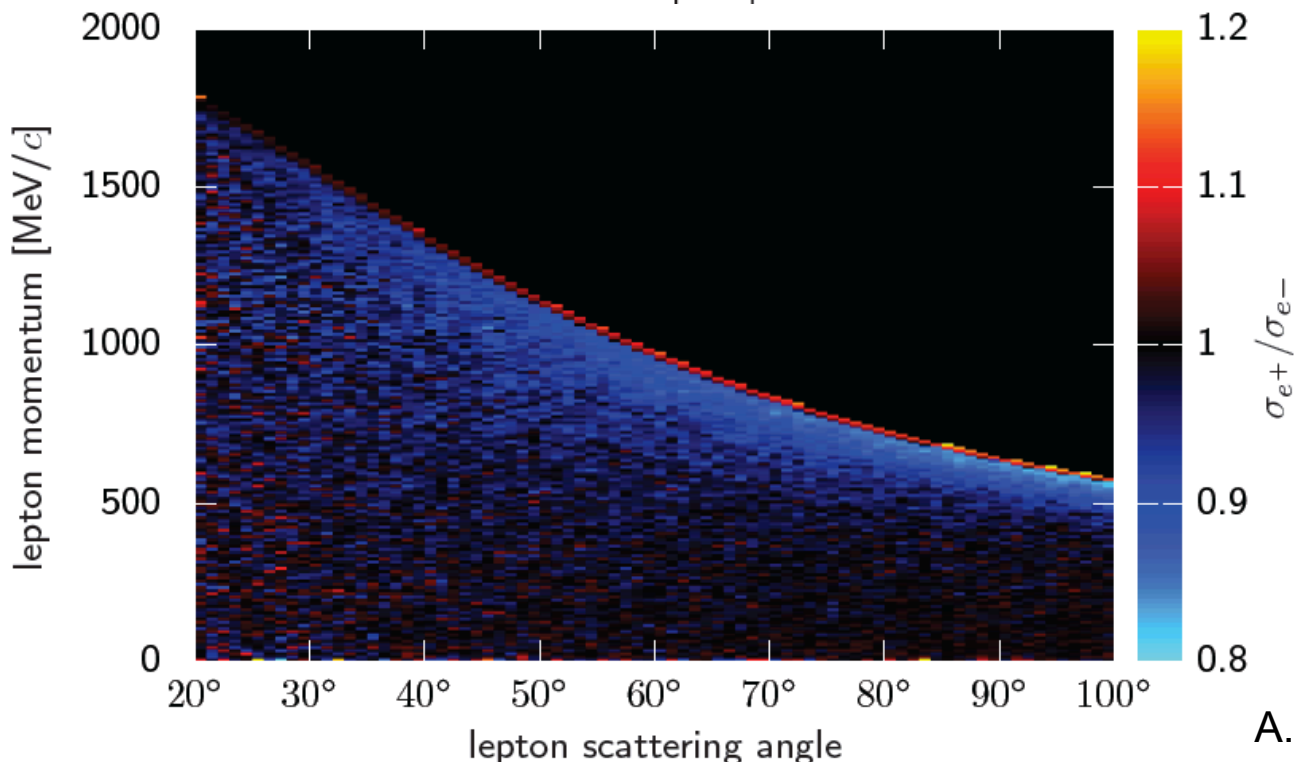
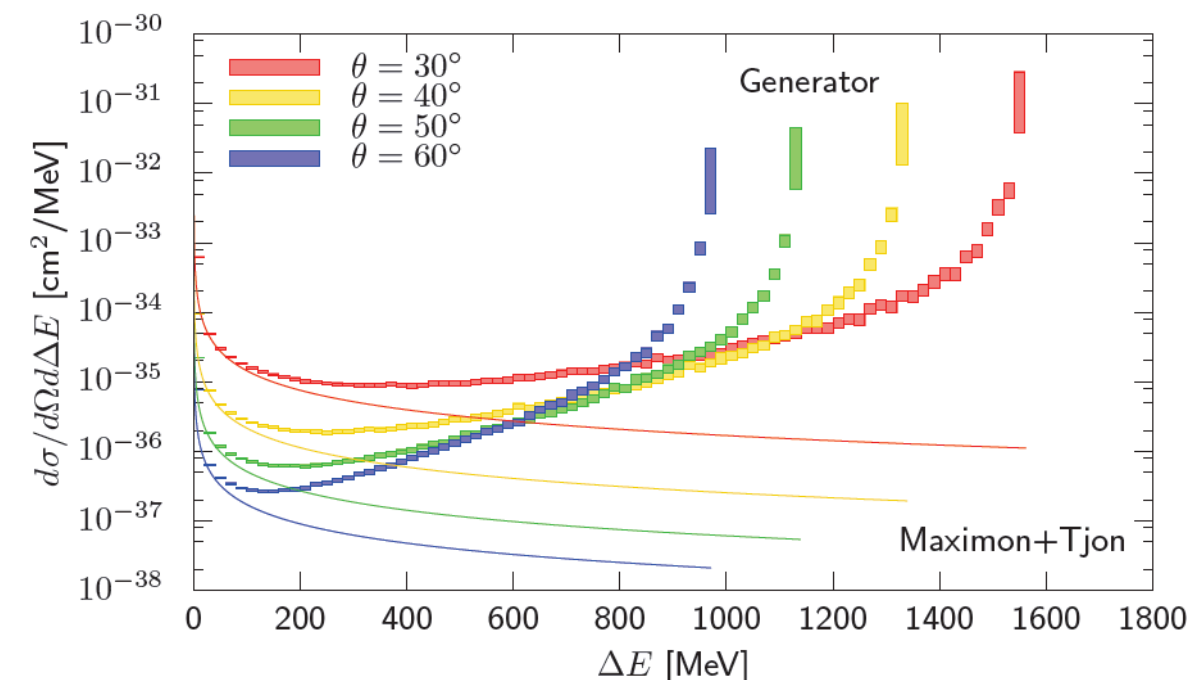
- Use MC framework to accurately implement all ‘standard’ RC and to extract effect from hard TPE
- Ensure consistency between different experiments



MIT radiative generator



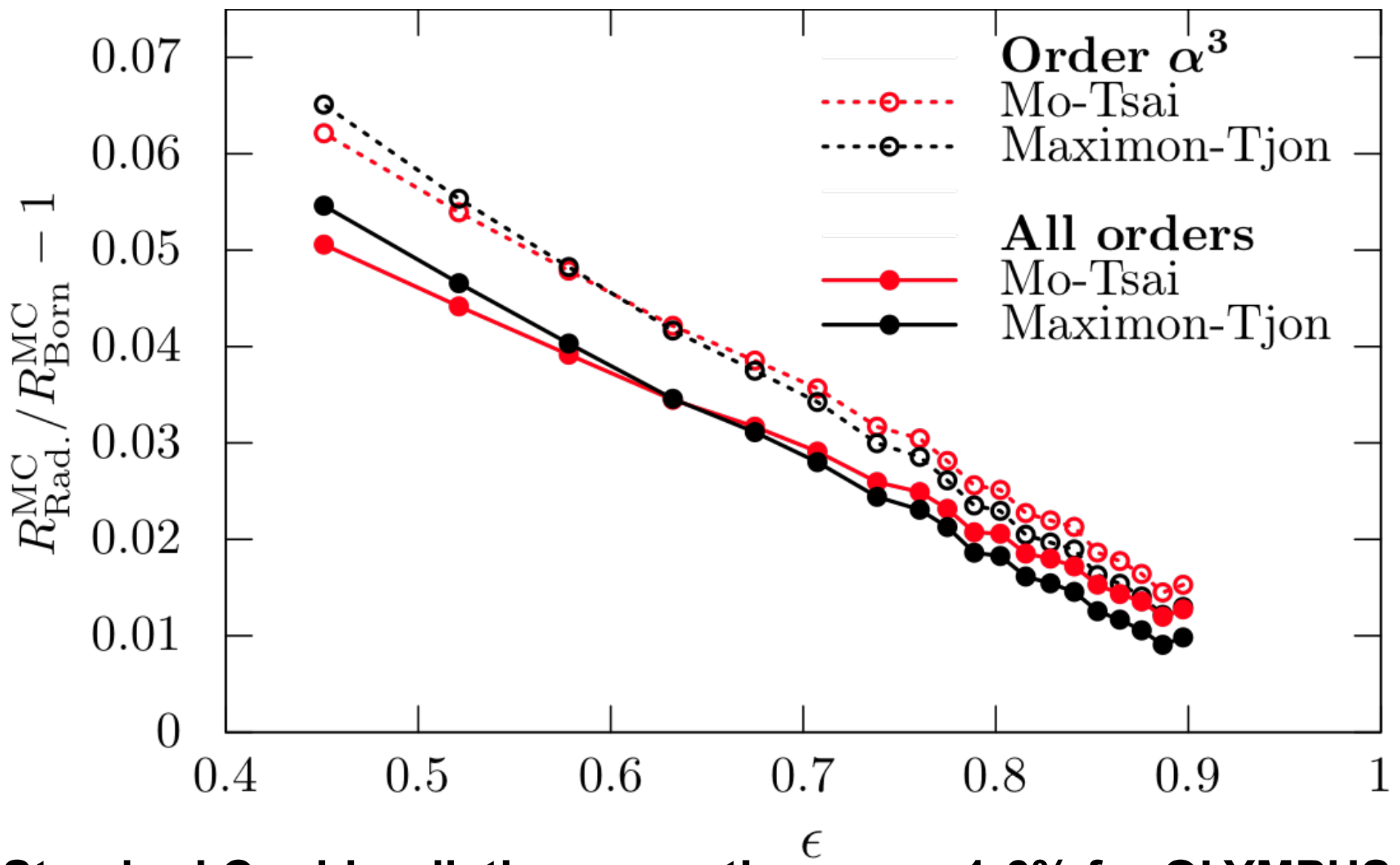
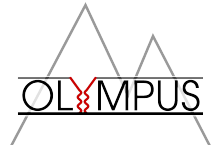
51



- **Avoids approximations**
- **Agreement with Maximon&Tjon (soft photons) at low ΔE**
- **Excellent agreement with VEPP-3 generator at $\mathcal{O}(\alpha^3)$**

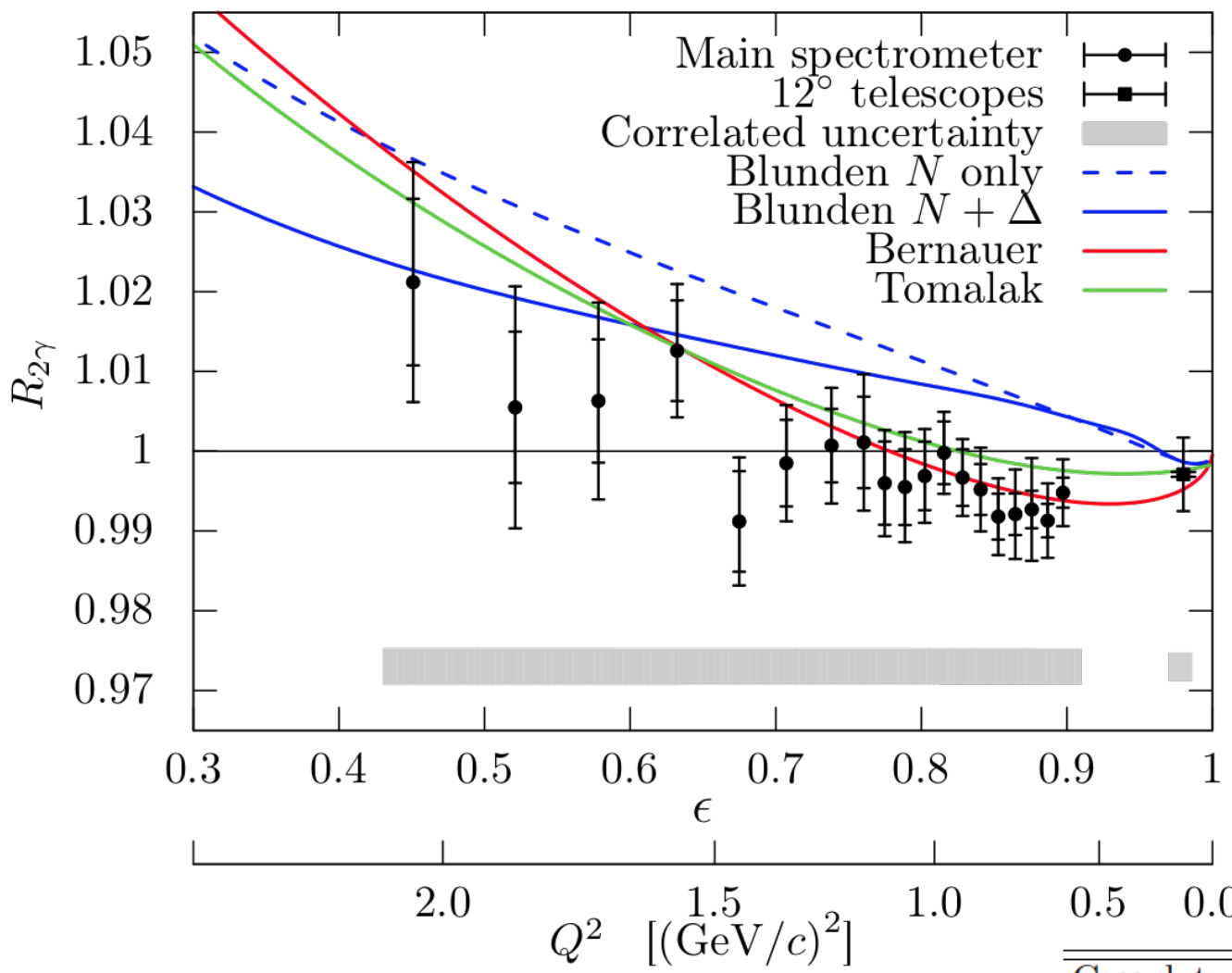
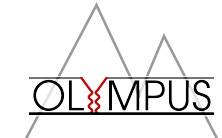
Effect on σ_{e+}/σ_{e-}

MIT radiative generator



- Standard C-odd radiative corrections are $\sim 1\text{-}6\%$ for OLYMPUS
- Variation due to higher orders at $\sim 1\%$ level

Result for hard two-photon exchange



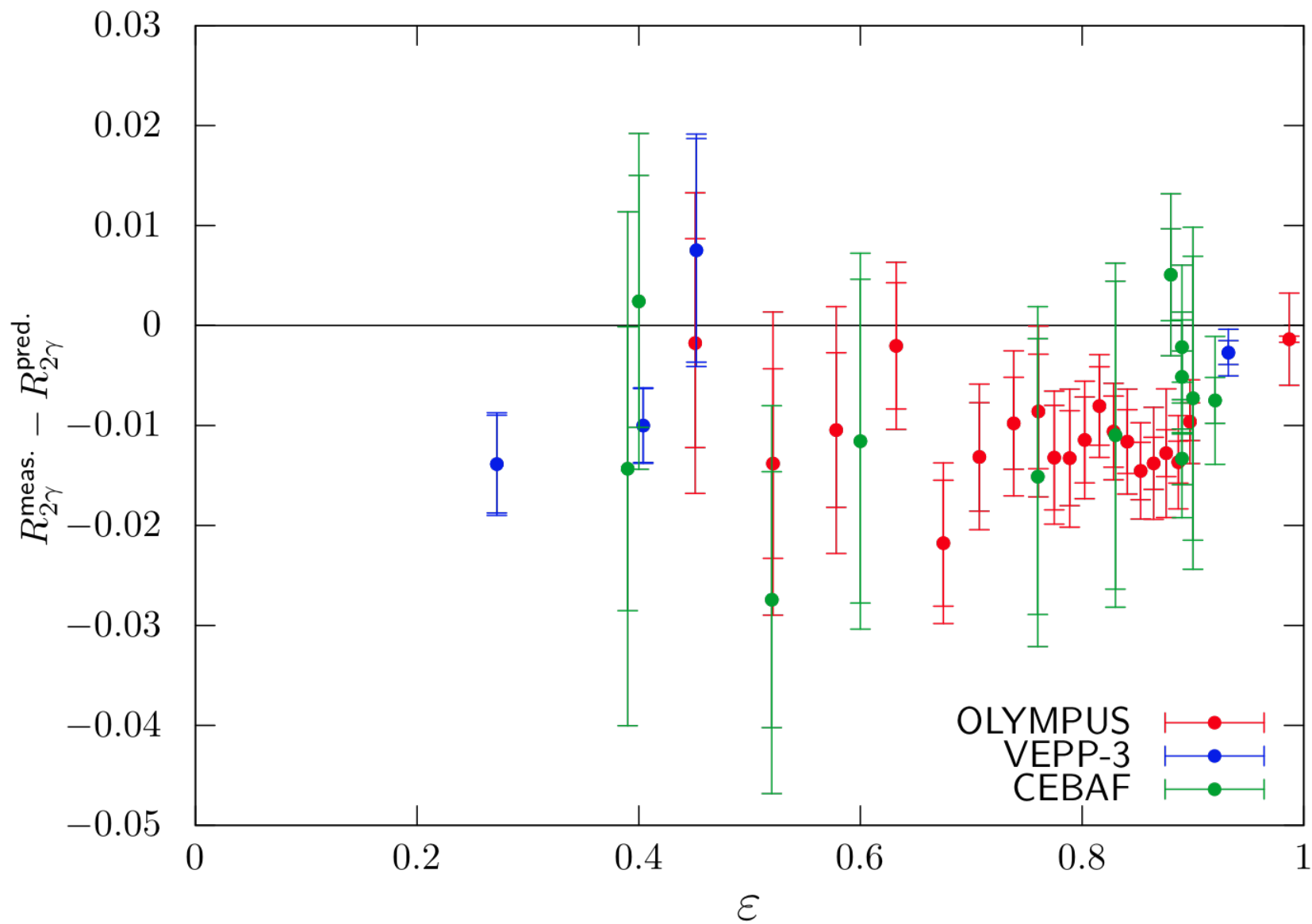
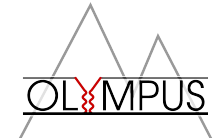
- Mo-Tsai to all orders
- Results based on 3.1 fb^{-1} , statistics 0.2 – 1%
- Hard TPE is small !
- Below Hadronic Model by Blunden at low Q^2
- Good agreement with phenomenology

Data needed at higher $Q^2 > 2.5 \text{ (GeV/c)}^2$ where TPE effects are expected to be larger

B.S. Henderson *et al.*, PRL 118, 092501 (2017)

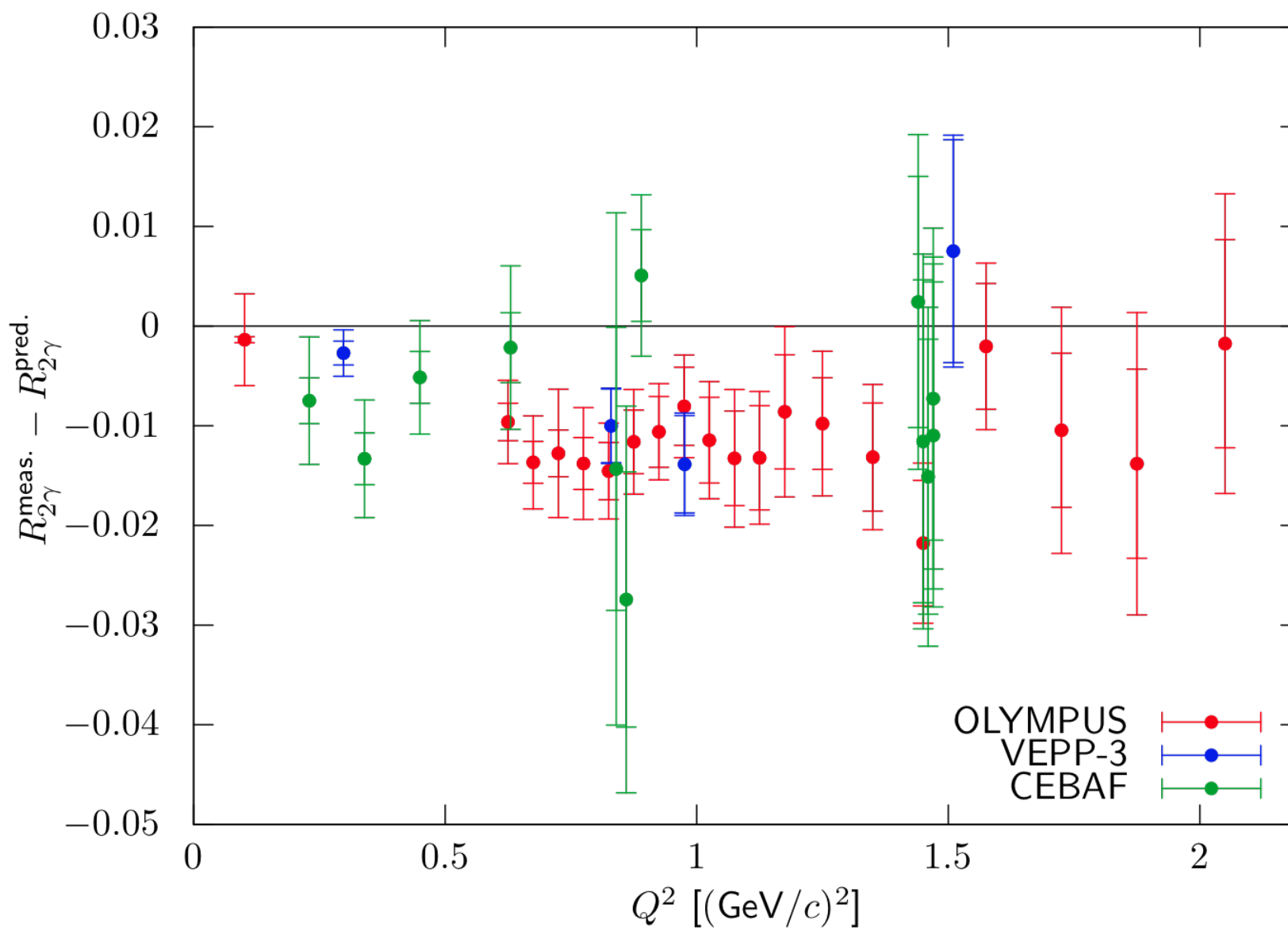
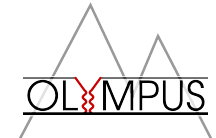
Correlated contributions	Uncertainty in $R_{2\gamma}$
Beam energy	0.04–0.13%
MIE luminosity	0.36%
Beam and detector geometry	0.25%
Uncorrelated contributions	
Tracking efficiency	0.20%
Elastic selection and background subtraction	0.25–1.17%

Comparison with VEPP-3 and CLAS



- OLYMPUS, VEPP-3 and CLAS (limited precision) all in agreement
- Hard TPE observed is small, below Blunden
- Need data at higher $Q^2 > 2.5 \text{ (GeV/c)}^2$ for validation where TPE *could* be sizable

Comparison with VEPP-3 and CLAS



- OLYMPUS, VEPP-3 and CLAS (limited precision) all in agreement
- Hard TPE observed is small, below Blunden
- Need data at higher $Q^2 > 2.5$ (GeV/c) 2 for validation where TPE *could* be sizable

Implications

Dedicated workshops and conference sessions:

- **NSTAR2017, Columbia, SC, August 20-23, 2017**
<http://nstar2017.physics.sc.edu/>
- **Hadronic Physics with Lepton and Hadron Beams, Jlab, Sep. 5-8, 2017**
<https://www.jlab.org/conferences/hadrons2017/index.html>
- **JPOS2017, JLab, Sep. 12-15, 2017**
<https://www.jlab.org/conferences/JPos2017/>
- **EW Box, Amherst, MA, Sep. 28-30, 2017**
<http://www.physics.umass.edu/acfi/seminars-and-workshops/the-electroweak-box>
- **EINN2017, Paphos, Cyprus, Oct. 29 – Nov. 4, 2017**
<http://einnconference.org/2017/>
- **This workshop (668. WE-Heraeus-Seminar), Bad Honnef, Germany, Apr. 23-27, 2018**
<https://indico.him.uni-mainz.de/event/14/>

More data!

Possible future high- Q^2 measurement of $R_{2\gamma}$:

Need 3 GeV e^+ and e^- beams to reach $Q^2 = 4.5 \text{ (GeV/c)}^2$

Add positron source to CEBAF?



Jefferson Lab Positron Working Group <https://wiki.jlab.org/pwgwiki>

E. Voutier, J. Grames

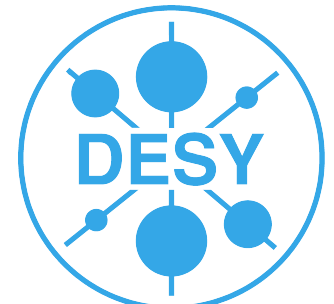
TPE measurements in Halls A (spectrometers), Hall B (CLAS12)

JLAB has detectors and equipment but no positrons

OLYMPUS-II (or “Above-OLYMPUS”) at DESY

D. Hasell, R. Milner, U. Schneekloth

DESY has positrons but no detectors and equipment

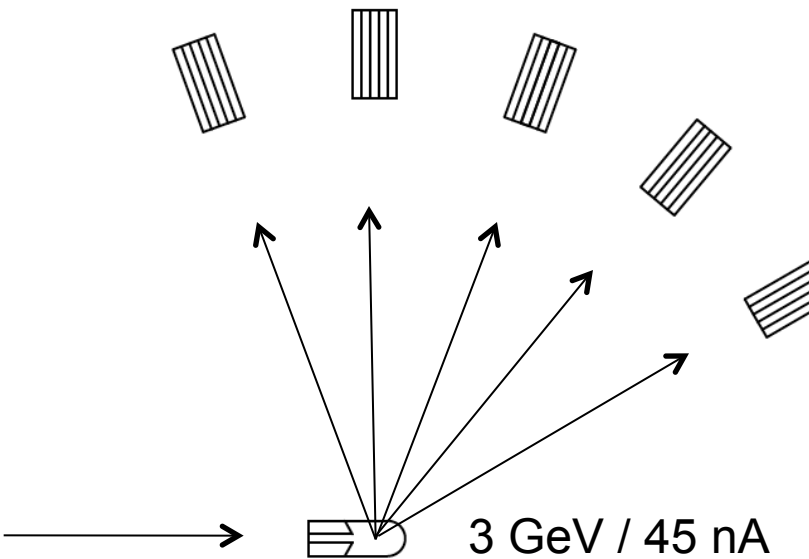


Above OLYMPUS

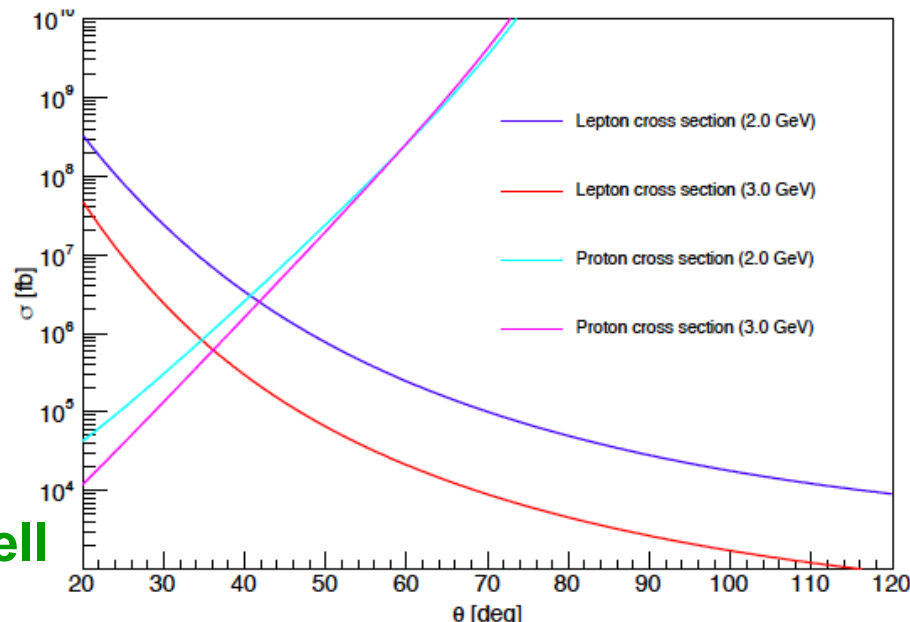
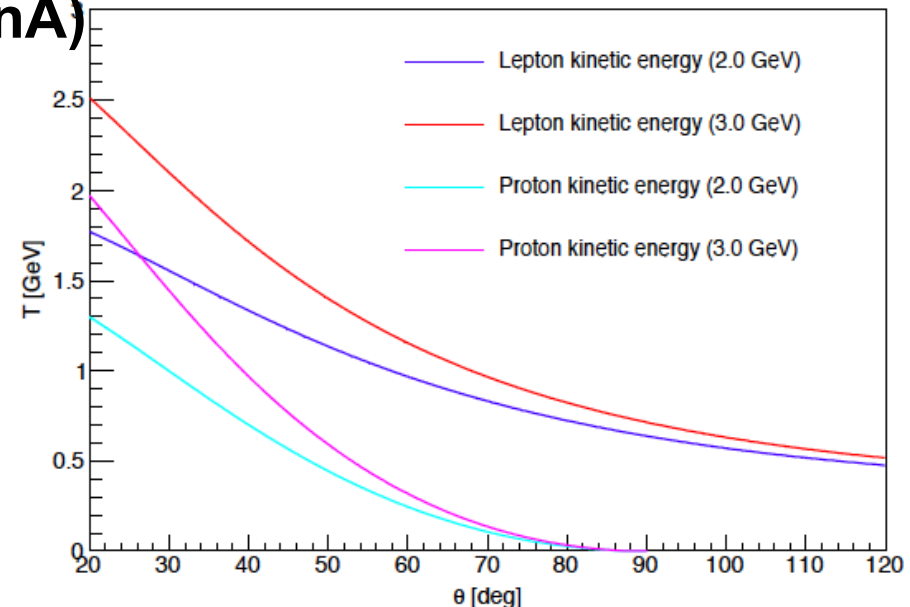
OLYMPUS-II (or “Above-OLYMPUS”) at DESY



- Considering test beamline to extract e^+/e^- beams from DESY-II (0.5-6.3 GeV, 12.5 Hz repetition, 30/60nA)
- PbWO₄ calorimeter arrays;
A4 liquid hydrogen target (Mainz)



θ	Q^2 (GeV/c) ²	ϵ	$d\sigma/d\Omega$ fb	Events/day
30°	1.69	0.825	2.41×10^6	8.91×10^4
50°	3.00	0.554	6.51×10^4	2.42×10^3
70°	3.82	0.329	8.94×10^3	3.30×10^2
90°	4.29	0.184	2.65×10^3	9.80×10^1
110°	4.57	0.096	1.20×10^3	4.44×10^1



D. Hasell

Summary

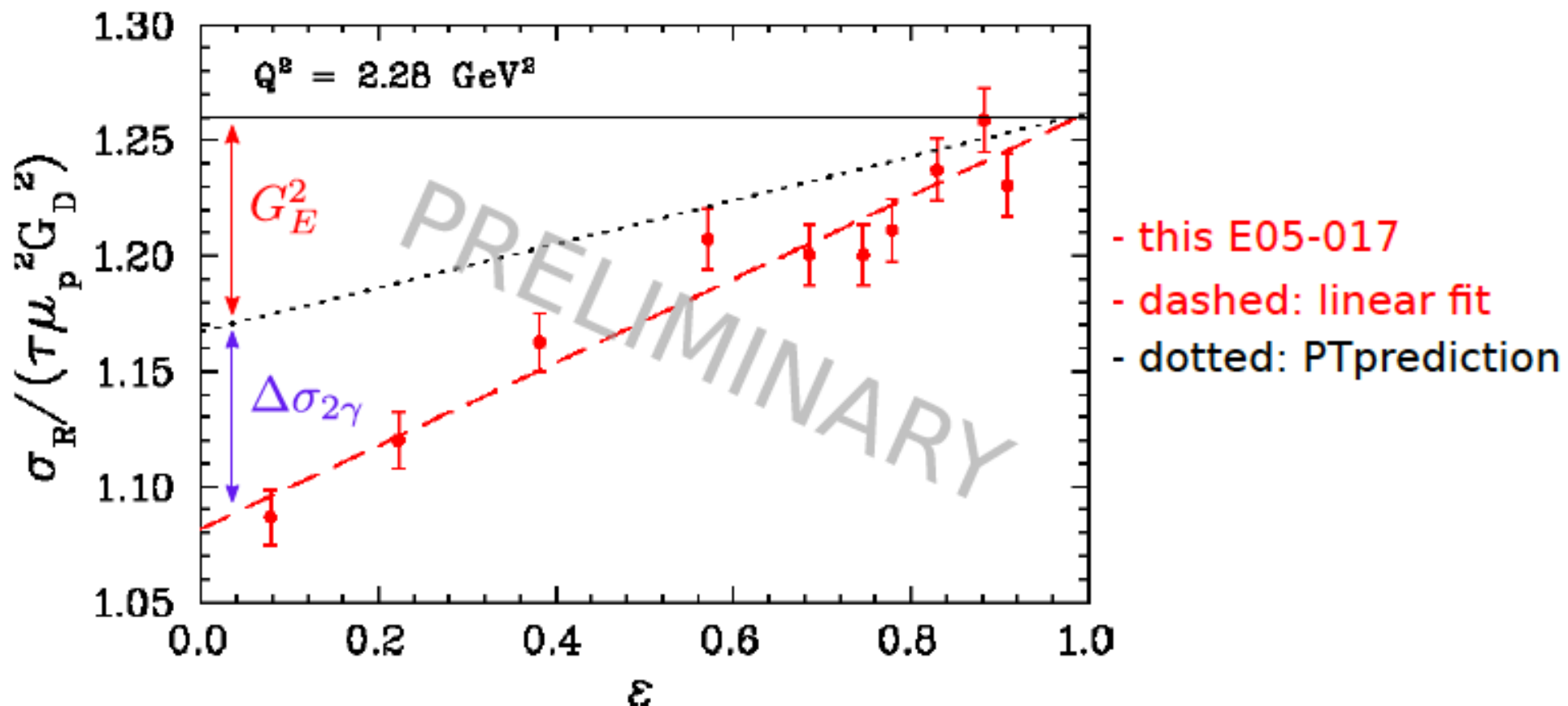
- The limits of OPE have been reached with the achieved precision
 - Large discrepancy between unpolarized and polarized data
 - Nucleon elastic form factors, particularly G_E^p under doubt
- The TPE hypothesis is suited to remove form factor discrepancy, however calculations of TPE are model-dependent
- New observables: ϵ dependence of polarization transfer, ϵ -nonlinearity of cross sections, single-spin asymmetries, e^+/e^- comparisons
- Positron/electron comparisons to test TPE: VEPP-3, CLAS, **OLYMPUS**
- **OLYMPUS:** Hard TPE found to be
 - consistent with other TPE experiments but more precise
 - smaller than expected by standard hadronic theory at low Q^2
 - consistent with phenomenology at $Q^2 < 2.5 \text{ (GeV/c)}^2$
- Need to improve theoretical precision for radiative corrections !
- TPE is to be tested at higher $Q^2 > 2.5 \text{ (GeV/c)}^2$ with future experiments (e.g. with positron source at CEBAF or extracted beams at DESY)
- Broader Impact:
 - gamma-Z box in PVES; TPE effects in eA and inelastic scattering;
 - Proton radius puzzle: elastic $\{\mu, e\}^\pm p$ scattering with MUSE@PSI

Backup

PRELIMINARY RESULTS

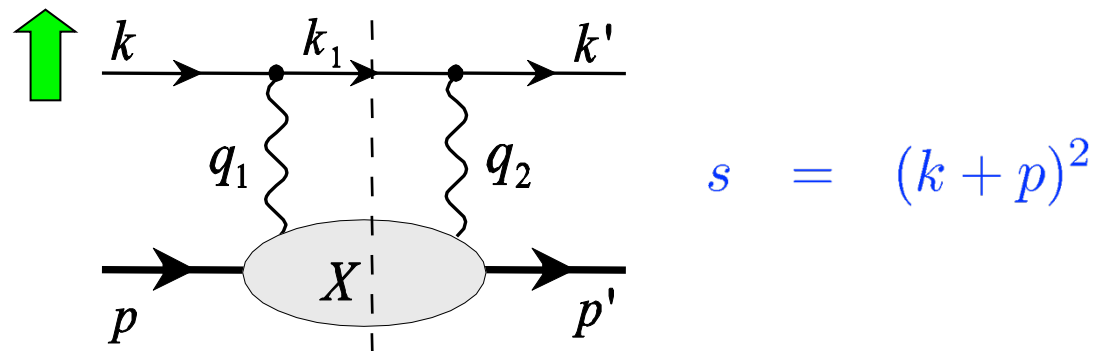
- Rosenbluth separation:

- linear fit to extract FF ratio
- second fit (not shown) with data shifted by δ_{slope} for systematics
- $\Delta\sigma_{2\gamma}$ separates TPE size from G_E^2 slope



Imaginary part: Single-spin asymmetries

spin of beam OR target
NORMAL to scattering plane



on-shell intermediate state ($M_X = W$)

$$A_n = -\frac{1}{(2\pi)^3} \frac{e^2 (1-\varepsilon)}{8 Q^2} \int_{M^2}^s dW^2 \frac{|\vec{k}_1|^2}{4\sqrt{s}} \int d\Omega_{k1} \frac{1}{Q_1^2 Q_2^2} \mathcal{I} (L_{\alpha\mu\nu} H^{\alpha\mu\nu})$$

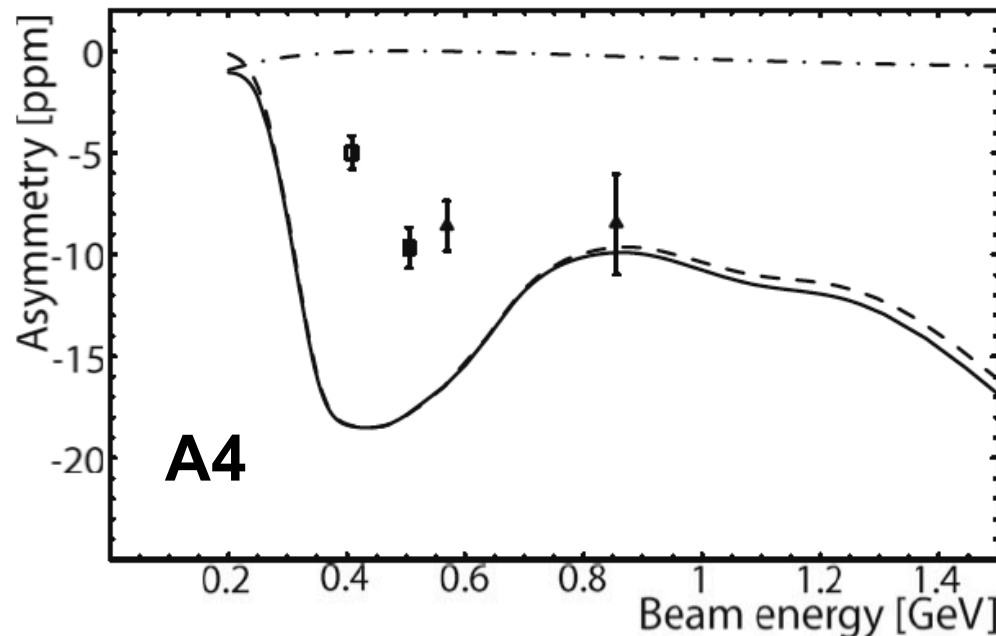
E.g. target normal spin asymmetry

$$A_n = \sqrt{\frac{2\varepsilon(1+\varepsilon)}{\tau}} \frac{1}{\sigma_R} \left\{ -G_M \mathcal{I} \left(\delta \tilde{G}_E + \frac{\nu}{M^2} \tilde{F}_3 \right) + G_E \mathcal{I} \left(\delta \tilde{G}_M + \left(\frac{2\varepsilon}{1+\varepsilon} \right) \frac{\nu}{M^2} \tilde{F}_3 \right) \right\},$$

↑Beam: PVES at Bates, MAMI and Jlab;

↑Target: (Quasi-)elastic: E05-015: ${}^3\text{He} \uparrow(\text{e}, \text{e}')$, E08-005: ${}^3\text{He} \uparrow(\text{e}, \text{e}'\text{n})$
Deep inelastic: E07-013; HERMES $\text{p} \uparrow(\text{e}, \text{e}')$

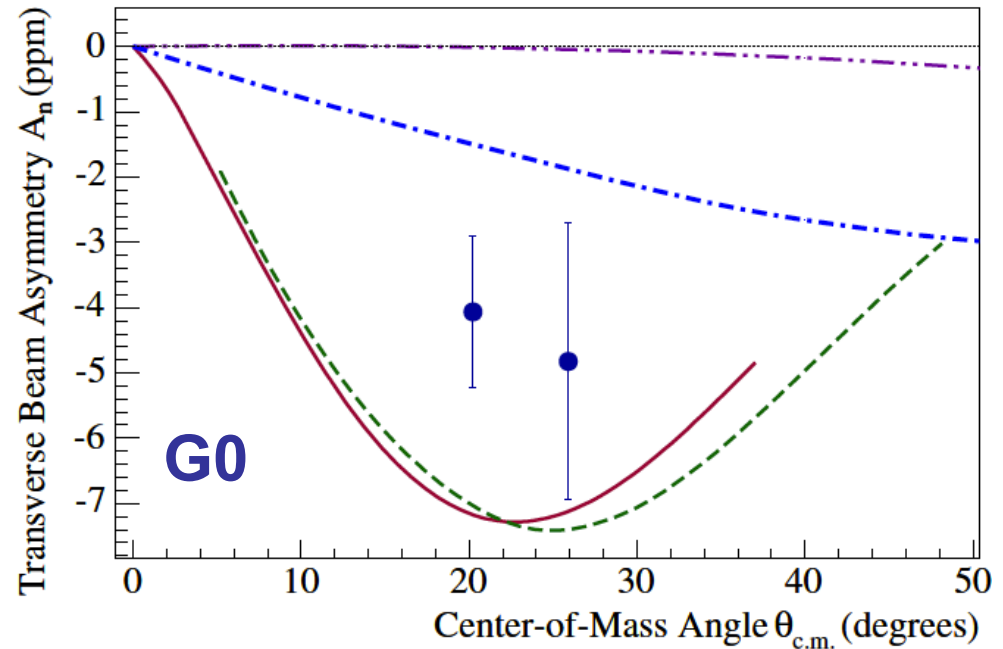
Beam-normal single spin asymmetry



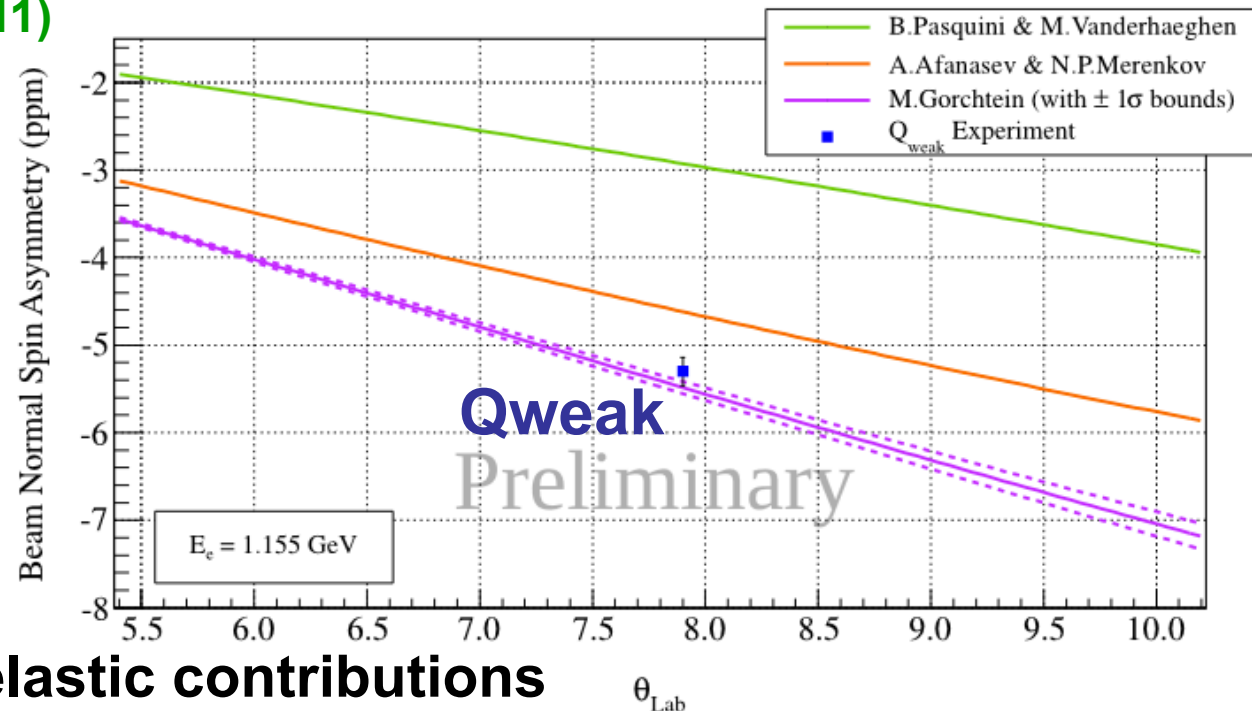
F. Maas *et al.*, PRL 99, 092301 (2005);
 S. Baunack, EPJ ST198, 343 (2011)

$p(e\uparrow, e')$ at forward angles

Qweak (preliminary):
 $A_n = (-5.35 \pm 0.07 \pm 0.15)$ ppm
 B.P. Waidyawansa, PAVI2014,
 arXiv:1604.04602

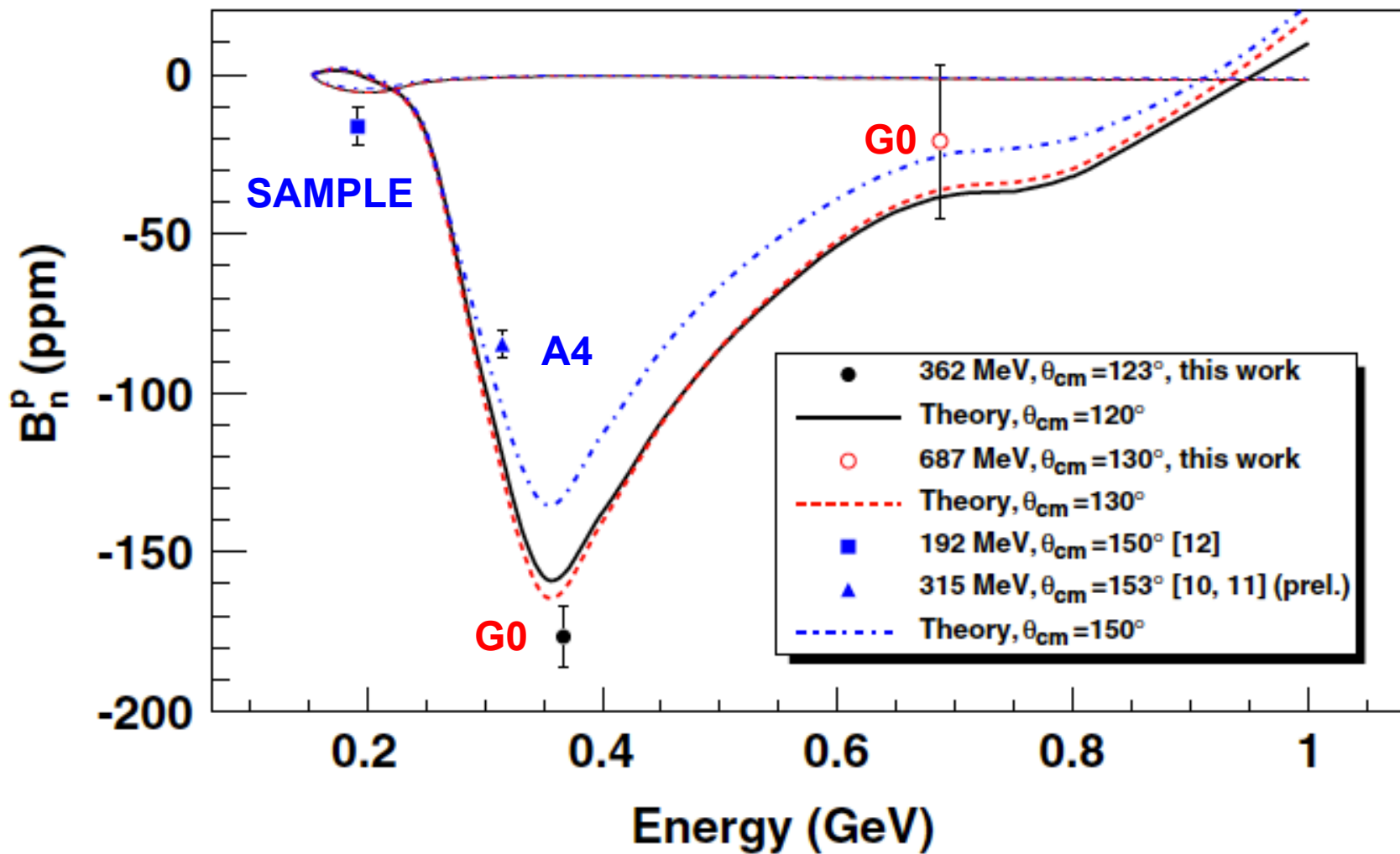


D. Armstrong *et al.*, PRL 99, 092301 (2007)



BNSSA's dominated by inelastic contributions

Beam-normal single spin asymmetry



$p(e\uparrow, e')$ at backward angles:

G0 bwd: D. Androic *et al.*, PRL 107, 022501 (2011)

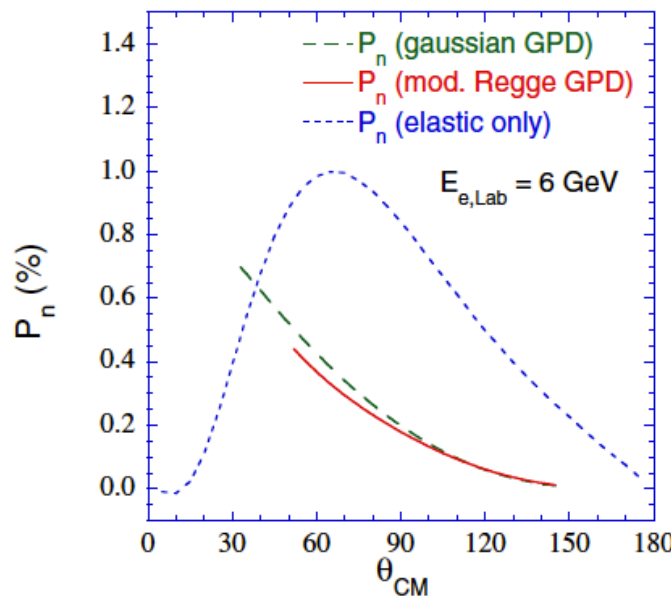
A4 bwd: S. S. Baunack, EPJ ST198, 343 (2011)

SAMPLE: S. Wells *et al.*, PRC 63, 064001 (2001)

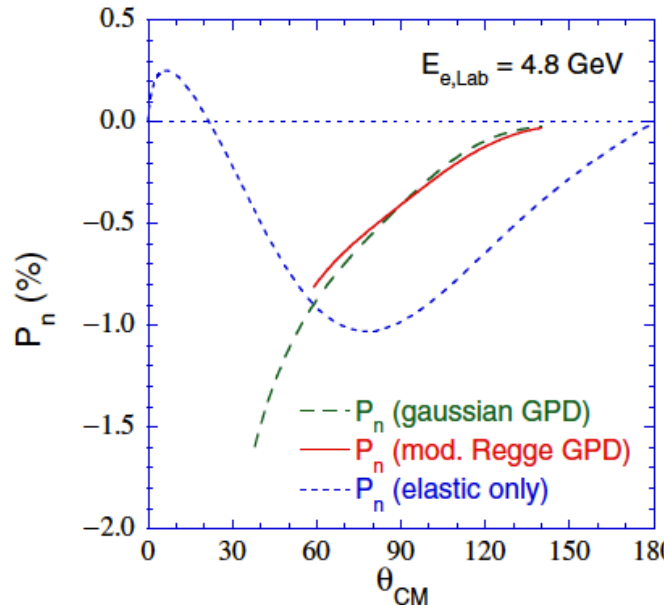
BNSSA's dominated by inelastic contributions

Target-normal single spin asymmetry

Normal Polarization or Analyzing Power - Proton

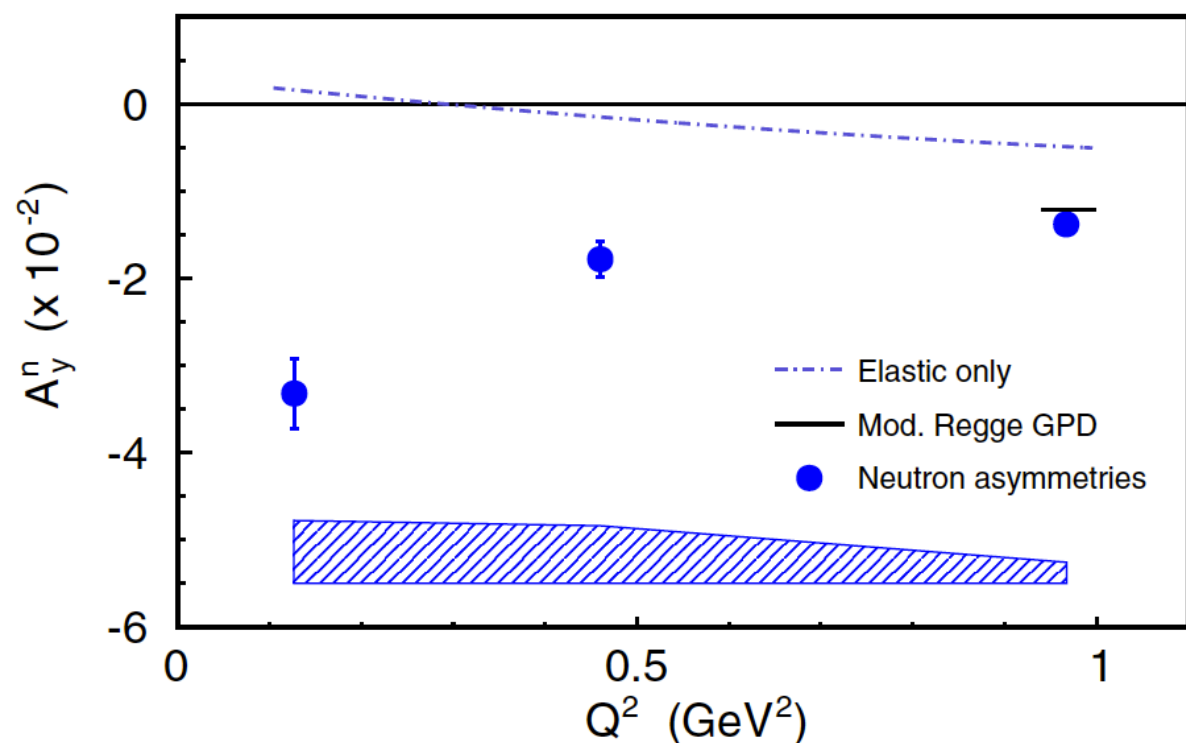


Normal Polarization or Analyzing Power - Neutron



A. Afanasev et al.,
PRD 72, 013008 (2005)
(elastic)

%-level asymmetries
opposite sign for p&n



${}^3\text{He} \uparrow(e,e')$: E05-015 (quasielastic)

Y.-W. Zhang et al.,
PRL 115, 172502 (2015)

Theory:
Y.C. Chen et al.,
PRL 93, 122301 (2004)

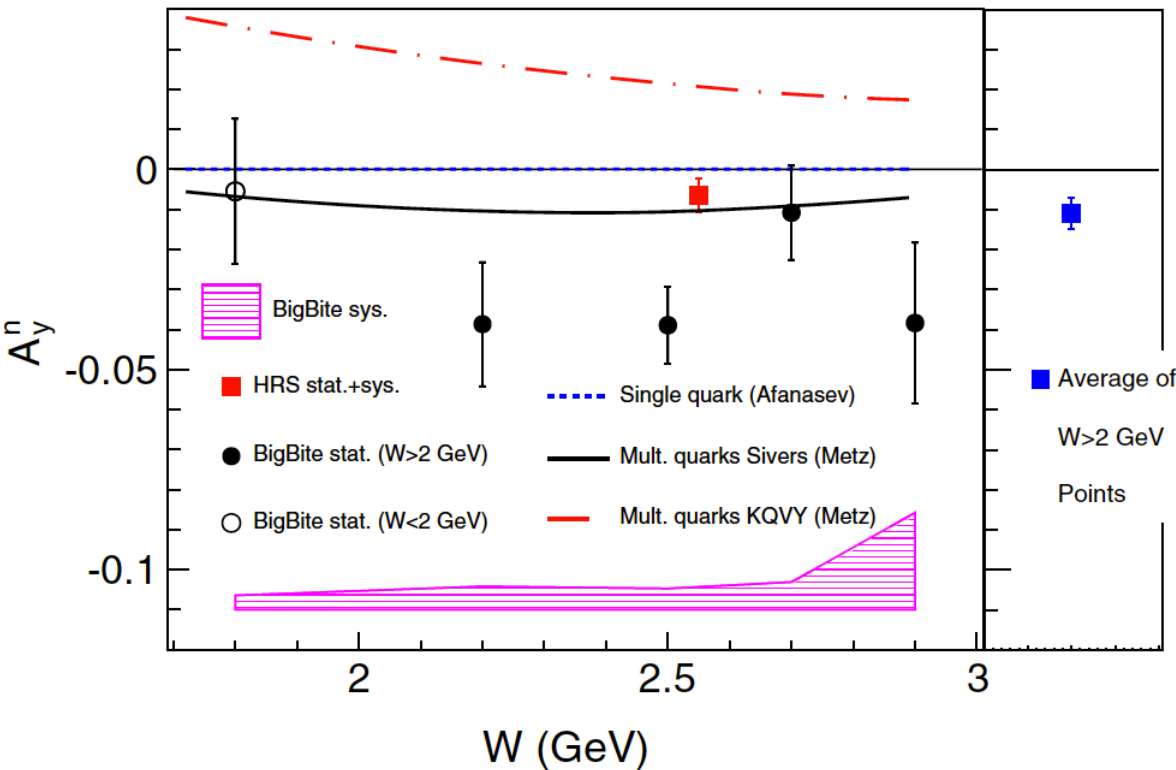
Further:

${}^3\text{He} \uparrow(e,e'n)$: E08-005 (quasielastic)

Target-normal single spin asymmetry

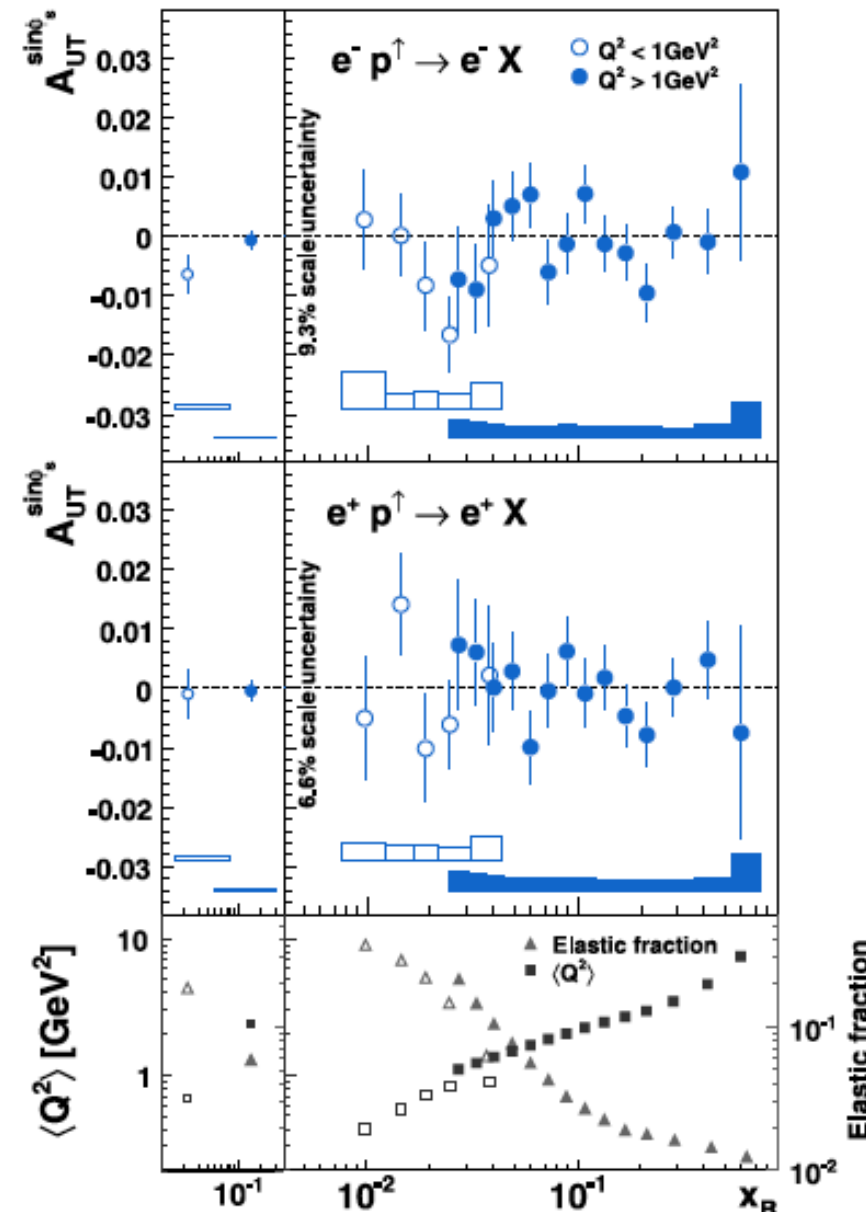
$^3\text{He} \uparrow(e, e')X$: E07-013 (DIS)

J. Katich *et al.*, PRL 113, 022502 (2014)



$p \uparrow(e, e')X$: HERMES (DIS)

A. Airapetian *et al.*, PLB 682, 351 (2010)



Single-quark: 10^{-4} -level asymmetries

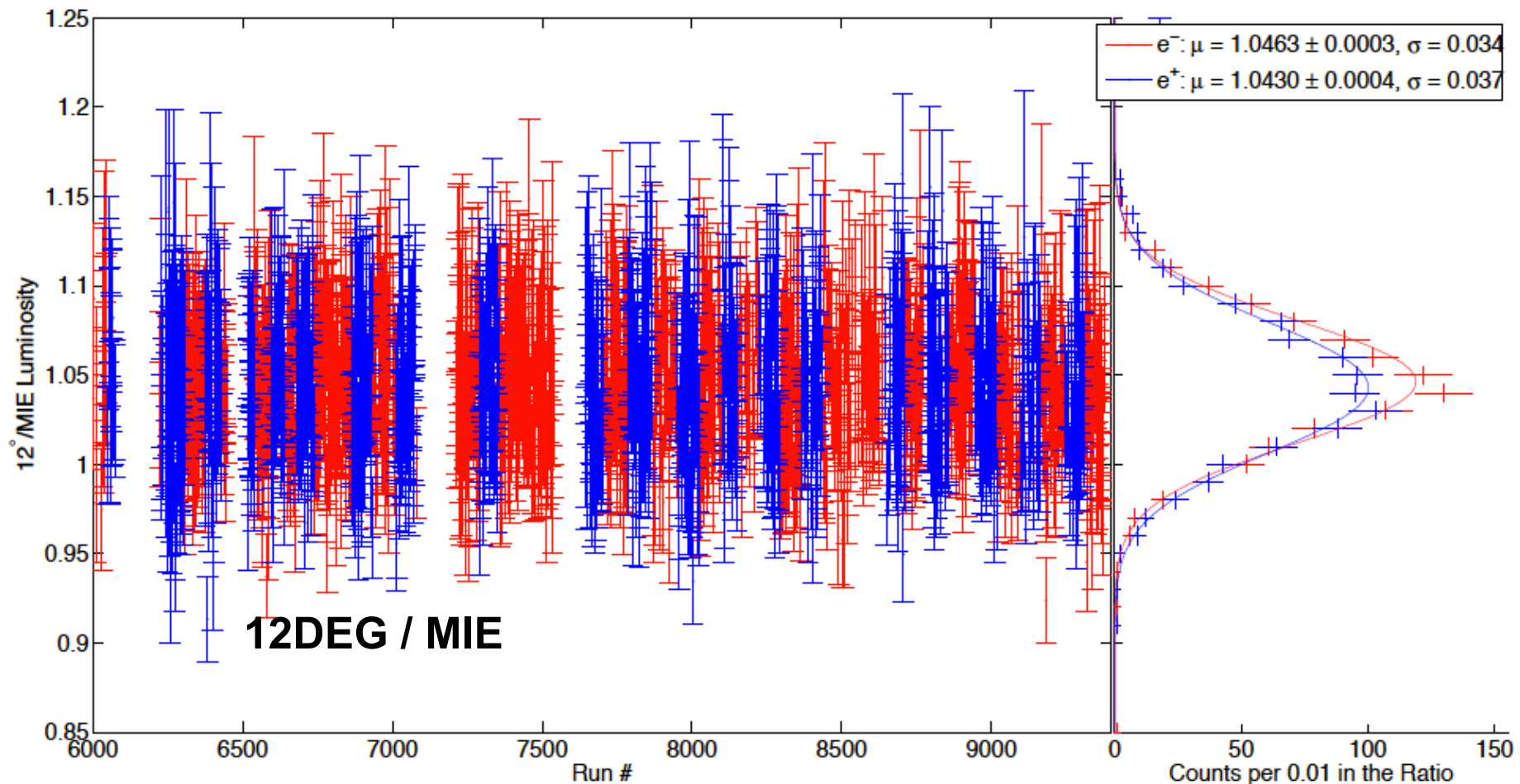
A. Afanasev *et al.*, PRD77, 014028 (2008)

Multi-quark: %-level asymmetries

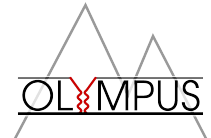
A. Metz *et al.*, PRD 86, 094039 (2012)

Luminosity monitoring

- Five redundant systems: Slow Control, SYMB, MIE, 12DEG-L,R
- Absolute luminosity from each rate to a few %
- Ratio of e^+/e^- luminosities for $R_{2\gamma}$ to sub %
- Time variation, mean and variance, systematics from comparisons
- Excellent agreement between SC, MIE, and 12DEG-L,R
- Final luminosity ratio from MIE, using 12DEG for high- ϵ data point

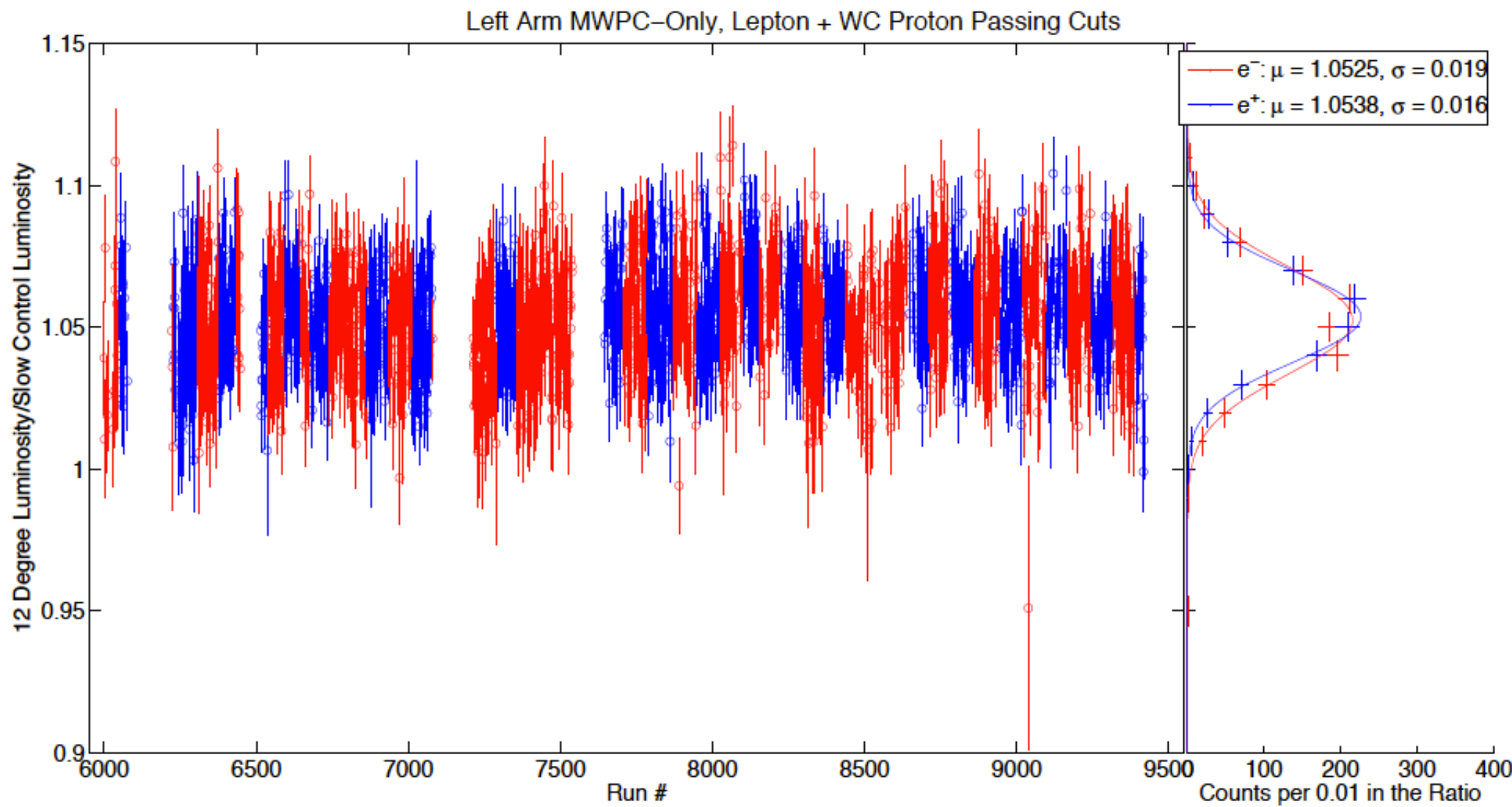


Luminosity monitoring

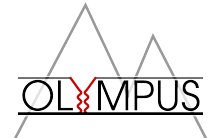


68

12DEG-L / SC

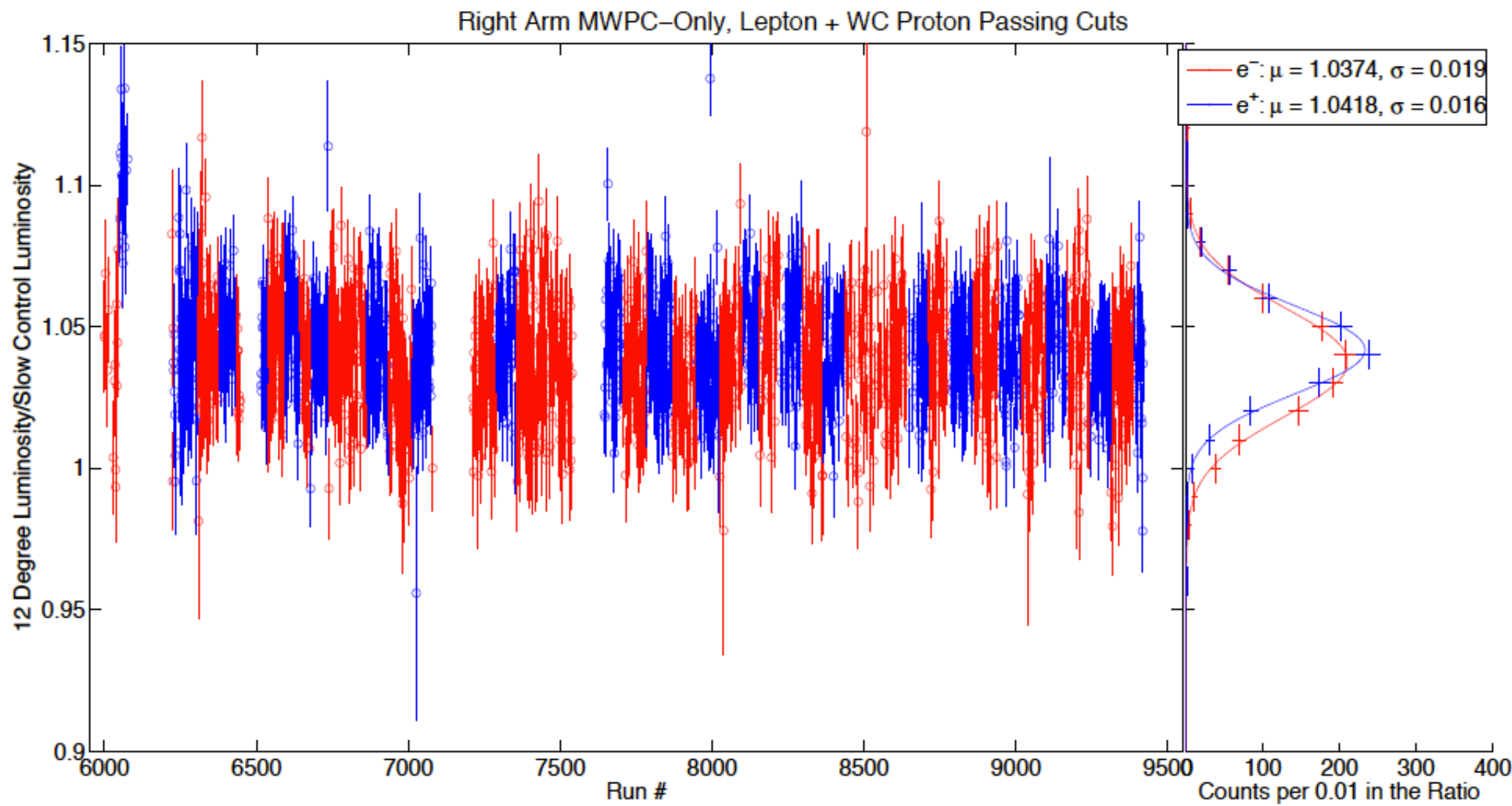


Luminosity monitoring

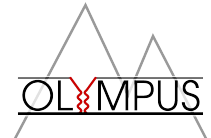


69

12DEG-R / SC

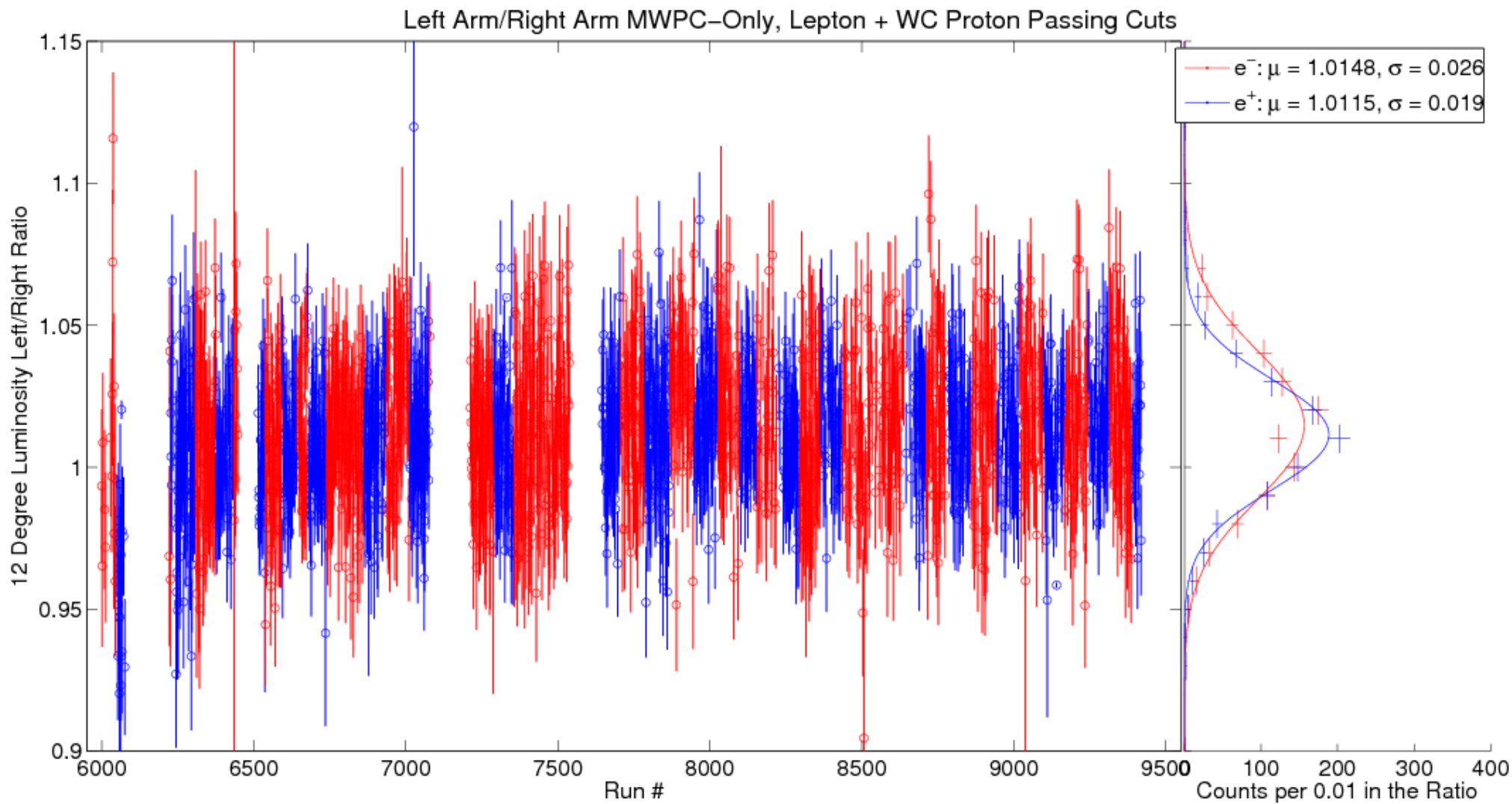


Luminosity monitoring

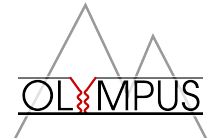


70

12DEG-L / R

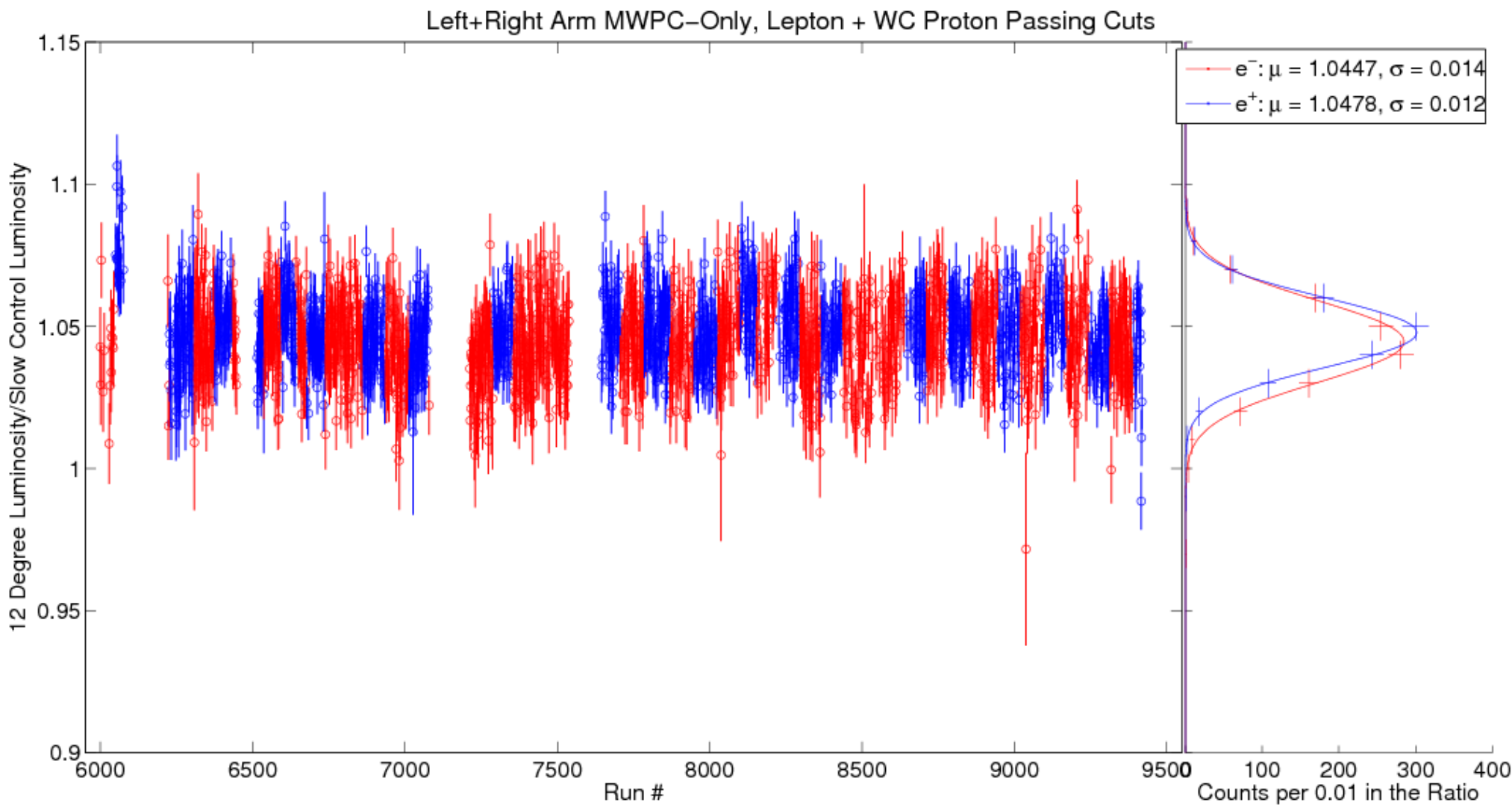


Luminosity monitoring



71

12DEG L+R / SC

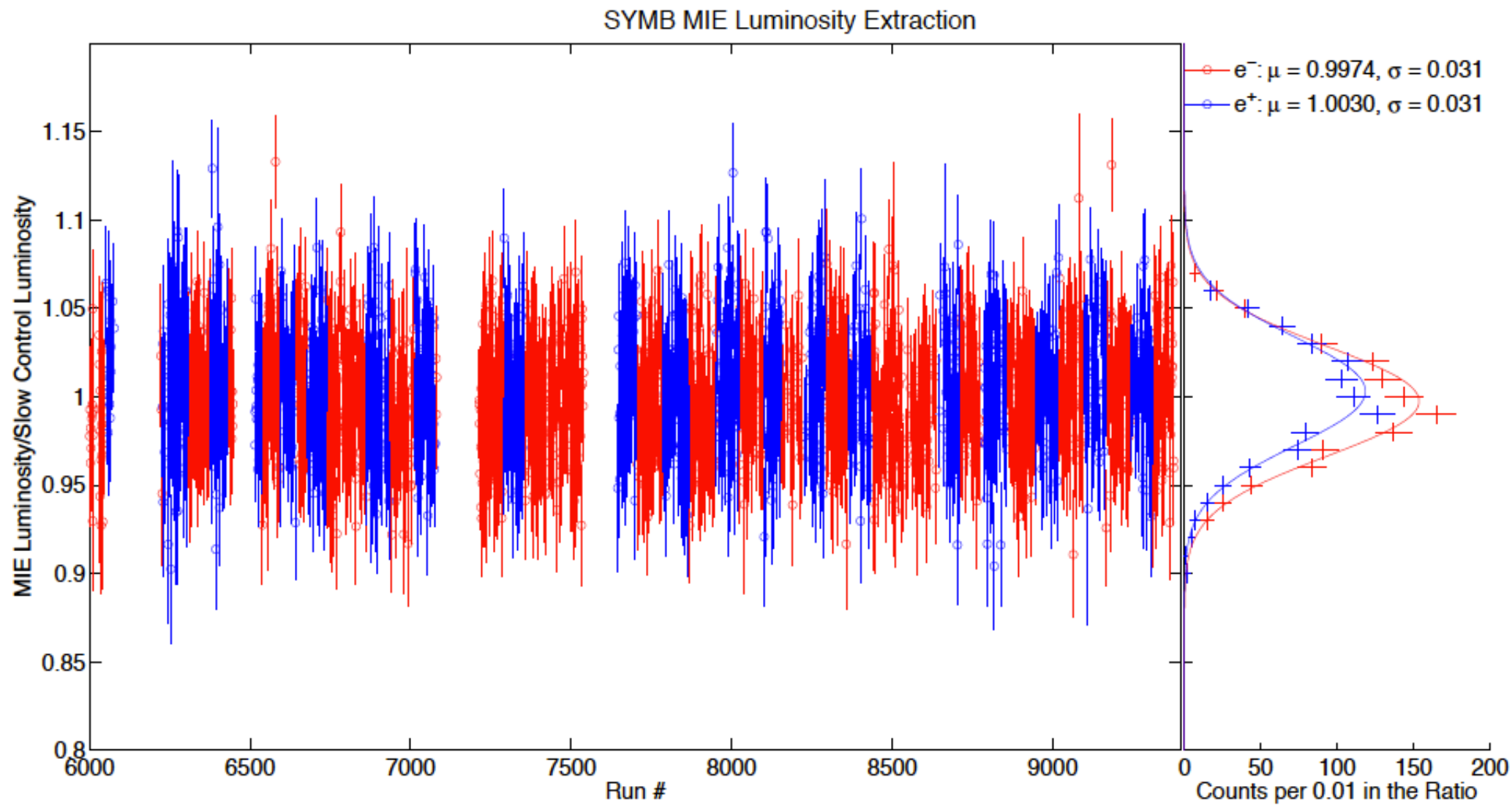


Luminosity monitoring

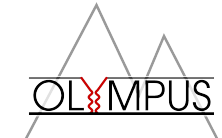


72

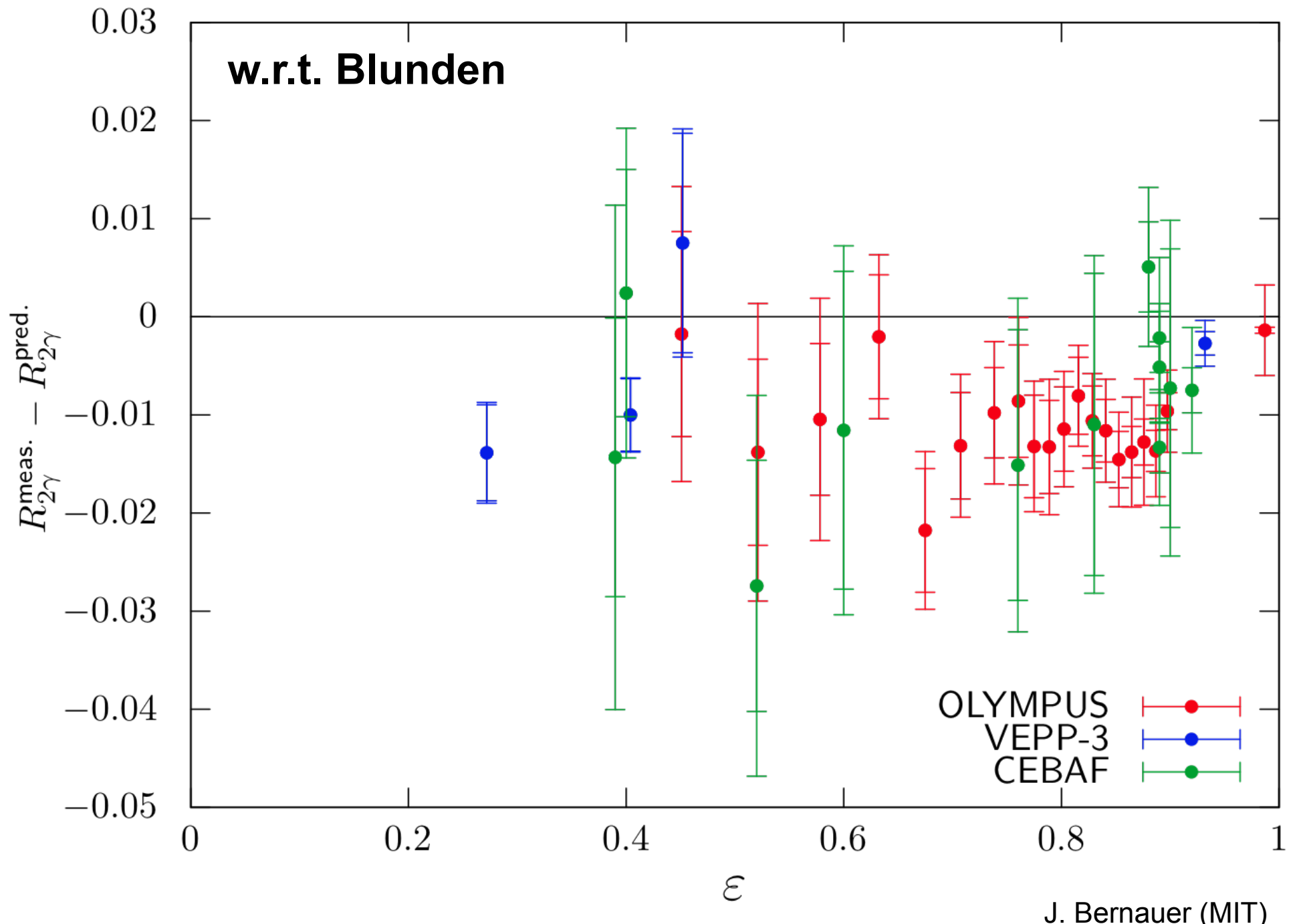
MIE / SC



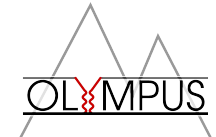
Comparison with VEPP-3 and CLAS



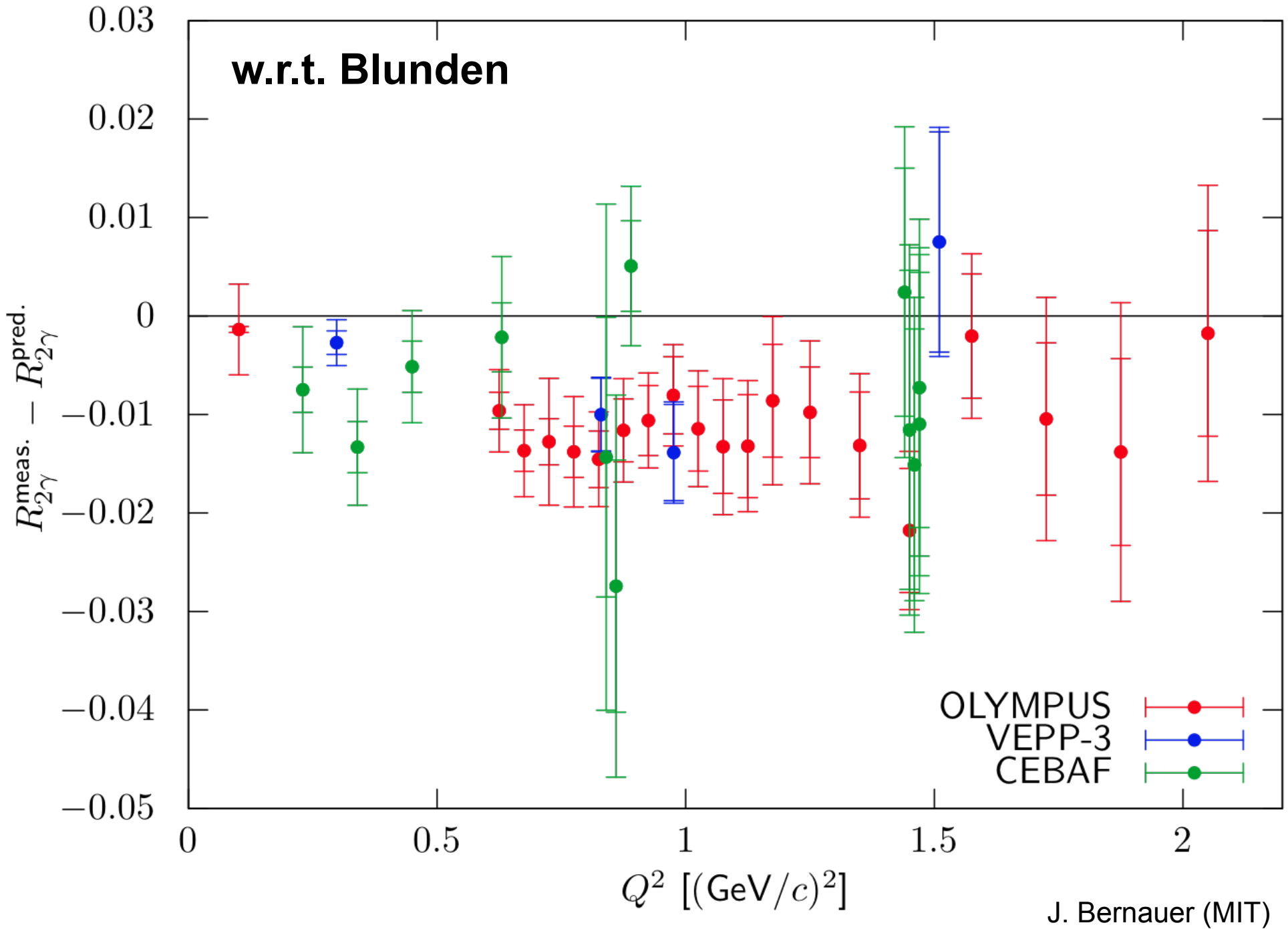
73



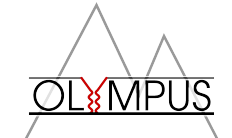
Comparison with VEPP-3 and CLAS



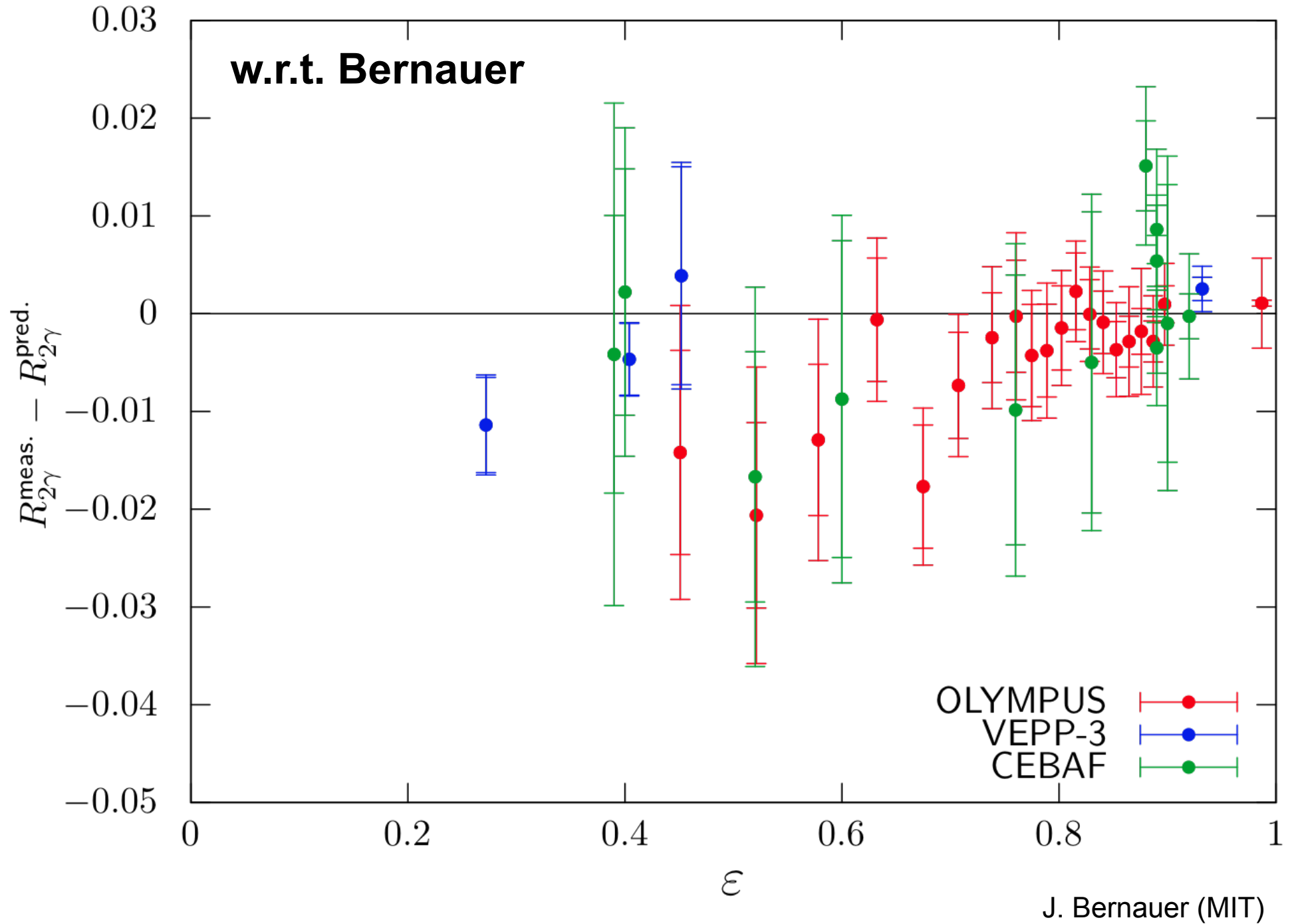
74



Comparison with VEPP-3 and CLAS



75



Comparison with VEPP-3 and CLAS



76

